

St. Lucie Unit 1 ECCS Performance Results
and
Isolated Safety Injection Tank Study

2-1-12-76

I. Introduction and Summary

On January 4, 1974, the Atomic Energy Commission issued New Acceptance Criteria for Emergency Core Cooling Systems for Light-Water-Cooled Reactors⁽¹⁾. The analysis presented herein demonstrates that the St. Lucie Unit 1 ECCS design satisfies these new criteria. The analysis has been performed using the Combustion Engineering (C-E) large break evaluation model^(2,3). The large break evaluation model results are presented in Section II and cover primary system ruptures larger than 0.5 ft². As demonstrated in CENPD-137⁽⁴⁾, breaks smaller than 0.5 ft² are not limiting. Therefore, a small break spectrum analysis is not presented.

C-E has recognized the similarities which exist for the NSSS of the 2560 Mwt Reactor Plants (Calvert Cliffs 1, Millstone Point 2, St. Lucie 1, and Calvert Cliffs II) and has performed a generic blowdown calculation to be used for all

CONTROL # 691

100-100000-100000



of these ECCS performance evaluation analyses. The features of each of these reactors have been compared and the appropriate parameters for the calculation were selected on the basis of conservatism (e.g., stored energy in the fuel has been maximized). However, due to the sensitivity of the thermal behavior of the hottest rod to the unique features of the fuel, containment building, and safeguard systems, explicit refill, reflood, and hot rod thermal transient calculations have been performed for St. Lucie 1.

Hot rod temperature calculations were performed for the entire spectrum of break sizes at a peak linear heat generation rate (PLHGR) of 15.8 kw/ft. The worst break (that which limits the PLHGR) was identified as the 0.8 DEG/PD*. The results of this study supersede those reported in Reference 5 and show that the plant meets the NRC Acceptance Criteria published in the Federal Register on January 4, 1974. Conformance is summarized as follows:

Criterion (1) Peak Clad Temperature. "The calculated maximum fuel element cladding temperature shall not exceed 2200°F."

The spectrum analysis yielded a peak clad temperature of 2192°F for the 0.8 DEG/PD break.

Criterion (2) Maximum Cladding Oxidation. "The calculated total oxidation of the cladding shall nowhere exceed 17% of the total cladding thickness before oxidation."

The spectrum analysis yielded a local peak clad oxidation

* 0.8 DEG/PD = 0.8 Double-Ended Guillotine rupture of the Pump Discharge leg.

percentage of 10.42% for the 0.8 DEG/PD break.

- Criterion (3) Maximum Hydrogen Generation. "The calculated total amount of hydrogen generated from the chemical reaction of the cladding with water or steam shall not exceed 1% of the hypothetical amount that would be generated if all of the metal in the cladding cylinders surrounding the fuel, excluding the cladding surrounding the plenum volume, were to react."

The 0.8 DEG/PD break produced the highest core-wide oxidation which was <.787%.

- Criterion (4) Coolable Geometry. "Calculated changes in core geometry shall be such that the core remains amenable to cooling."

The clad swelling and rupture model which is part of the C-E Evaluation Model⁽²⁾ accounts for the effects of changes in core geometry if such changes are predicted to occur. With these core geometry changes, core cooling was enough to lower temperatures. No further rupture can occur since the calculations were carried to the point at which the temperatures were decreasing. Thus, a coolable geometry has been maintained.

- Criterion (5) Long Term Cooling. "After any calculated successful initial operation of the ECCS, the calculated core temperature shall be maintained at an acceptably low value and decay heat shall be removed for the extended period of time required by the long-lived radioactivity remaining in the core."

The spectrum analysis presented in this report shows that the rapid insertion of borated water from the ECCS will suitably limit the peak clad temperature and cool the core within a short period of time. Subsequently, the safety injection pumps would supply cooling water from the refueling water tank to remove decay heat resulting from the long-lived radioactivity remaining in the core. When the refueling water tank is nearly empty, the safety injection pumps would then be lined up to recirculate water from the containment sump. In this manner, the core would be cooled for an indefinite period of time.

In addition to the spectrum analysis summarized above and discussed in Section II, a reanalysis was performed in which one Safety Injection Tank was isolated from the primary system. The method of analysis and the results are presented in Section III. Worst break results, for the cases with and without an isolated SIT, are compared below at a PLHGR of 15.8 kw/ft:

0.8 DEG/PD Results

	One SIT Isolated	No SIT Isolated
Peak Clad Temperature ($^{\circ}\text{F}$)	2191	2192
Local Clad Oxidation (%)	10.97	10.42
Core-Wide Clad Oxidation (%)	<.880	<.787

It is concluded that the LOCA criteria⁽¹⁾ are met for the case in which one SIT is isolated. Since all calculations assumed full power operation, there is no need to reduce power when one SIT is isolated. The PLHGR limit for both types of operation (SIT isolated and not isolated) is 15.8 kw/ft.

II. Large Break Analysis

A. Method of Calculation

The calculations reported in this section were performed using Combustion Engineering's large break evaluation model which is described in Reference 2. In addition, the following modifications to the model, as documented in Reference 3, have been included in these calculations:

1. The containment wall nodding technique has been revised in order to provide a converged wall temperature solution.
2. Based on a recent review of steam-water mixing data, the resistance across the ECCS injection section during the period after the safety injection tanks have emptied has been revised.

In the C-E model, the CEFLASH-4A⁽⁶⁾ computer program is used to determine the primary system flow parameters during the blowdown phase, and the COMPERC-II⁽⁷⁾ computer program is used to describe the system behavior during the refill and reflood phases. The core flow and thermodynamic parameters from these two codes are used as input to the STRIKIN-II⁽⁸⁾ program which is used to calculate the hot rod clad temperature transient. The peak clad temperature and peak local clad oxidation percentage are



therefore obtained from the STRIKIN-II calculation. The core-wide clad oxidation percentage is obtained from the results of both STRIKIN-II and the COMZIRC^(7; Suppl. 1) computer programs.

B. Emergency Core Cooling System Assumptions

The Emergency Core Cooling System consists of two high pressure pumps, two low pressure pumps and four safety injection tanks. Automatic operation of the pumps is actuated by a low-low pressurizer pressure signal or a high containment pressure signal. Flow is initiated from the safety injection tanks when the cold leg pressure drops below 215 psia plus the elevation head. Parameters pertinent to the calculation of the LOCA are presented in Table II-1.

In performing the LOCA calculations, conservative assumptions are made concerning the availability of safety injection flow. It is assumed that off-site power is lost and all safety injection pumps must await diesel startup before they can begin to deliver flow. (It is assumed, however, that off-site power is available for the containment spray pumps). Also, it is assumed that all safety injection flow delivered to the broken cold leg is lost.

An analysis of the possible single failures that can occur within the ECCS has shown that the worst single failure for large breaks is the failure of one of the low pressure pumps to start⁽²⁾. Thus, only one low pressure pump is used in the current LOCA analysis for St. Lucie Unit 1.

The above assumptions lead to the conclusion that the following safety

injection flows are available:

75% of the flow from two high pressure pumps

75% of the flow from one low pressure pump

Flow from three safety injection tanks

In the analysis reported in this section, no credit is taken for pump flow until the tanks are empty.

C. Core, System and Containment Parameters

The significant core and system parameters used in the large break calculations are presented in Table II-1. The peak linear heat rate was assumed to occur in the top of the core, the conservative location as identified in Section IV.A.4 of Reference 2. A conservative beginning-of-life moderator temperature coefficient ($+0.2 \times 10^{-4} \Delta\rho/^{\circ}\text{F}$) was used for all cases.

Hot fuel rod conditions, as determined by the FATES⁽⁹⁾ computer program, were evaluated at a rod-average burnup of 3389 MTD/MTU; a parameter study was performed which indicated that clad temperature and oxidation were maximized at this exposure.

Containment parameters as presented in Table II-2 are chosen to minimize containment pressure such that a conservative determination of core reflood rate is made. Pressure suppression equipment startup times are selected at their minimum values corresponding to off-site power being available.



D. Break Spectrum

In general, all possible break locations are considered in a LOCA analysis. However, as demonstrated in other Appendix K LOCA calculations (References 2 and 10, for example), hot leg ruptures and cold leg ruptures on the suction side of the pump yield clad temperatures substantially lower than those observed for cold leg ruptures on the discharge side of the pump. Pump discharge leg ruptures are limiting due to the minimization of blowdown core flow and reflood rate for this break location. Thus, only these breaks need to be considered in order to identify that rupture which results in the highest clad temperature or largest amount of clad oxidation. Since core flow is a function of the break size, calculations have been performed for both guillotine and slot breaks over a range of break sizes from 0.5 ft² to twice the flow area of the cold leg.

E. Results

Table II-3 presents a listing of the large break sizes analyzed in this study along with the figure numbers presenting the pertinent transient data for each break.

As noted in Table II-3, the results for each of the breaks analyzed are displayed graphically in Figures II.1 through II.7. For each break, the nine variables listed in Table II-4 are plotted as a function of time. For the break having the highest clad temperature and clad oxidation (0.8 DEG/PD), the additional quantities listed in Table II-5 are also presented. The water level in the downcomer (Figure II.5-M) is presented



only for one break because all breaks have the same transient behavior. Times of interest for the various breaks are shown in Table II-6, while Table II-7 summarizes peak clad temperatures and clad oxidation percentages.

As described in Reference 2, the method used to calculate core-wide clad oxidation is conveniently simple, but is very conservative. The following major conservatisms can be enumerated:

- (1) During blowdown, all rods experience the same amount of oxidation as the hot rod.
- (2) During the entire transient, all rods experience the same rupture region oxidation as the hot rod.
- (3) In initializing the multi-region COMZIRC calculation, the CEFLASH-4A hot assembly clad and fuel temperatures are used for all rods having above average power.
- (4) During refill/reflood, the flattest possible power distribution is used, even though inconsistent with the PLHGR.

In addition to the above four conservative features of the method, there is also a major conservatism in the particular manner in which the core-wide oxidation percentages were determined for St. Lucie Unit 1. The hot assembly region power in CEFLASH-4A was based on a peak LHGR of 17.0 kw/ft, thus allowing flexibility during the determination of the allowable peak LHGR based on the STRIKIN-II prediction of the hot rod thermal behavior. However, since the STRIKIN-II calculations yielded an allowable PLHGR of only 15.8 kw/ft, this procedure

leads to a very conservative core-wide clad oxidation calculation since the CEFLASH-4A hot assembly fuel and clad temperatures are used to initialize COMZIRC at the beginning of refill/reflood. An evaluation of this conservatism for another plant showed that the core-wide clad oxidation was reduced from 0.933% to 0.776% when the CEFLASH-4A hot assembly reference PLHGR was reduced from 17.0 to 15.2 kw/ft. Thus, the actual values for core-wide clad oxidation would be appreciably less than those reported in Table II-7.

Figure II-8 shows peak clad temperature plotted versus break size and type, showing the worst break to be the 0.8 DEG/PD rupture.

Mass and energy release to the containment during blowdown is presented in Table II-8. Also shown in this table is the steam expulsion data during reflood. The ECC water spillage and containment spray flow rates are presented graphically in Figure II.9.



III. Isolated Safety Injection Tank Analysis

The calculations reported in this section were performed using the CE evaluation model as described in Section II-A. Additionally, a portion of the study required a modification to the noding scheme employed in the CEFLASH-4A blowdown model. The change was necessary in order to explicitly model a safety injection tank in each of the intact cold legs, thus allowing for the study of possible asymmetric effects. Figure IV.A.1-1 of Reference 2 shows the CEFLASH-4A nodal map used for the evaluation model. In this model, the intact loop cold legs are lumped together; in the new model these cold legs have been separated and modeled individually.

In order to determine if asymmetric effects exist, the standard and modified CEFLASH-4A nodal models were used to analyze the 1.0 DEG/PD break. Cases were run in which a Safety Injection Tank was successively isolated from each intact cold leg until all three SIT locations had been examined. In all cases, the SIT attached to the broken cold leg is assumed to spill directly to the containment. Results indicated there were no asymmetric effects during blowdown due to isolating the various safety injection tanks.

Based on the above findings, the standard CEFLASH-4A nodal model was used to analyze the worst break (0.8 DEG/PD as defined in Section II). Refill/reflood calculations were performed using the COMPERC-II computer code. COMPERC-II cannot model safety injection asymmetry, but can treat such asymmetry conservatively; i.e., the total SIT flow rate entering the vessel was reduced by one third, but the injection section pressure drop in the cold leg having the isolated SIT was maintained at 0.4 psi, the value used when SIT flow is present. A more detailed calculation in which the asymmetry was modeled would show a larger steam flow rate through the cold leg having the isolated SIT;

the higher steam flow rate would lead to higher reflood rates and lower clad temperatures.

As done in the spectrum analysis, core flow and thermodynamic parameters from the CEFLASH-4A and COMPERC-II analyses were used as input to the STRIKIN-II code for the determination of the hot rod clad temperature transient as well as the peak local clad oxidation percentage. The core-wide clad oxidation percentage was obtained from the results of both STRIKIN-II and the COMZIRC computer programs.

Table III-1 presents a list of variables plotted as a function of time for the isolated Safety Injection Tank study. Table III-2 compares parameters of interest for the worst break (0.8 DEG/PD) analyzed with and without an isolated SIT at a PLHGR of 15.8 kw/ft.

The results of this study indicate that the LOCA criteria are not exceeded at a PLHGR of 15.8 kw/ft when one SIT is isolated. The study also shows that, although the temperatures and oxidation percentages increased somewhat during reflood due to the longer refill period, the limiting clad temperature occurs during blowdown, as it did for the reference case described in Section II. Therefore, since the peak clad temperature is limiting and occurs during blowdown, and since blowdown asymmetry effects are insignificant, the worst break will be the same for the isolated SIT configuration as it was for the reference configuration in which all tanks were operative.

IV. Computer Code Version Identification

The following versions of the Combustion Engineering ECCS Evaluation Model computer codes were used for this analysis:

CEFLASH-4A: Version No. 74329

STRIKIN-II: Version No. 75105*

COMPERC-II: Version No. 75097

COMZIRC : Version No. 75055

* The STRIKIN-II Version 75066 has been modified to prevent occurrence of a negative square root (due to computer round-off error) when in nucleate boiling. Versions 75066 and 75105 predict the same results upon successful computation.

V. References

1. Acceptance Criteria for Emergency Core Cooling Systems for Light-Water-Cooled Nuclear Power Reactors, Federal Register, Vol. 39, No. 3 - Friday, January 4, 1974.
2. CENPD-132, "Calculative Methods for the C-E Large Break LOCA Evaluation Model," August, 1974 (Proprietary).
CENPD-132, Supplement 1, "Updated Calculative Methods for the C-E Large Break LOCA Evaluation Model," December 1974 (Proprietary).
3. CENPD-132, Supplement 2, "Calculational Methods for the C-E Large Break LOCA Evaluation Model," July 1975.
4. CENPD-137, "Calculation Methods for the C-E Small Break LOCA Evaluation Model," Combustion Engineering Proprietary Report, August, 1974 (Proprietary).
5. St. Lucie Unit 1 FSAR, Large Break Analysis, Section 6.3.3.6.1 as amended by Revision #45, May 27, 1975.
6. CENPD-133, "CEFLASH-4A, A FORTRAN IV Digital Computer Program for Reactor Blowdown Analysis," April 1974 (Proprietary).
CENPD-133, Supplement 2, "CEFLASH-4A, A FORTRAN IV Digital Computer Program for Reactor Blowdown Analysis (Modification)," December, 1974 (Proprietary).
7. CENPD-134, "COMPERC-II, A Program for Emergency Refill-Reflood of the Core," April 1974 (Proprietary).
CENPD-134, Supplement 1, "COMPERC-II, A Program for Emergency Refill-Reflood of the Core (Modification)," December 1974 (Proprietary).
8. CENPD-135, "STRIKIN-II, A Cylindrical Geometry Fuel Rod Heat Transfer Program," April 1974 (Proprietary).
CENPD-135, Supplement 2, "STRIKIN-II, A Cylindrical Geometry Fuel Rod Heat Transfer Program (Modification)," December 1974 (Proprietary).
9. CENPD-139, "C-E Fuel Evaluation Model," July 1974 (Proprietary).
10. Letter D. C. Switzer (NNECO) to O. D. Parr (NRC) re: Millstone Nuclear Power Station, Unit 2 ECCS Re-evaluation, July 10, 1975, Docket No. 50-336.



Table II-1
General System Parameters

<u>Quantity</u>	<u>Value</u>	
Reactor Power Level (102% of Nominal)	2611	MWt
Average Linear Heat Rate (102% of Nominal)	6.2126	kw/ft
Peak Linear Heat Rate	15.8	kw/ft
Gap Conductance at Peak Linear Heat Rate*	820.2	BTU/hr-ft ² -°F
Fuel Centerline Temperature at Peak Linear Heat Rate*	4055.1	°F
Fuel Average Temperature at Peak Linear Heat Rate*	2656.5	°F
Hot Rod Gas Pressure*	1147.6	psia
Moderator Temperature Coefficient at Initial Density	+0.2 x 10 ⁻⁴	Δρ/°F
System Flow Rate (Total)	139.44 x 10 ⁶	lbs/hr
Core Flow Rate	134.6 x 10 ⁶	lbs/hr
Initial System Pressure	2250	psia
Core Inlet Temperature	548	°F
Core Outlet Temperature	598	°F
Active Core Height	11.39	ft
Fuel Rod OD	.44	in.
Number of Cold Legs	4	
Number of Hot Legs	2	
Cold Leg Diameter	30	in.
Hot Leg Diameter	42	in.
Safety Injection Tank Pressure	215	psia
Safety Injection Tank Gas/Water Volume	930/1090	ft ³

*These quantities correspond to the burnup (3389 MWD/MTU, hot rod average) yielding the highest peak clad temperature.

Table II-2

Containment Physical Parameters

Net Free Volume $2.5111 \times 10^6 \text{ Ft}^3$

Containment Initial Conditions:

Humidity 100%

Containment Temperature 60°F

Enclosure Building Temperature 38°F

Initial Pressure 14.6 psia

Initial Time For:

Spray Flow 25 seconds

Fans (4) 0.0 seconds

Containment Spray Water:

Temperature 55°F

Flow Rate (Total, both pumps) 3375 gpm

Fan Cooling Capacity (per fan)

Vapor Temperature ($^\circ\text{F}$)Capacity (BTU/Sec)

60	0.0
120	3472.0
180	7388.8
220	11611.1
264	20833.3

Heat Transfer Coefficient

- Containment structure to enclosure building atmosphere heat transfer coefficient - $13.0 \text{ BTU/hr-ft}^2\text{-}^\circ\text{F}$.
- Sump to base slab - $10 \text{ BTU/hr-ft}^2\text{-}^\circ\text{F}$.
- Containment atmosphere to sump - $500 \text{ BTU/hr-ft}^2\text{-}^\circ\text{F}$.



Table II-2 Continued

St. Lucie 1 Revised Passive Heat Sink Information

	<u>Wall</u>	<u>Material</u>	<u>Thickness Ft</u>	<u>Area Ft²</u>	<u>k BTU Hr-ft-°F</u>	<u>ρC_p BTU Ft³-°F</u>	<u>Exposure Side 1</u>	<u>Exposure Side 2</u>
1.	Containment Shell	Steel	.1171	86700	25.9	53.57	Cont. Vapor	Annulus
2.	Floor Slab	Concrete	20.0	12682	1.0	34.2	Cont. Vapor	Insulated
3.	Misc. Concrete	Concrete	1.5	87751	1.0	34.2	Cont. Vapor	Insulated
4.	Galvanized Steel	Zinc Steel	0.0005833 0.01417	130000	64.0 25.9	40.6 53.57	Cont. Vapor	Insulated
5.	Carbon Steel	Steel	0.03125	25000	30.0	53.8	Cont. Vapor	Insulated
6.	Stainless Steel	Steel	0.0375	22300	9.8	54.0	Cont. Vapor	Insulated
7.	Misc. Steel	Steel	0.0625	40000	25.9	53.57	Cont. Vapor	Insulated
8.	Misc. Steel	Steel	0.02083	41700	25.9	53.57	Cont. Vapor	Insulated
9.	Misc. Steel	Steel	0.17708	7000	25.9	53.57	Cont. Vapor	Insulated
10.	Imbedded Steel	Steel Concrete	0.0708 7.00	18000	25.9 1.0	53.57 34.2	Cont. Vapor	Insulated



Table II-3
Large Break Spectrum

<u>Break Size, Type and Location</u>	<u>Abbreviation</u>	<u>Figure</u>
1.0 x Double-Ended Slot Break in Pump Discharge Leg	1.0 x DES/PD	II.1
0.8 x Double-Ended Slot Break in Pump Discharge Leg	0.8 x DES/PD	II.2
0.6 x Double-Ended Slot Break in Pump Discharge Leg	0.6 x DES/PD	II.3
0.5 Ft ² Slot Break in Pump Discharge Leg	0.5 ft ² S/PD	II.4
1.0 x Double-Ended Guillotine Break in Pump Discharge Leg	1.0 x DEG/PD	II.5
0.8 x Double-Ended Guillotine Break in Pump Discharge Leg	0.8 x DEG/PD	II.6
0.6 x Double-Ended Guillotine Break in Pump Discharge Leg	0.6 x DEG/PD	II.7



Table II-4

Variables Plotted as a Function of Time
for Each Large Break in the Spectrum

<u>Variable</u>	<u>Figure Designation</u>
Core Power	A
Pressure in Center Hot Assembly Node	B
Leak Flow	C
Hot Assembly Flow (below hot spot)	D.1
Hot Assembly Flow (above hot spot)	D.2
Hot Assembly Quality	E
Containment Pressure	F
Mass Added to Core During Reflood	G
Peak Clad Temperature	H

Table II-5

Additional Variables Plotted as a Function
of Time for the Worst Large Break

<u>Variables</u>	<u>Figure Designation</u>
Mid Annulus Flow	I
Qualities Above and Below the Core	J
Core Pressure Drop	K
Safety Injection Flow into Intact Discharge Legs	L
Water Level in Downcomer During Reflood	M
Gap Conductance	N
Local Clad Oxidation	O
Clad Temperature, Centerline Fuel Temperature, Average Fuel Temperature and Coolant Temperature for Hottest Node	P
Hot Spot Heat Transfer Coefficient	Q
Hot Spot Heat Transfer Coefficient During Reflood	R
Containment Temperature	S
Sump Temperature	T
Hot Pin Pressure	U
Core Bulk Channel Flow Rate	V

Table II-6

Times of Interest for Each Large Break (PLHGR = 15.8 kw/ft)
(Seconds)

<u>Break</u>	<u>Hot Rod Rupture</u>	<u>SI Tanks on</u>	<u>Start of Reflood</u>	<u>SI Tanks Empty</u>
1.0 x DES/PD	10.0	17.3	37.6	70.4
0.8 x DES/PD	9.9	17.6	38.0	70.8
0.6 x DES/PD	10.4	19.3	39.6	72.6
0.5 ft ² S/PD	288.9	173.0	193.2	225.4
1.0 x DEG/PD	10.8	17.4	37.7	70.5
0.8 x DEG/PD	10.0	17.9	38.3	71.1
0.6 x DEG/PD	29.3	20.1	40.6	73.4

Table II-7

Peak Clad Temperatures and Oxidation Percentages
for the Break Spectrum at a PLHGR of 15.8 kw/ft

<u>Break</u>	<u>Peak Clad Temperature (^oF)</u>	<u>Clad Oxidation %</u>	
		<u>Local</u>	<u>Core-Wide</u>
1.0 DES/PD	2137	10.07	<.735
0.8 DES/PD	2149	9.98	<.726
0.6 DES/PD	2099	9.18	<.659
0.5 Ft ² S/PD	1777	2.85	<.141
1.0 DEG/PD	2150	10.29	<.762
0.8 DEG/PD	2192	10.42	<.787
0.6 DEG/PD	2056	7.71	<.524

Table II.8

St. Lucie Unit I
 Blowdown Mass and Energy Release Data
 0.8 x DEG/PD

TIME	MASS FLOW	ENERGY RELEASE	INTEGRAL OF MASS FLOW	INTEGRAL OF ENERGY RELEASE
SEC	LBM/SEC	BTU/SEC	LBM	BTU
0.0	0.0	0.0	0.0	0.0
.05	7.9404 $\times 10^4$	4.2793 $\times 10^7$	3.0800 $\times 10^3$	1.6582 $\times 10^6$
.10	6.8758	3.7109	6.7872 $\times 10^3$	3.6553
.15	7.0586	3.7989	1.0274 $\times 10^4$	5.5324
.20	6.8127	3.6668	1.3737	7.3962
.25	6.8865	3.7093	1.7178	9.2488 $\times 10^6$
.35	6.7299	3.6297	2.3965	1.2907 $\times 10^7$
.45	6.6087	3.5676	3.0624	1.6500
.60	6.6010	3.5669	4.0519	2.1861
.80	6.5845	3.5616	5.3723	2.8983
1.0	6.5559	3.5501	6.6855	3.6090
1.4	6.4260	3.4897	9.2917 $\times 10^4$	5.0222
1.8	6.0147	3.2751	1.1792 $\times 10^5$	6.3822
2.2	5.2523	2.8623	1.4040	7.6068
2.6	4.7898	2.6140	1.6046	8.7004
3.0	4.6063	2.5188	1.7919	9.7239 $\times 10^7$
3.4	4.3221	2.3684	1.9709	1.0703 $\times 10^8$
3.8	4.1283	2.2718	2.1393	1.1628
4.4	3.7965	2.1124	2.3775	1.2945
5.2	3.3374	1.9050	2.6625	1.4550
6.0	3.0142	1.7544	2.9157	1.6010
6.8	2.7546	1.6285	3.1463	1.7362
7.6	2.5215	1.512	3.3569	1.8618
8.4	2.3554	1.4085	3.5516	1.9784
9.2	2.1841	1.3045	3.7335	2.0870
10.0	1.9793 $\times 10^4$	1.1929 $\times 10^7$	3.9002 $\times 10^5$	2.1870 $\times 10^8$

Table II.8 Cont'd

TIME	MASS FLOW	ENERGY RELEASE	INTEGRAL OF MASS FLOW	INTEGRAL OF ENERGY RELEASE
SEC	LBM/SEC	BTU/SEC	LEM	BTU
11.0	1.6893 $\times 10^4$	1.0467 $\times 10^7$	4.0840 $\times 10^5$	2.2988 $\times 10^8$
12.0	1.3611 $\times 10^4$	9.0048 $\times 10^6$	4.2382	2.3963
13.0	8.2968 $\times 10^3$	7.2779	4.3468	2.4774
14.0	6.6074	6.2601	4.4199	2.5448
15.0	4.9331	5.2050	4.4776	2.6022
16.0	3.8203	4.1496	4.5210	2.6488
17.0	2.8101	3.3269	4.5539	2.6860
18.0	2.1394	2.6011	4.5785	2.7155
19.0	1.4563 $\times 10^3$	1.7916	4.5964	2.7374
20.0	9.8988 $\times 10^2$	1.2358 $\times 10^6$	4.6084	2.7523
21.0	4.4192	5.6219 $\times 10^5$	4.6164	2.7622
21.7	4.4460 $\times 10^2$	5.7162 $\times 10^5$	4.6197 $\times 10^5$	2.7660 $\times 10^8$
Time of Annulus Downflow				
Start of Reflood (Values below are for steam only)				
38.31	0.0	0.0	4.6197 $\times 10^5$	2.7660 $\times 10^8$
48.31	0.0	0.0	4.6197	2.7660
58.31	0.0	0.0	4.6197	2.7660
68.31	0.0	0.0	4.6197	2.7660
78.31	1.8671 $\times 10^2$	2.4280 $\times 10^5$	4.6337	2.7842
88.31	1.9948	2.5940	4.6521	2.8081
98.31	1.9559	2.5434	4.6718	2.8338
108.31	1.9172	2.4931	4.6913	2.8591
118.31	1.9128	2.4874	4.7106	2.8842
128.31	1.9045 $\times 10^2$	2.4767 $\times 10^5$	4.7297 $\times 10^5$	2.9090 $\times 10^8$



Table II. 8 Cont'd

TIME	MASS FLOW	ENERGY RELEASE	INTEGRAL OF MASS FLOW	INTEGRAL OF ENERGY RELEASE
SEC	LBM/SEC	BTU/SEC	LBM	BTU
138.31	1.8629 $\times 10^2$	2.4225 $\times 10^5$	4.7486 $\times 10^5$	2.9337 $\times 10^8$
148.31	1.8868	2.4536	4.7676	2.9583
158.31	1.8945	2.4637	4.7865	2.9829
168.31	1.8859	2.4525	4.8054	3.0074
178.31	1.8922	2.4607	4.8242	3.0320
188.31	1.8986	2.4690	4.8432	3.0566
198.31	1.9096	2.4832	4.8622	3.0813
208.31	1.9040	2.4760	4.8812	3.1060
228.31	1.9217	2.4990	4.9194	3.1558
248.31	1.9352	2.5166	4.9579	3.2058
268.31	1.9560	2.5436	4.9968	3.2563
288.31	1.9473	2.5323	5.0358	3.3071
308.31	1.9617	2.5510	5.0751	3.3582
328.31	1.9817	2.5770	5.1147	3.4097
348.31	1.9871	2.5840	5.1545	3.4614
368.31	2.0081	2.6113	5.1944	3.5134
388.31	2.0146	2.6198	5.2346	3.5656
408.31	2.0191	2.6257	5.2750	3.6181
438.31	2.0108 $\times 10^2$	2.6148 $\times 10^5$	5.3357 $\times 10^5$	3.6970 $\times 10^8$

Table III-1

Variables Plotted as a Function of Time
for Isolated Safety Injection Tank Analysis

<u>Variable</u>	<u>Figure Designation</u>
Core Power	A
Pressure in Center Hot Assembly Node	B
Leak Flow	C
Hot Assembly Flow (below hot spot)	D.1
Hot Assembly Flow (above hot spot)	D.2
Hot Assembly Quality	E
Containment Pressure	F
Mass Added to Core During Reflood	G
Peak Clad Temperature	H*
Mid Annulus Flow	I
Qualities Above and Below the Core	J
Core Pressure Drop	K
Safety Injection Flow into Intact Discharge Legs	L
Water Level in Downcomer During Reflood	M
Gap Conductance	N
Local Clad Oxidation	O
Clad Temperature, Centerline Fuel Temperature, Average Fuel Temperature and Coolant Temperature for Hottest Node	P
Hot Spot Heat Transfer Coefficient	Q
Hot Spot Heat Transfer Coefficient During Reflood	R
Containment Temperature	S
Sump Temperature	T
Hot Pin Pressure	U
Core Bulk Channel Flow Rate	V

*For the worst case, the temperature of the rupture node is also shown.

Table III-2

A Comparison of Times, Temperatures, and
Oxidation Percentages for the Worst Break (0.8 DEG/PD)
with and without an Isolated SIT

PLHGR = 15.8 kw/ft

<u>Break</u>	<u>Hot Rod Rupture</u>	<u>SI Tanks on</u>	<u>Start of Reflood</u>	<u>SI Tanks Empty</u>	<u>Peak Clad Temperature (^oF)</u>	<u>Clad Oxidation % Local</u>	<u>Core-Wide</u>
<u>One SIT Isolated</u>	10.0	17.9	46.5	71.3	2191	10.97	<.880
<u>No SIT Isolated</u>	10.0	17.9	38.3	71.1	2192	10.42	<.787

Figure II:1-A
2560 MWt PLANTS
1.0 x DOUBLE ENDED SLOT BREAK IN PUMP DISCHARGE LEG
CORE POWER

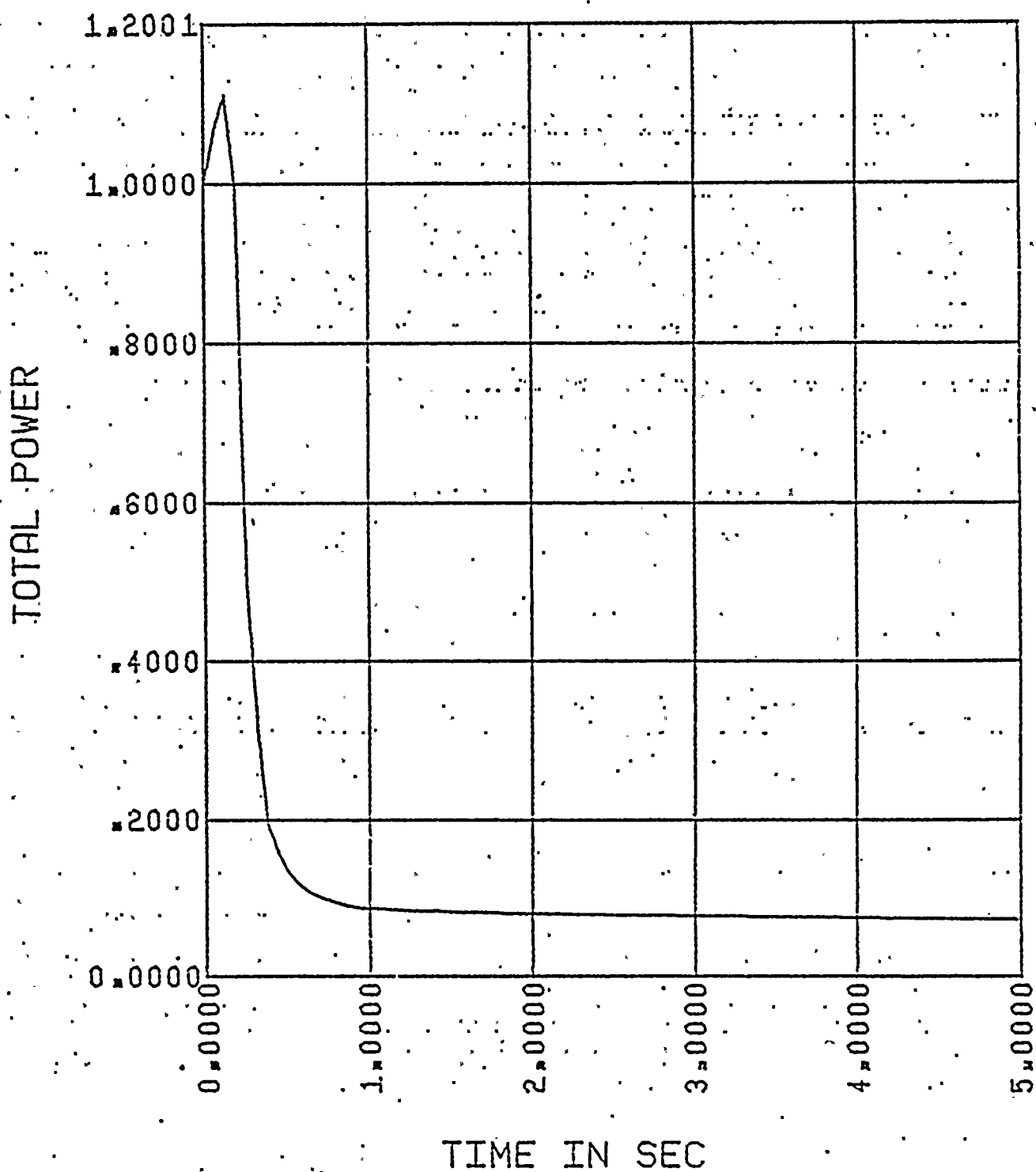




Figure II.1-B

2560 MWt PLANTS

1.0 x DOUBLE ENDED SLOT BREAK IN PUMP DISCHARGE LEG
PRESSURE IN CENTER HOT ASSEMBLY NODE

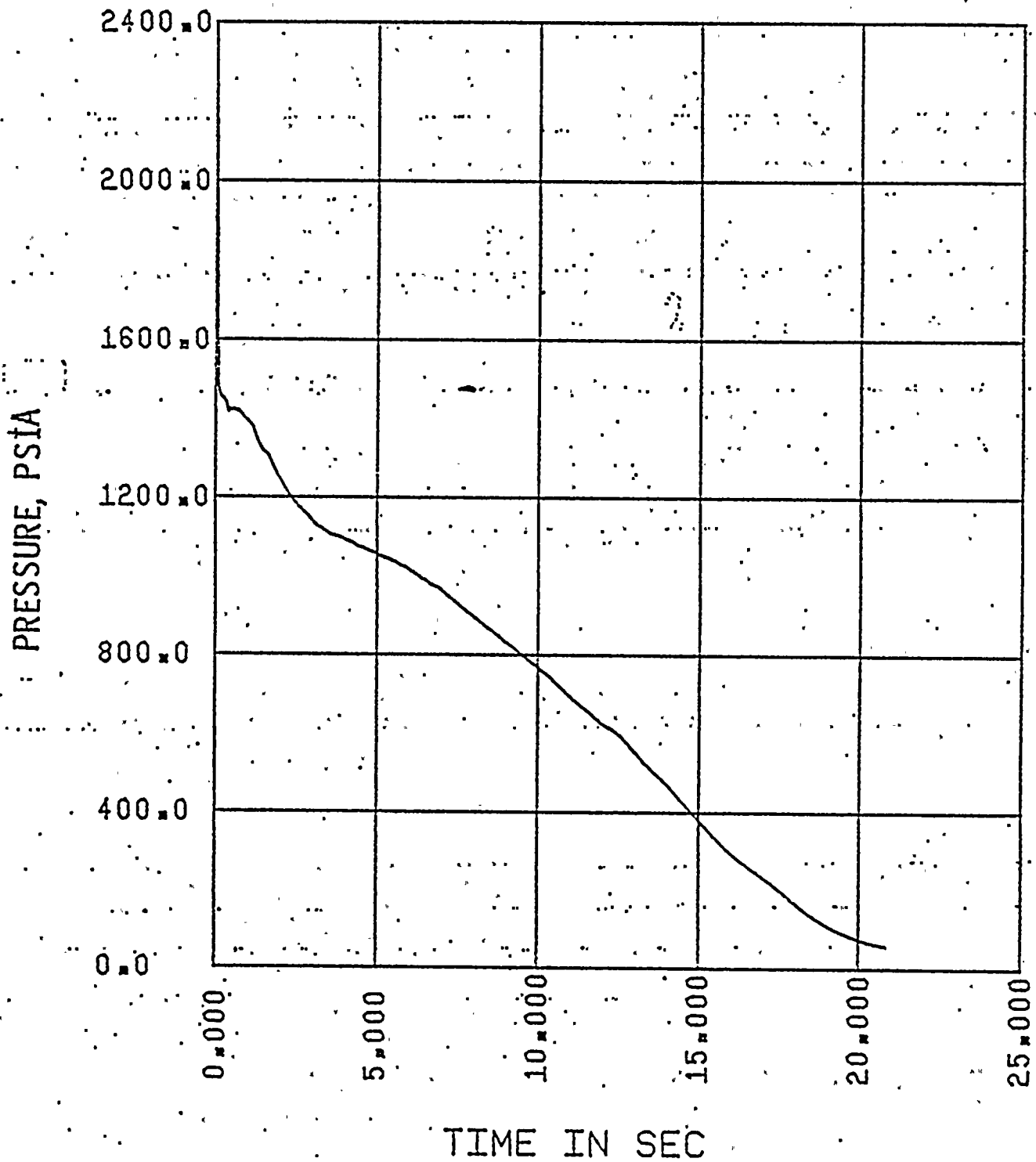
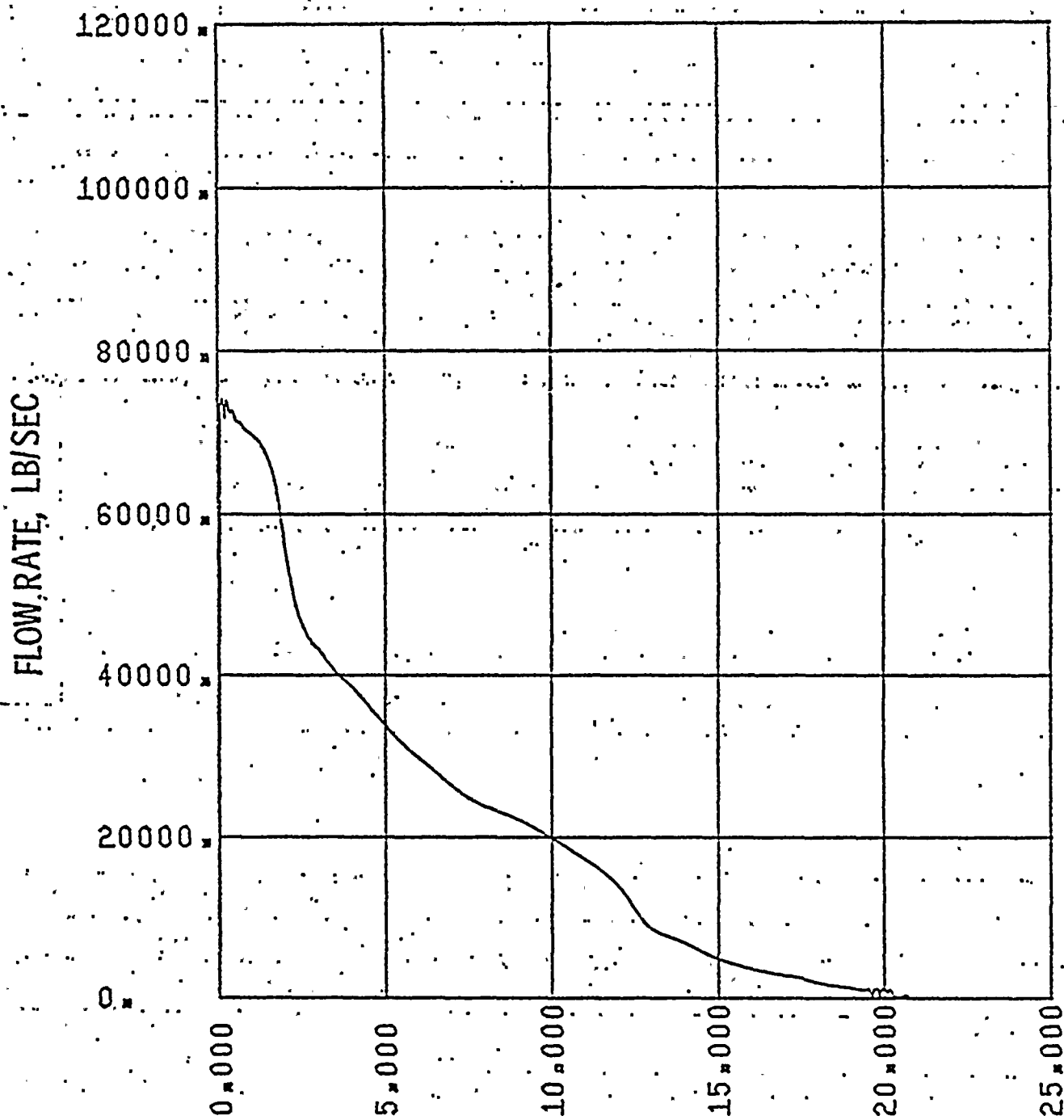


Figure II.1-C
2560 MWt PLANTS
1.0 x DOUBLE ENDED SLOT BREAK IN PUMP DISCHARGE LEG
LEAK FLOW



TIME IN SEC

Figure II.1-D.1

2560 MWt PLANTS

1.0 x DOUBLE ENDED SLOT BREAK IN PUMP DISCHARGE LEG
FLOW IN HOT ASSEMBLY - PATH 16, BELOW HOT SPOT

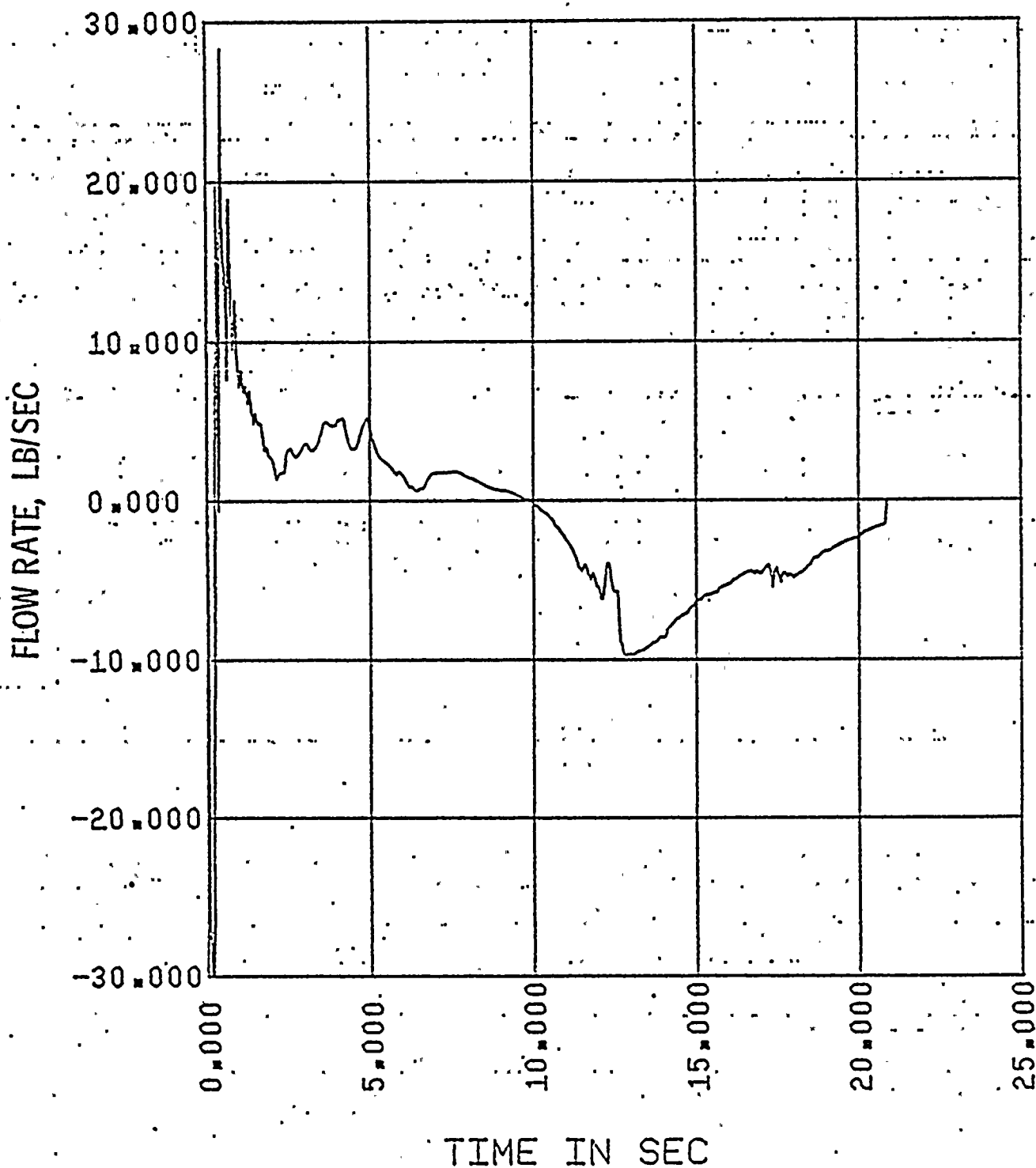
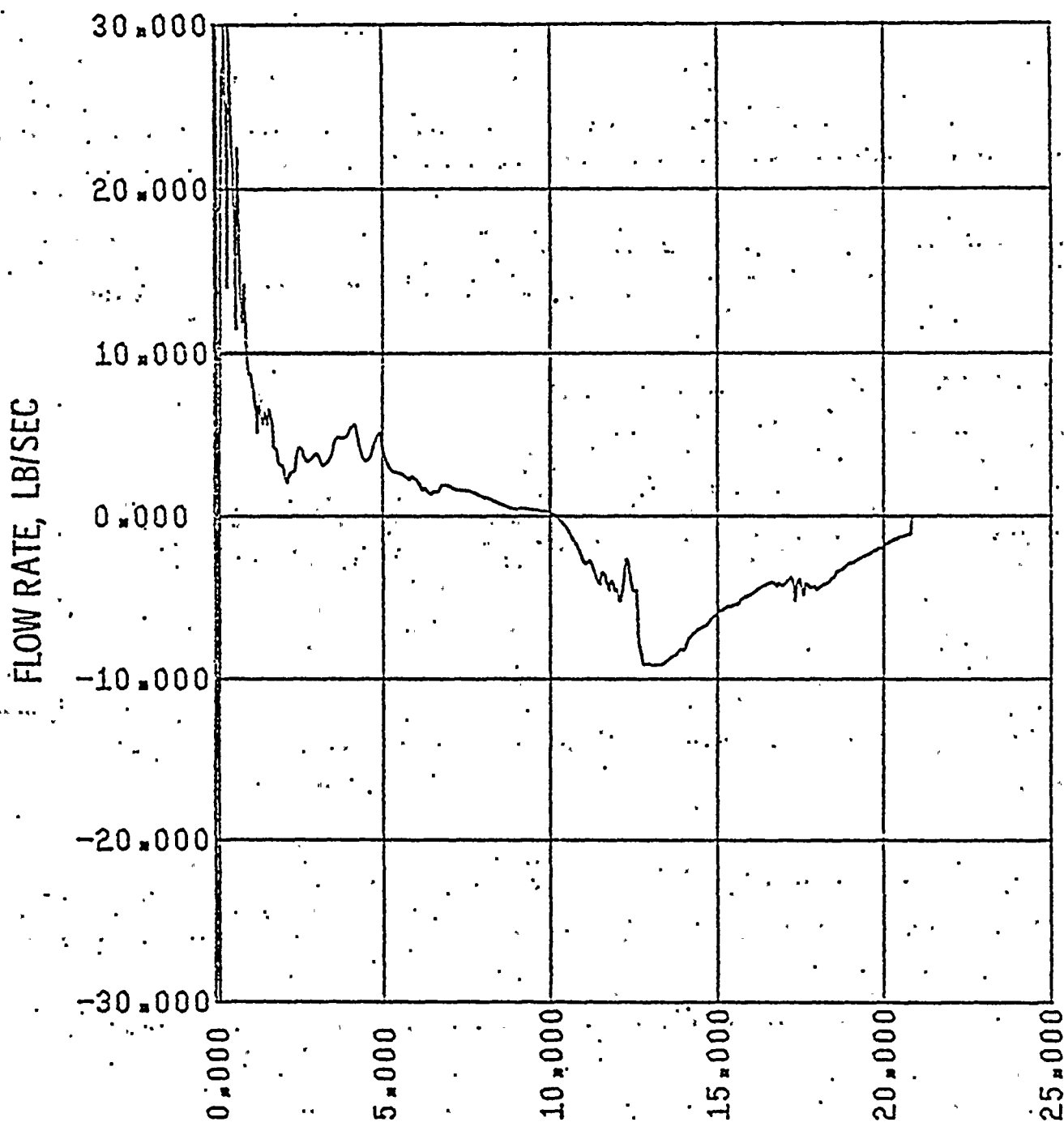


Figure II.1-D.2

2560 MWt PLANTS

1.0 x DOUBLE ENDED SLOT BREAK IN PUMP DISCHARGE LEG
FLOW IN HOT ASSEMBLY - PATH 17, ABOVE HOT SPOT



TIME IN SEC

Figure II.1-E

2560 MWT PLANTS

1.0x DOUBLE ENDED SLOT BREAK IN PUMP DISCHARGE LEG
HOT ASSEMBLY QUALITY

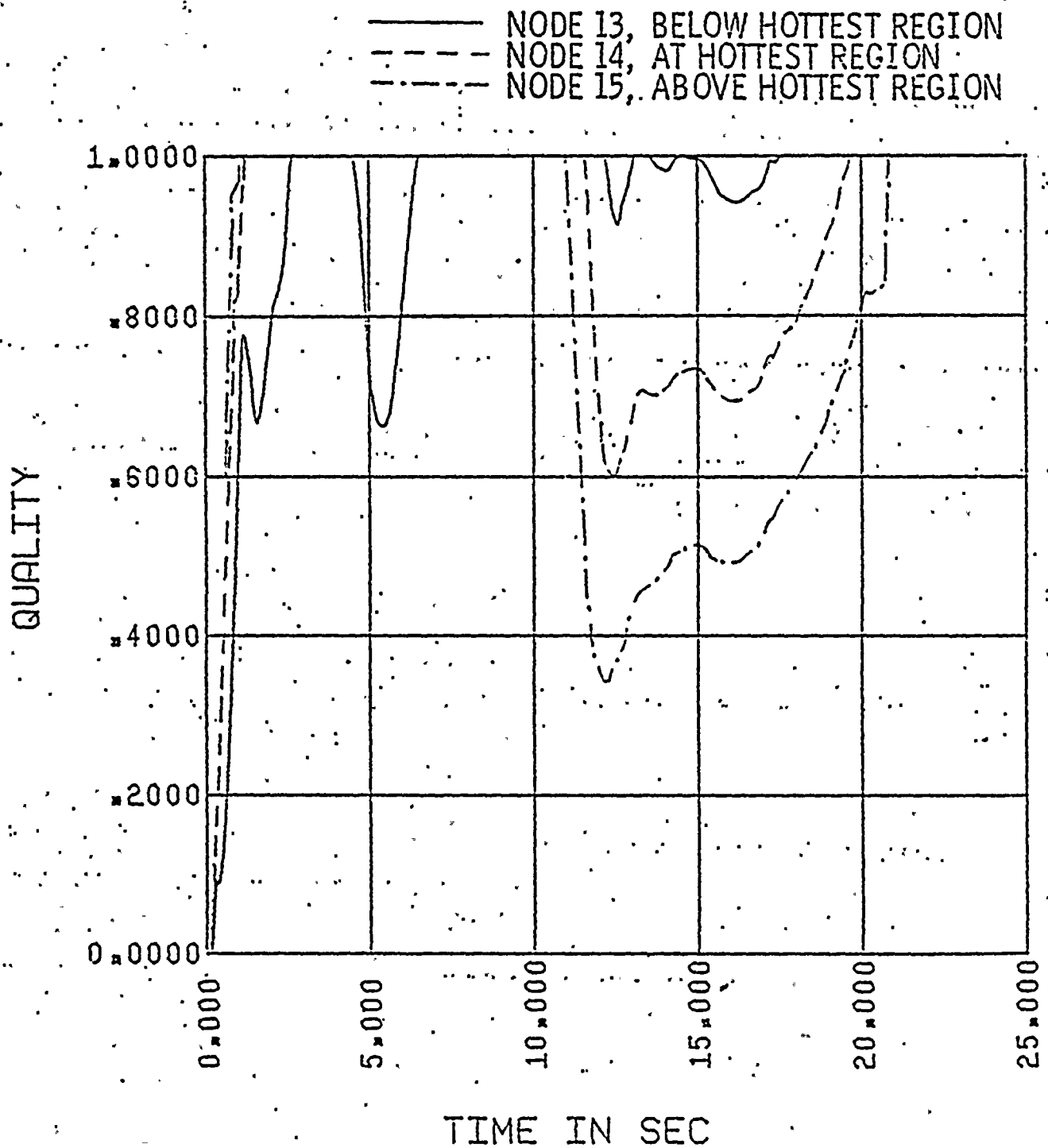


FIGURE II.1-F
ST. LUCIE UNIT I
1.0 x DOUBLE ENDED SLOT BREAK IN PUMP DISCHARGE LEG
CONTAINMENT PRESSURE

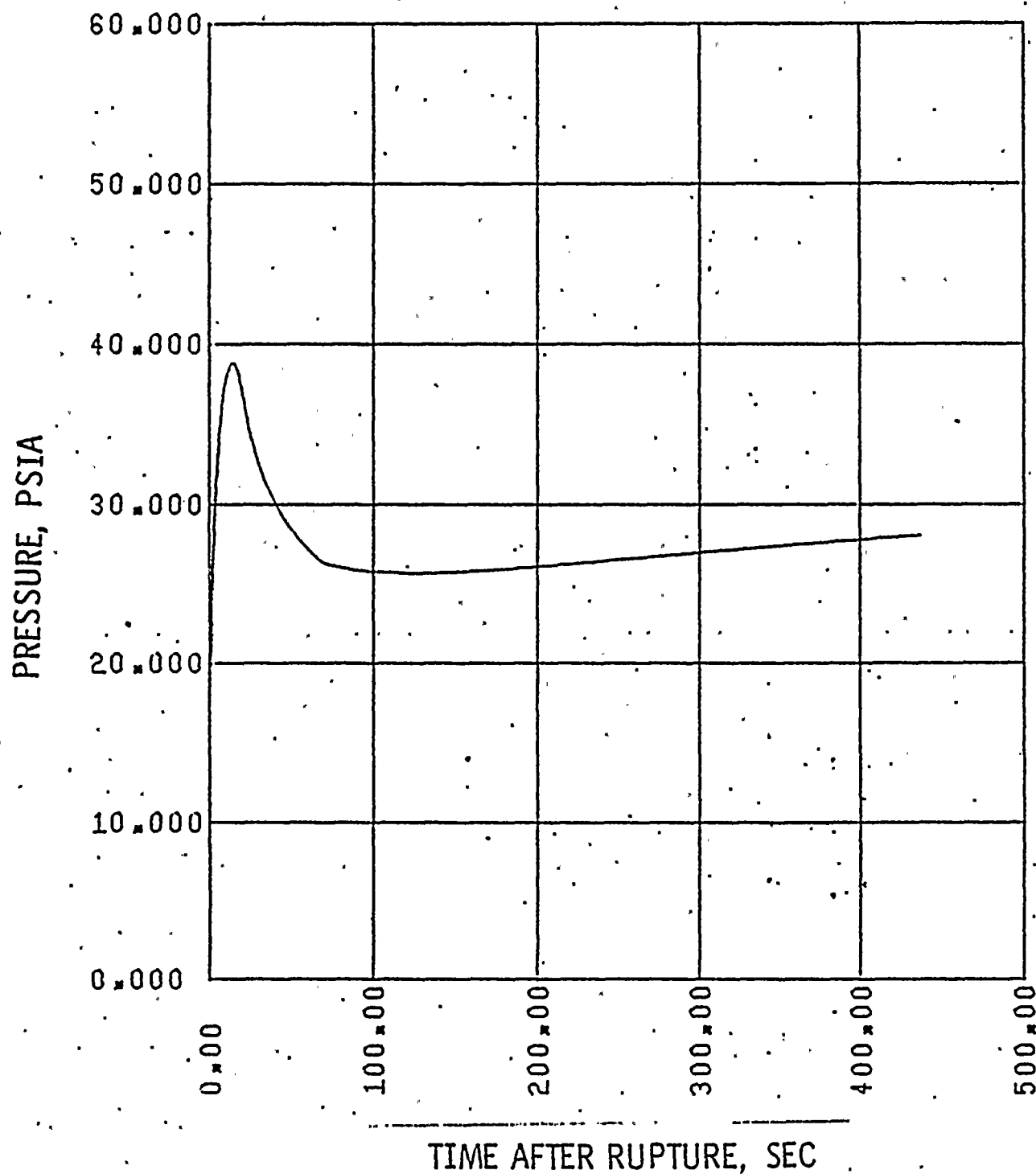
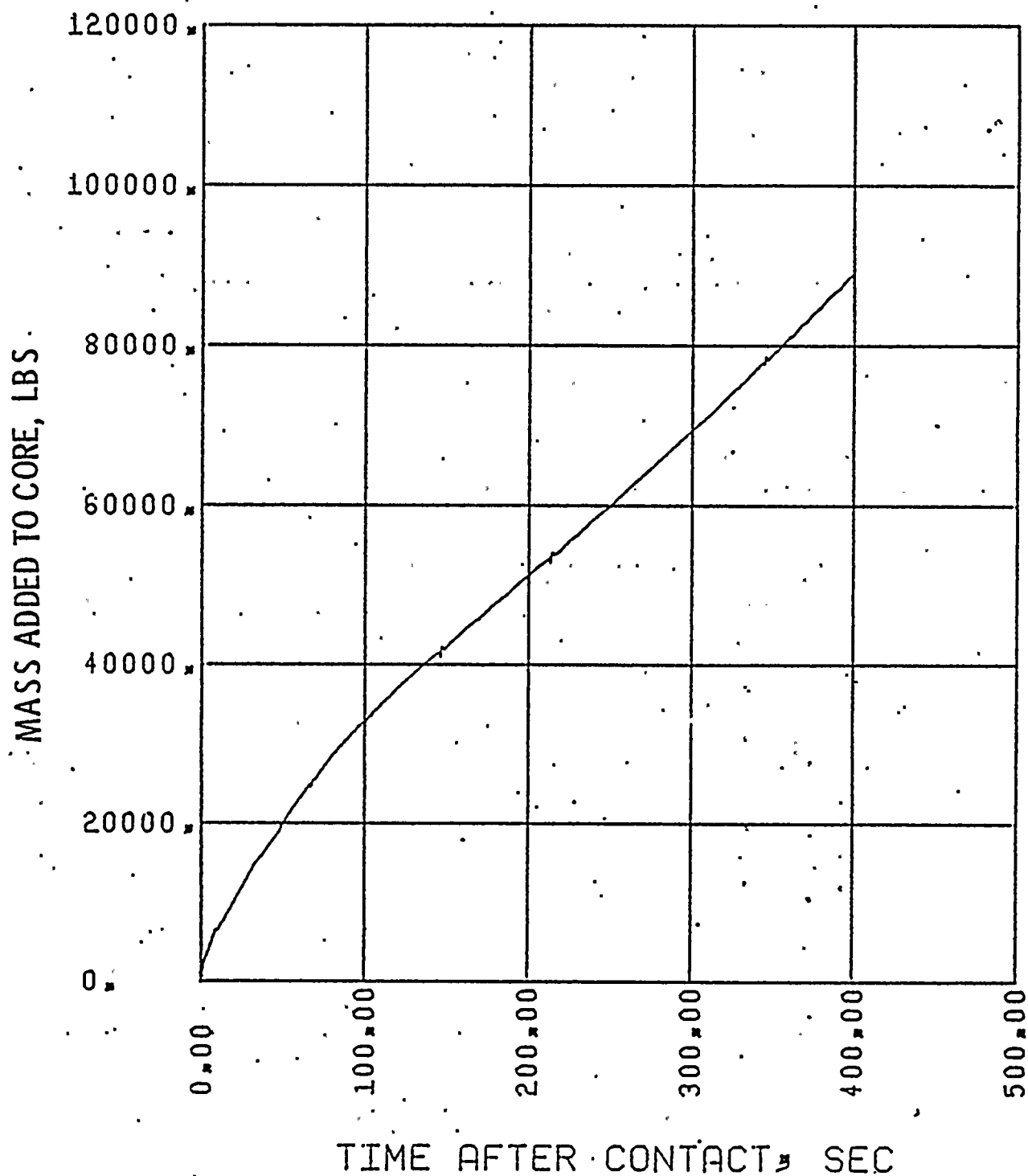


FIGURE II.1-G
ST. LUCIE UNIT I
1.0 x DOUBLE ENDED SLOT BREAK IN PUMP DISCHARGE LEG
MASS ADDED TO CORE DURING REFLOOD



ST. LUCIE UNIT I
1.0 x DOUBLE ENDED SLOT BREAK IN PUMP DISCHARGE LEG
PEAK CLAD TEMPERATURE

CLAD TEMPERATURE, °F

2200

2000

1800

1600

1400

1200

1000

800

600

400

0

100

200

300

400

500

600

700

TIME, SECONDS

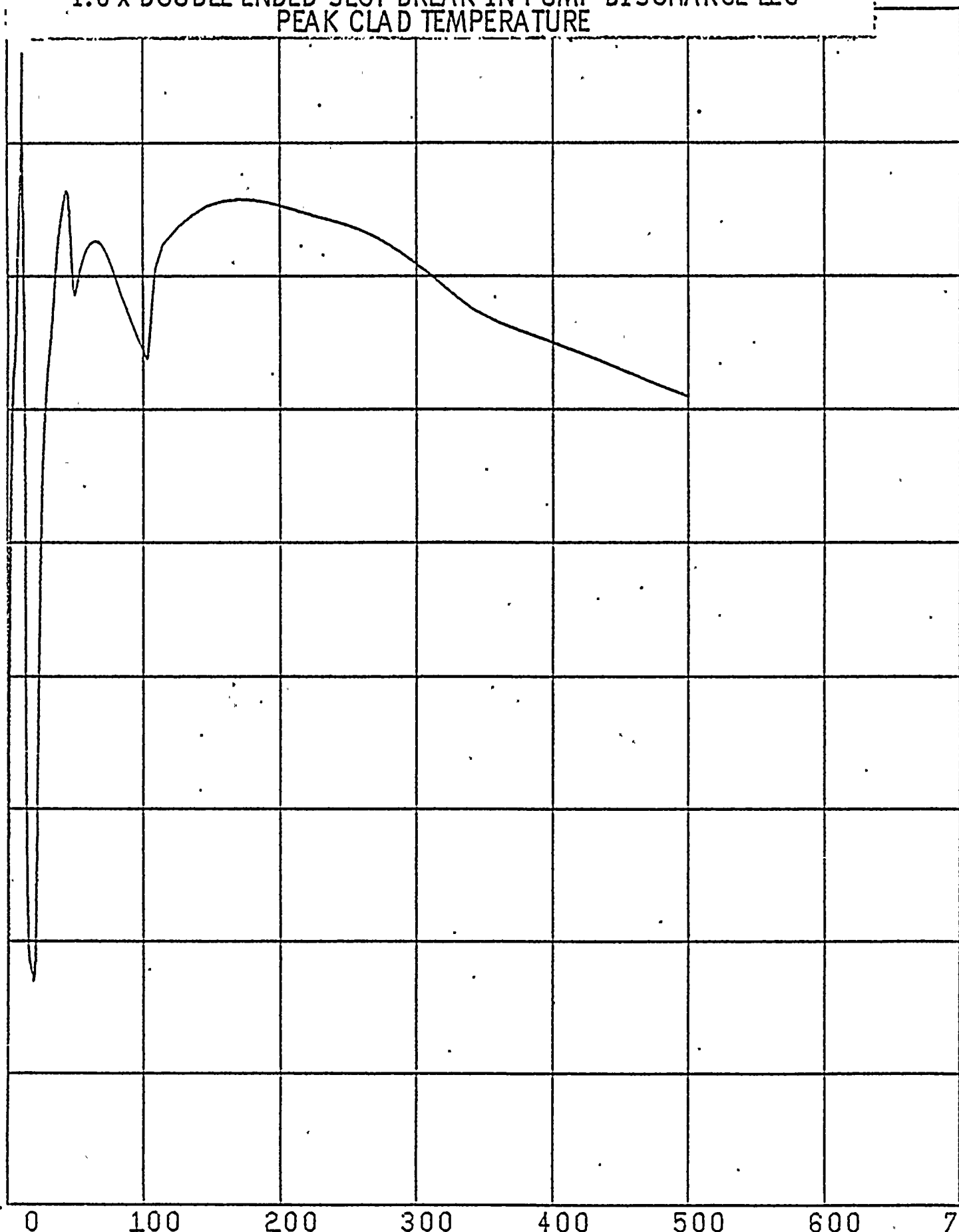
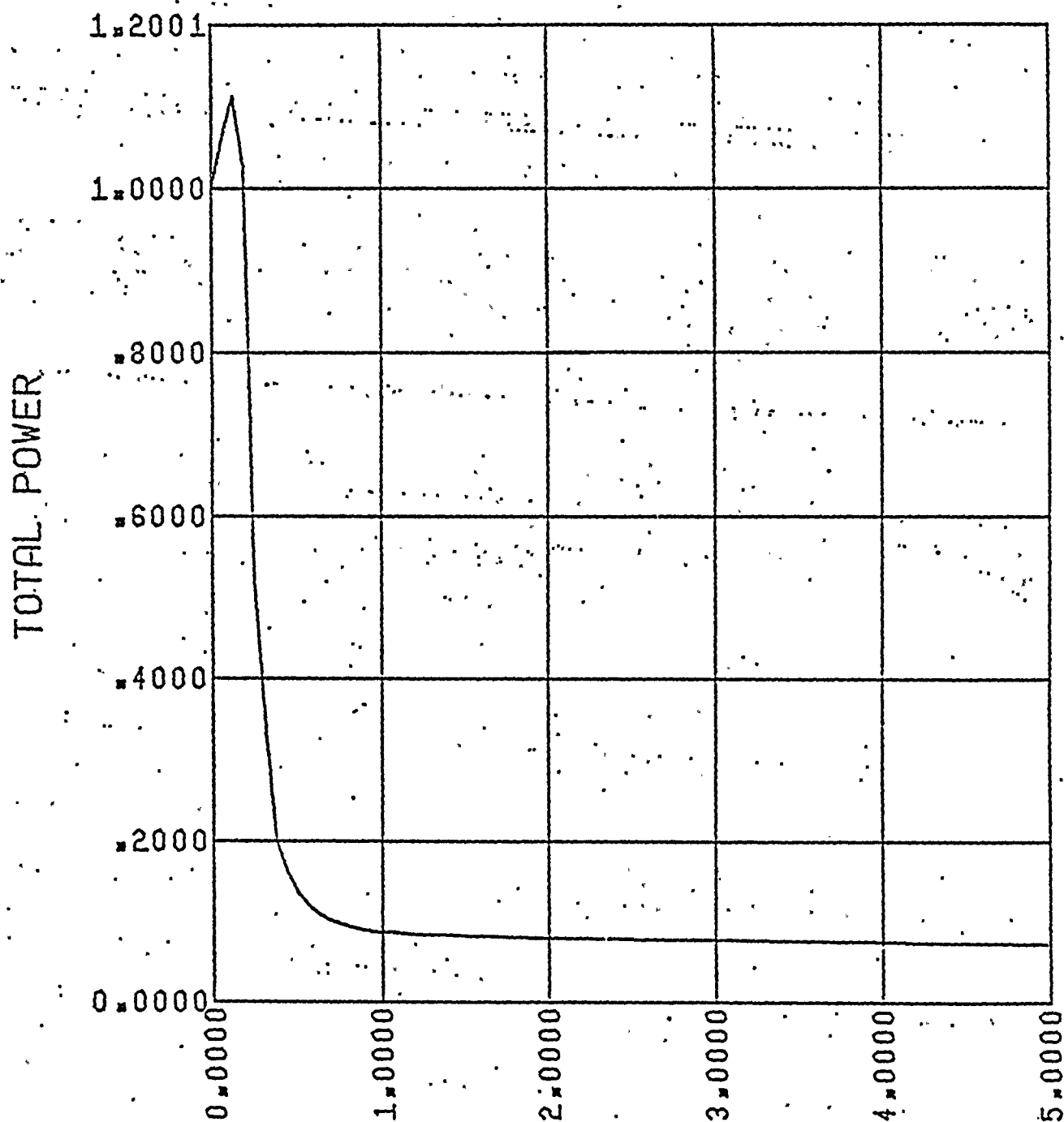


Figure II.2-A
2560 MWt PLANTS
0.8 x DOUBLE-ENDED SLOT BREAK IN PUMP DISCHARGE LEG
CORE POWER



TIME IN SEC



Figure II.2-B

2560 MWt PLANTS
0.8 x DOUBLE ENDED SLOT BREAK IN PUMP DISCHARGE LEG.
PRESSURE IN CENTER HOT ASSEMBLY NODE

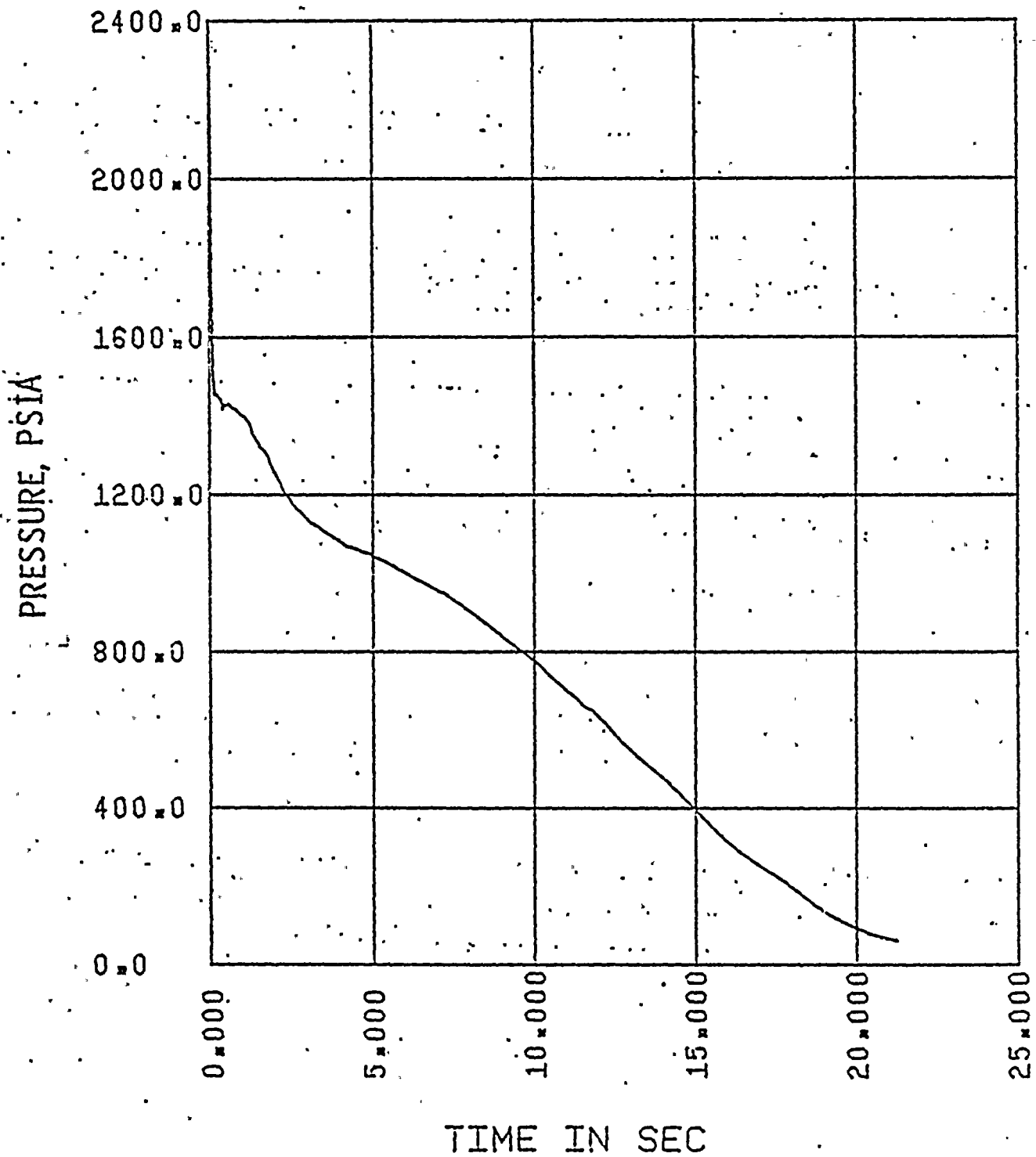




Figure II.2-C

2560 MWt PLANTS.

0.8 x DOUBLE ENDED SLOT BREAK IN PUMP DISCHARGE LEG
LEAK FLOW

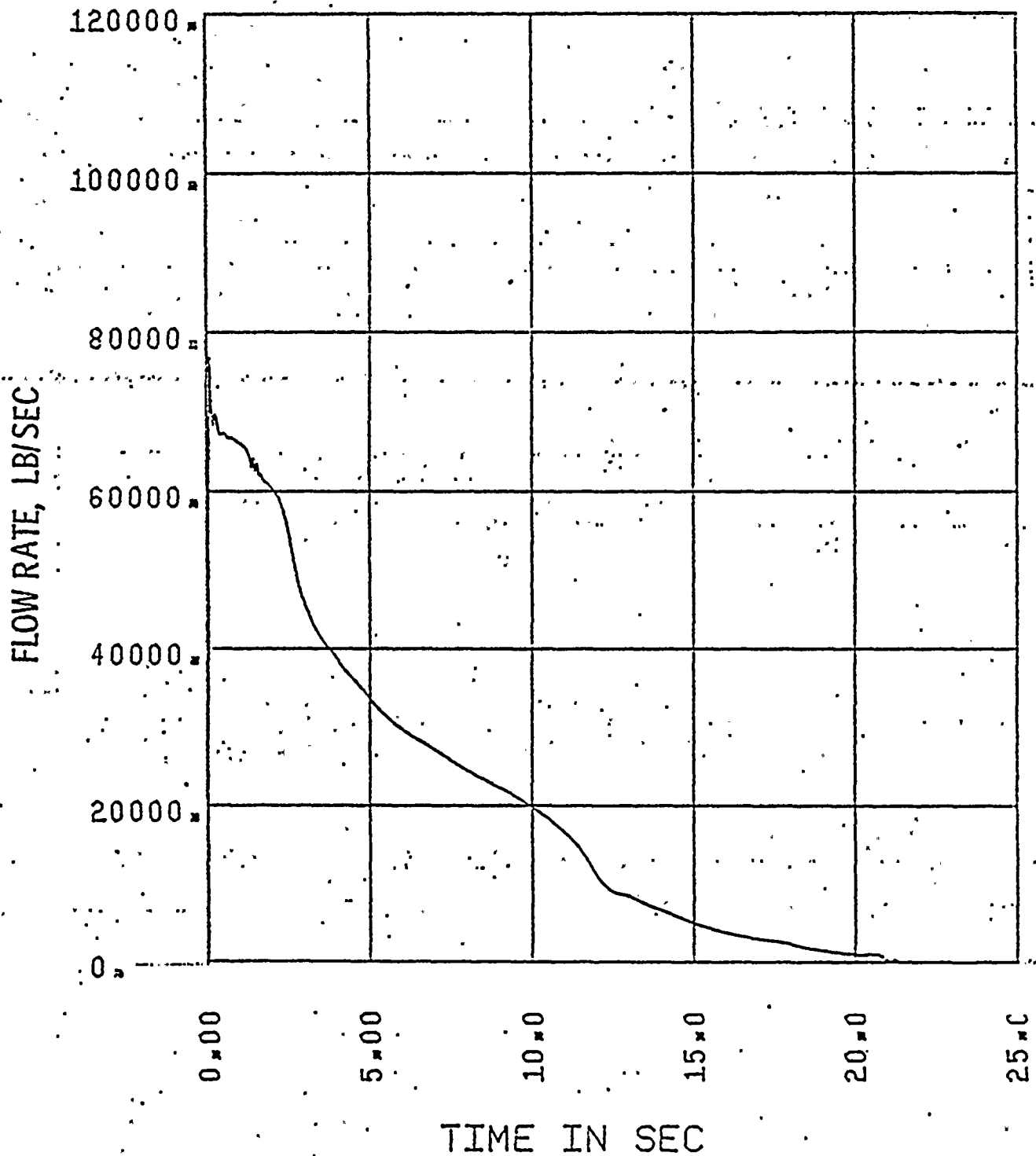




Figure II.2-D.1

2560 MWt PLANTS
0.8 x DOUBLE ENDED SLOT BREAK IN PUMP DISCHARGE LEG
FLOW IN HOT ASSEMBLY - PATH 16, BELOW HOT SPOT

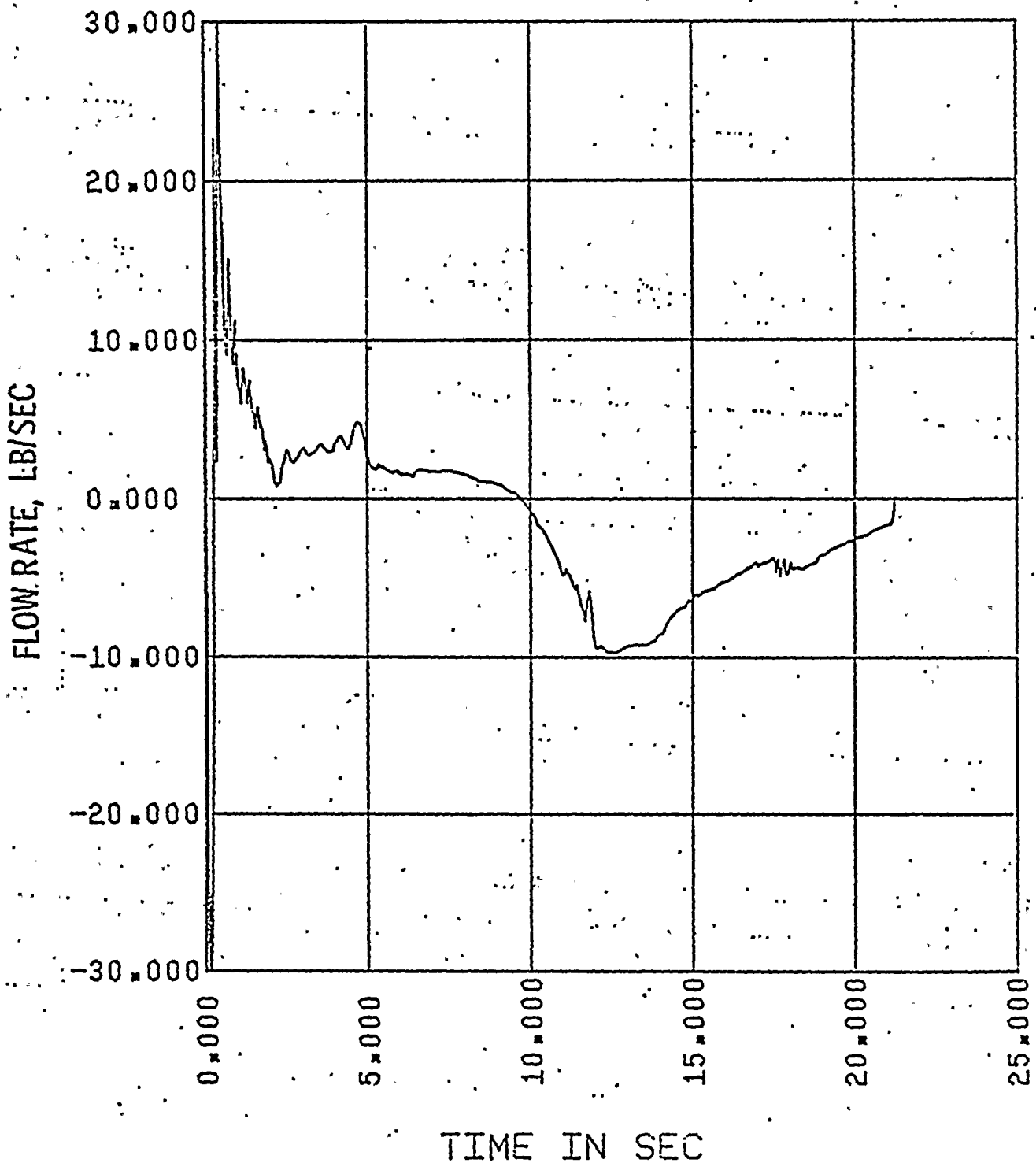


Figure II.2-D.2

2560 MWt PLANTS

0.8x DOUBLE ENDED SLOT BREAK IN PUMP DISCHARGE LEG
FLOW IN HOT ASSEMBLY - PATH 17, ABOVE HOT SPOT

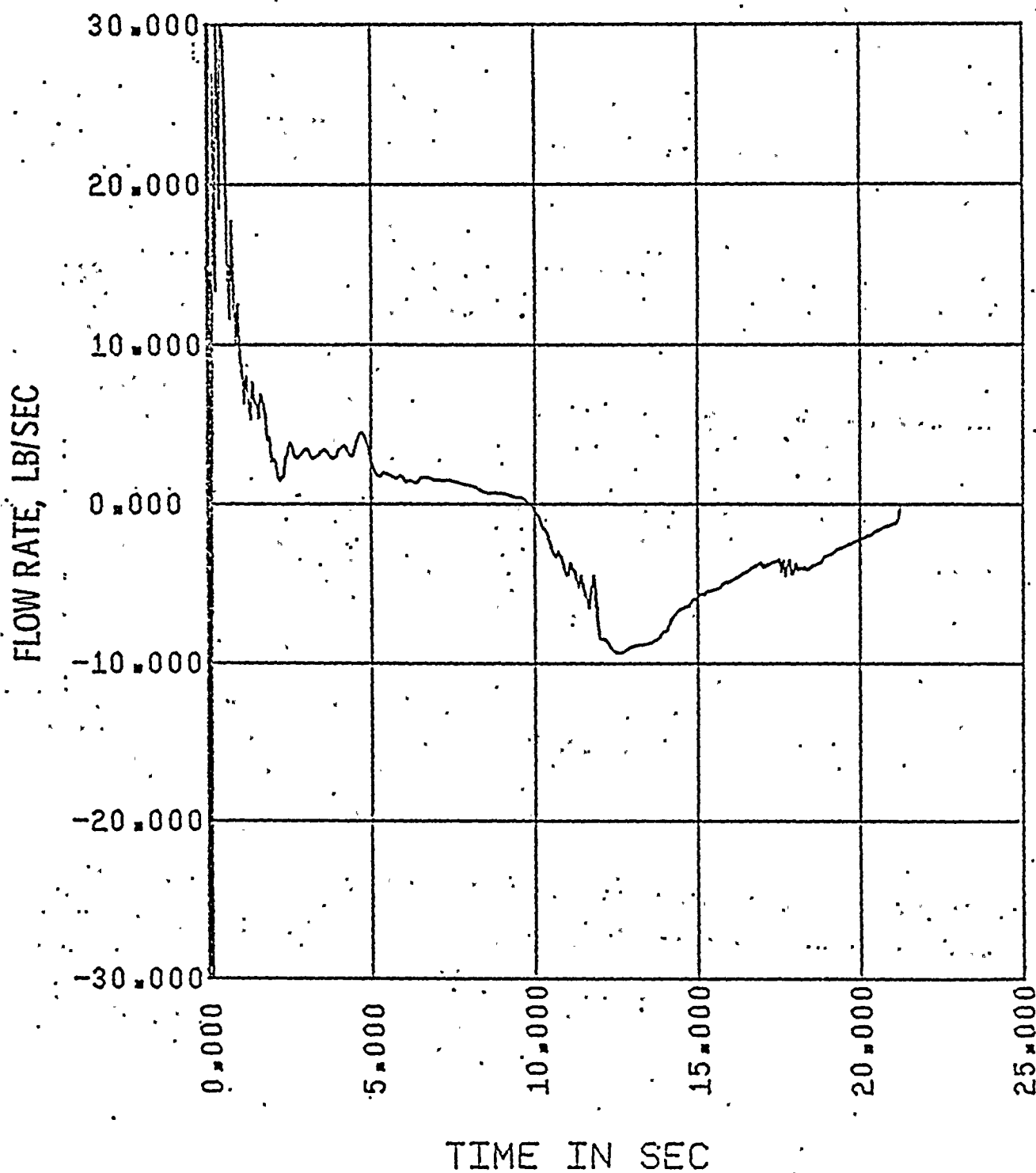




Figure II.2-E
2560 MWt PLANTS
0.8 x DOUBLE ENDED SLOT BREAK IN PUMP DISCHARGE LEG
HOT ASSEMBLY QUALITY

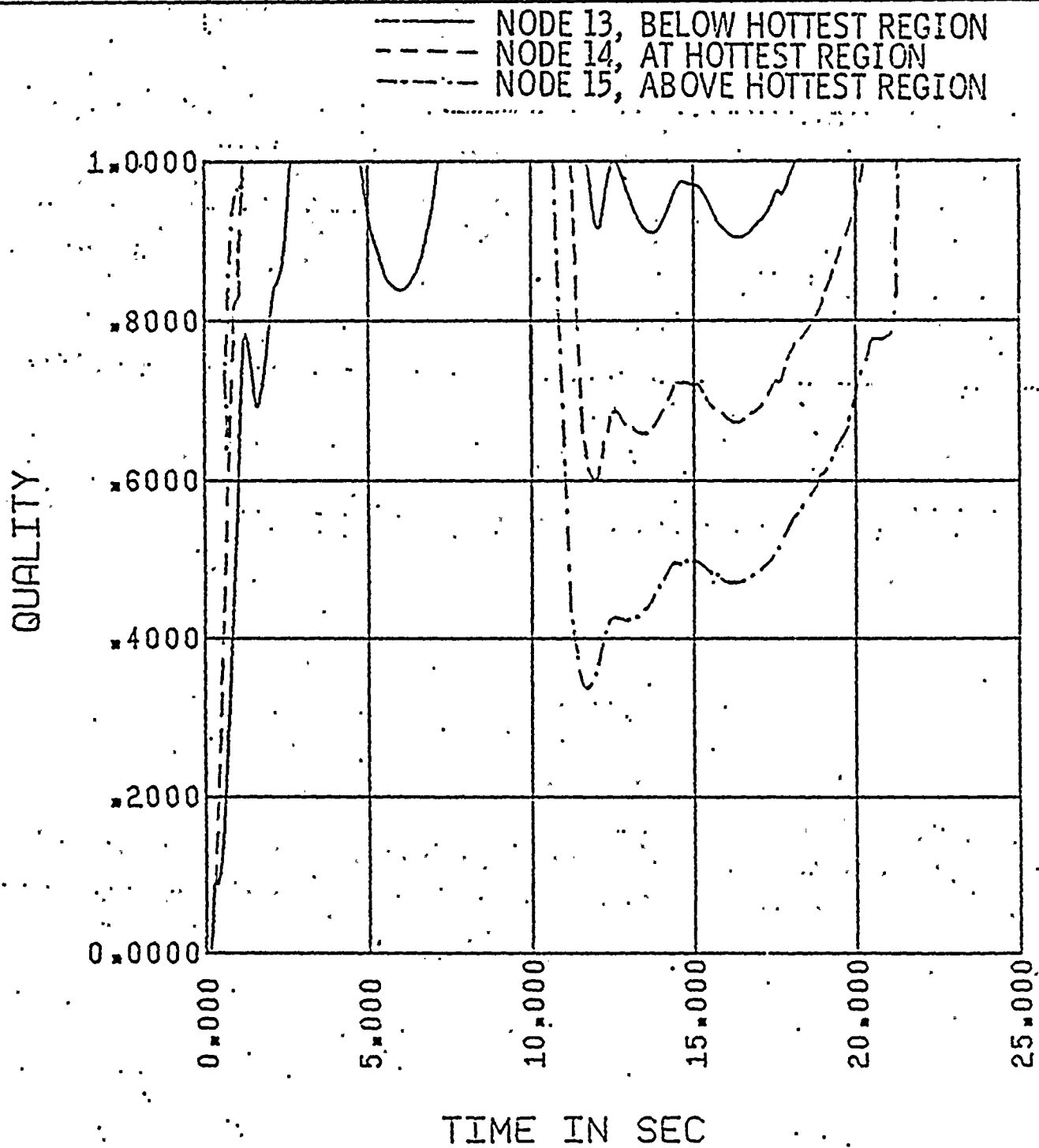




FIGURE II.2-F
ST. LUCIE UNIT I
0.8 x DOUBLE ENDED SLOT BREAK IN PUMP DISCHARGE LEG
CONTAINMENT PRESSURE

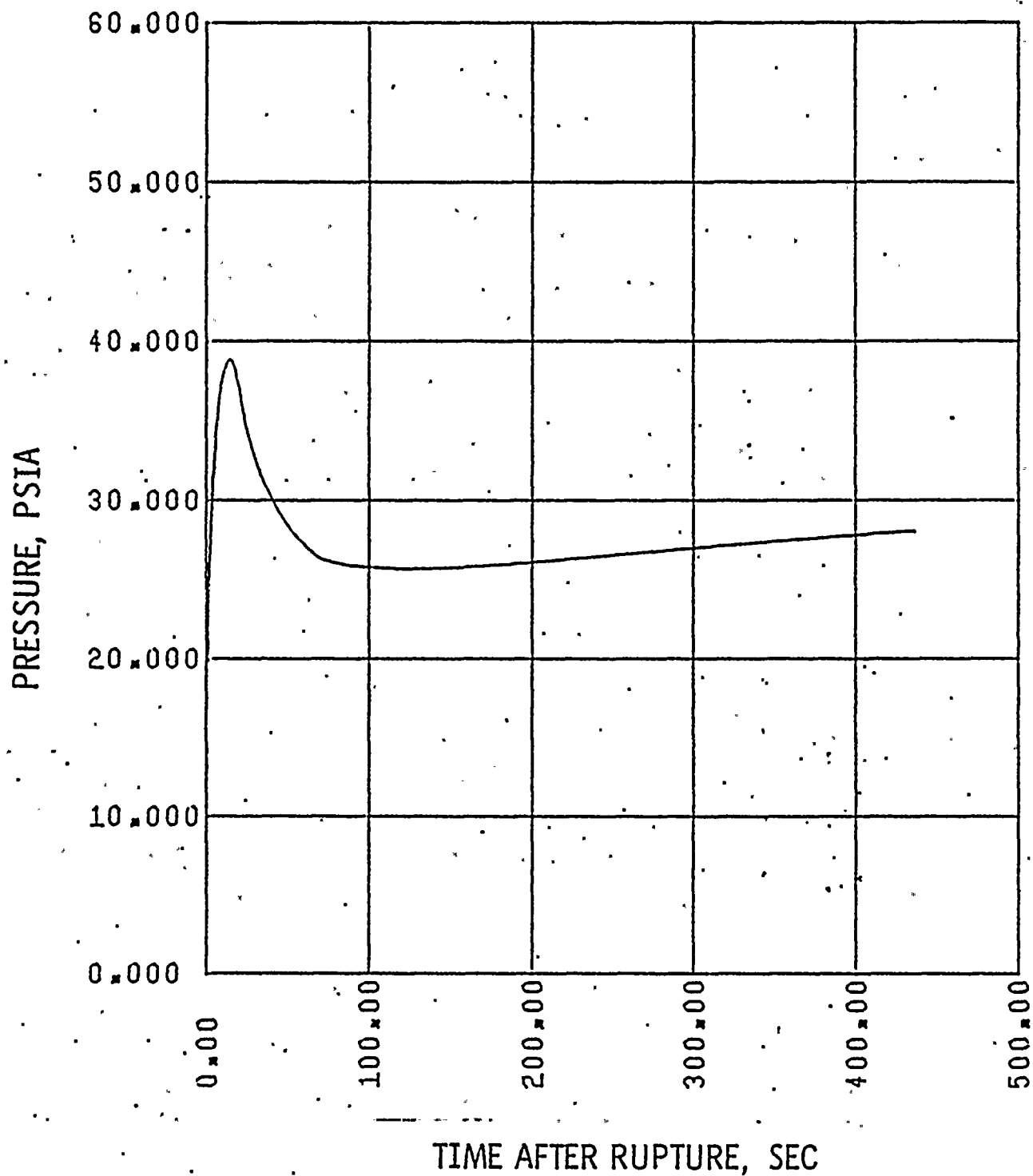
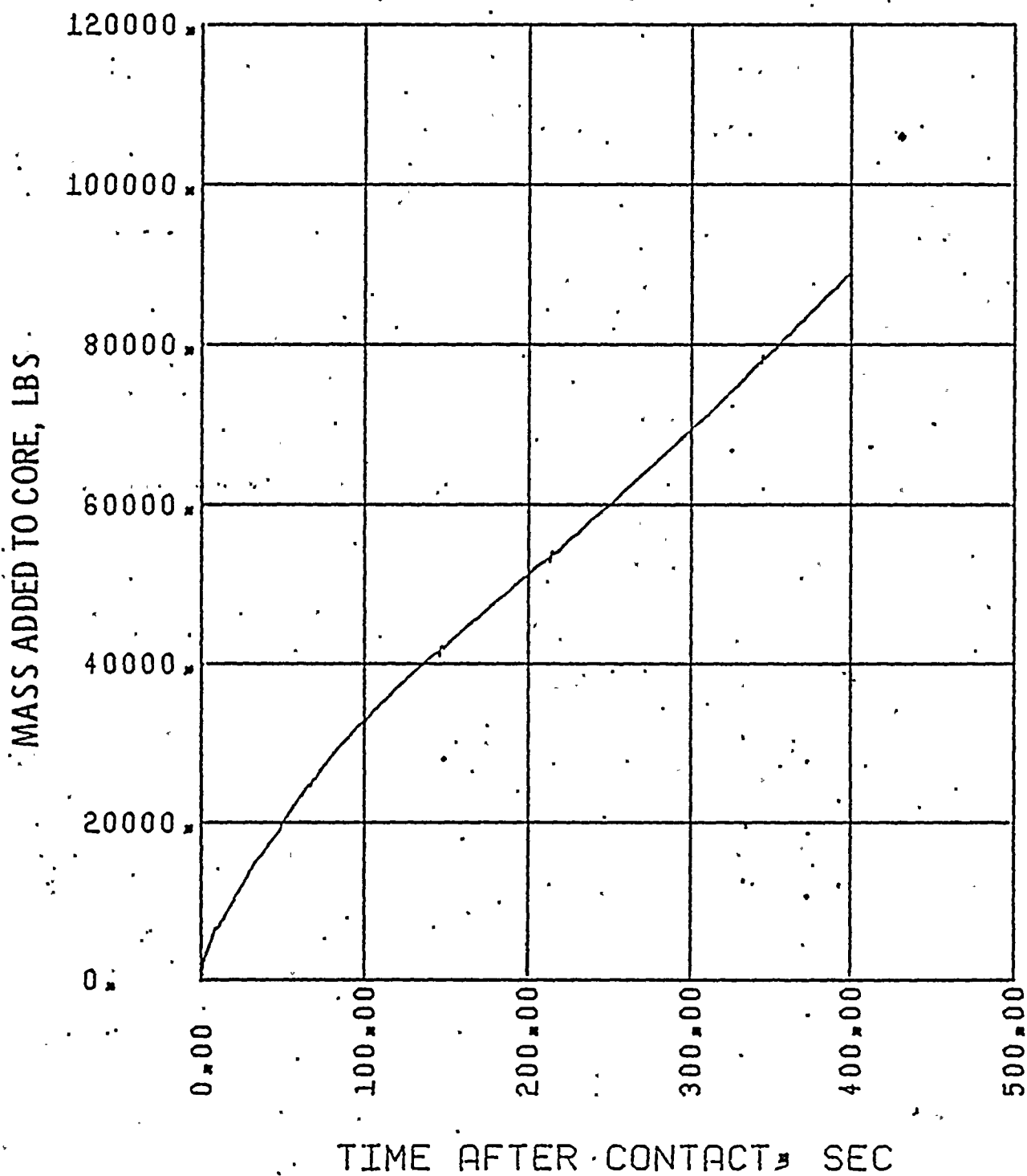


FIGURE II.2-G
ST. LUCIE UNIT I
0.8 x DOUBLE ENDED SLOT BREAK IN PUMP DISCHARGE LEG
MASS ADDED TO CORE DURING REFLOOD





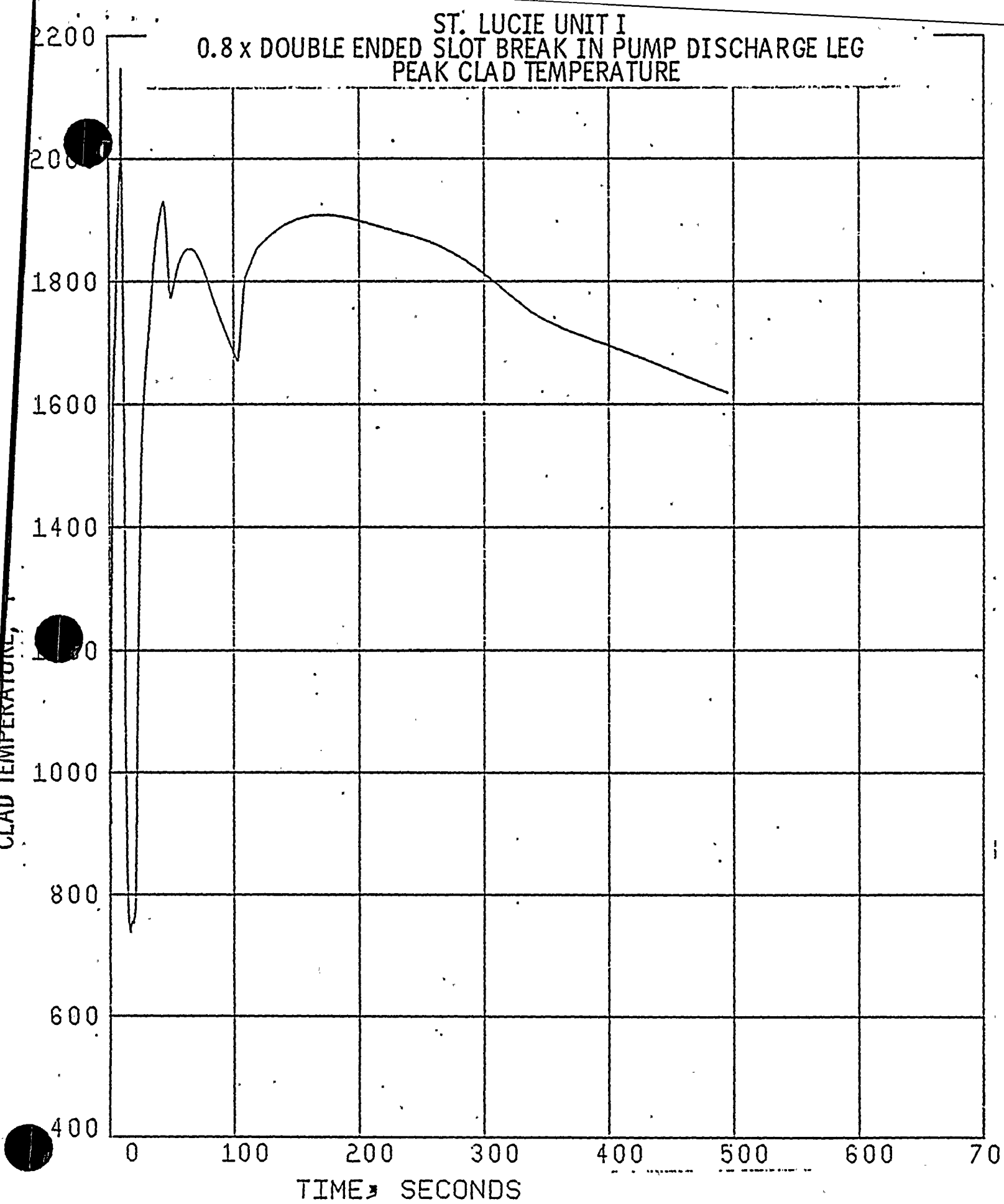


Figure II.3-A
2560 MW_t PLANTS
0.6 x DOUBLE ENDED SLOT BREAK IN PUMP DISCHARGE LEG
CORE POWER

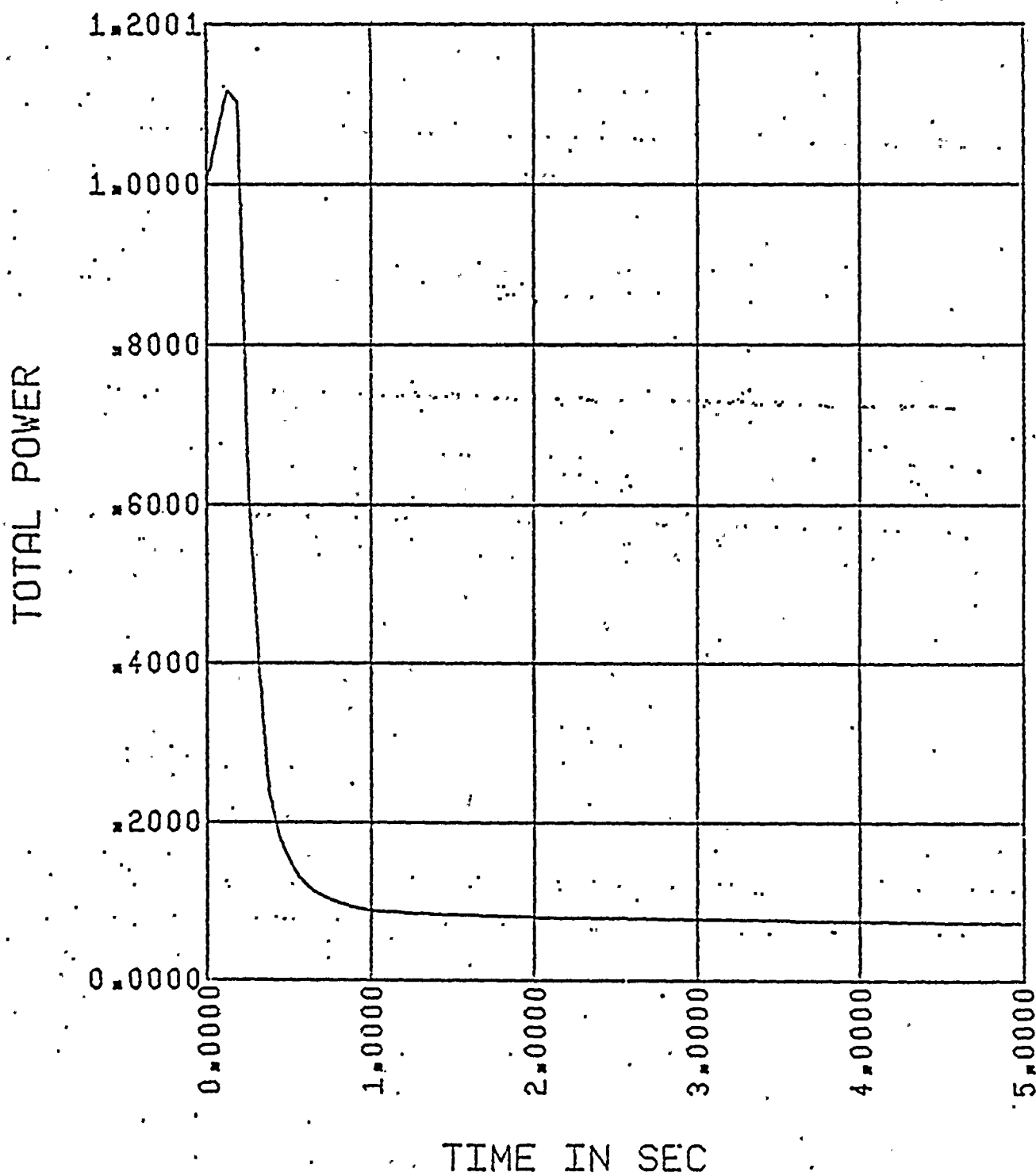


Figure II.3-B
2560 MWt PLANTS
0.6 x DOUBLE ENDED SLOT BREAK IN PUMP DISCHARGE LEG
PRESSURE IN CENTER HOT ASSEMBLY NODE

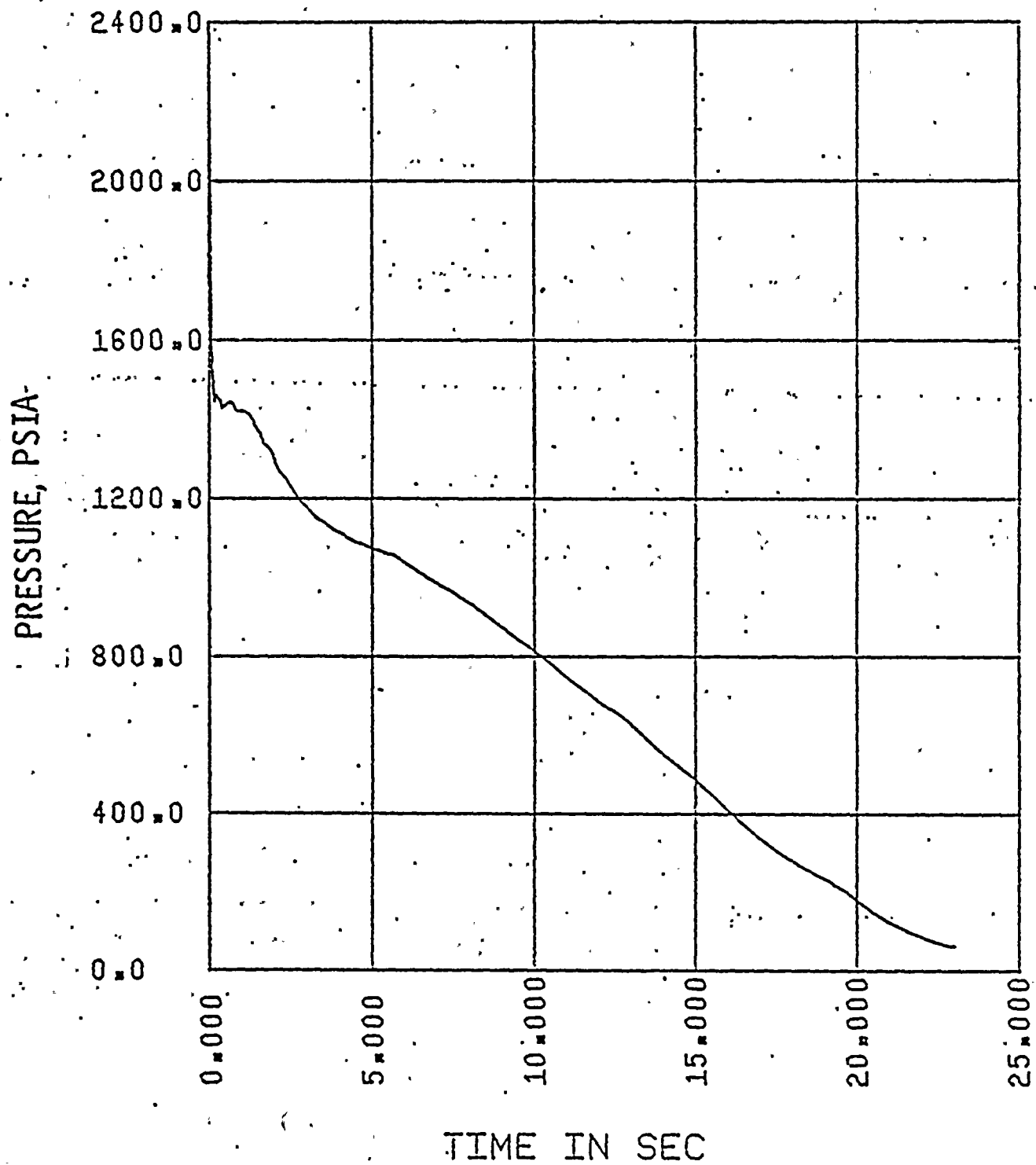




Figure II.3-C

2560 MWt PLANTS

0.6 x DOUBLE ENDED SLOT BREAK IN PUMP DISCHARGE LEG
LEAK FLOW

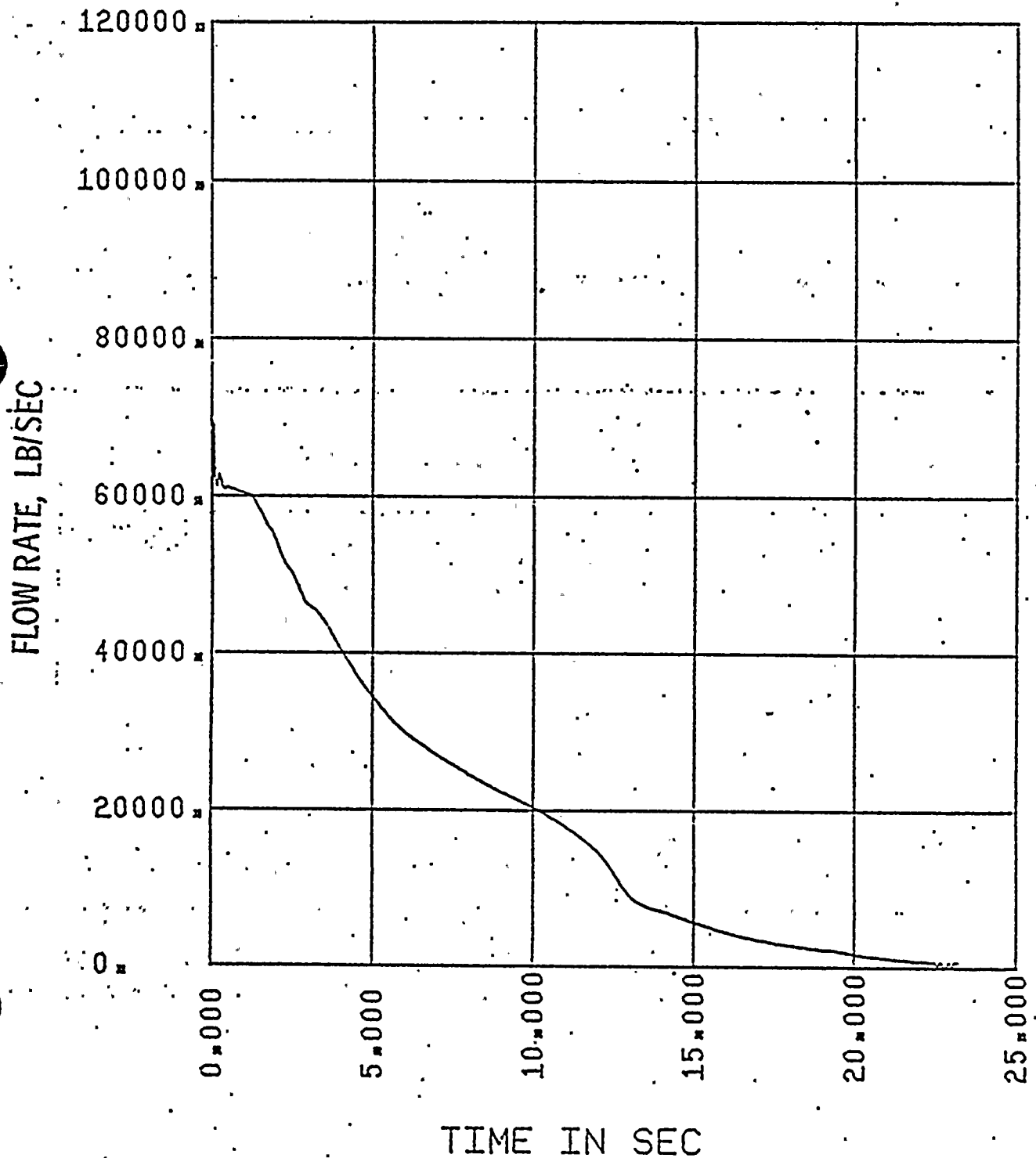
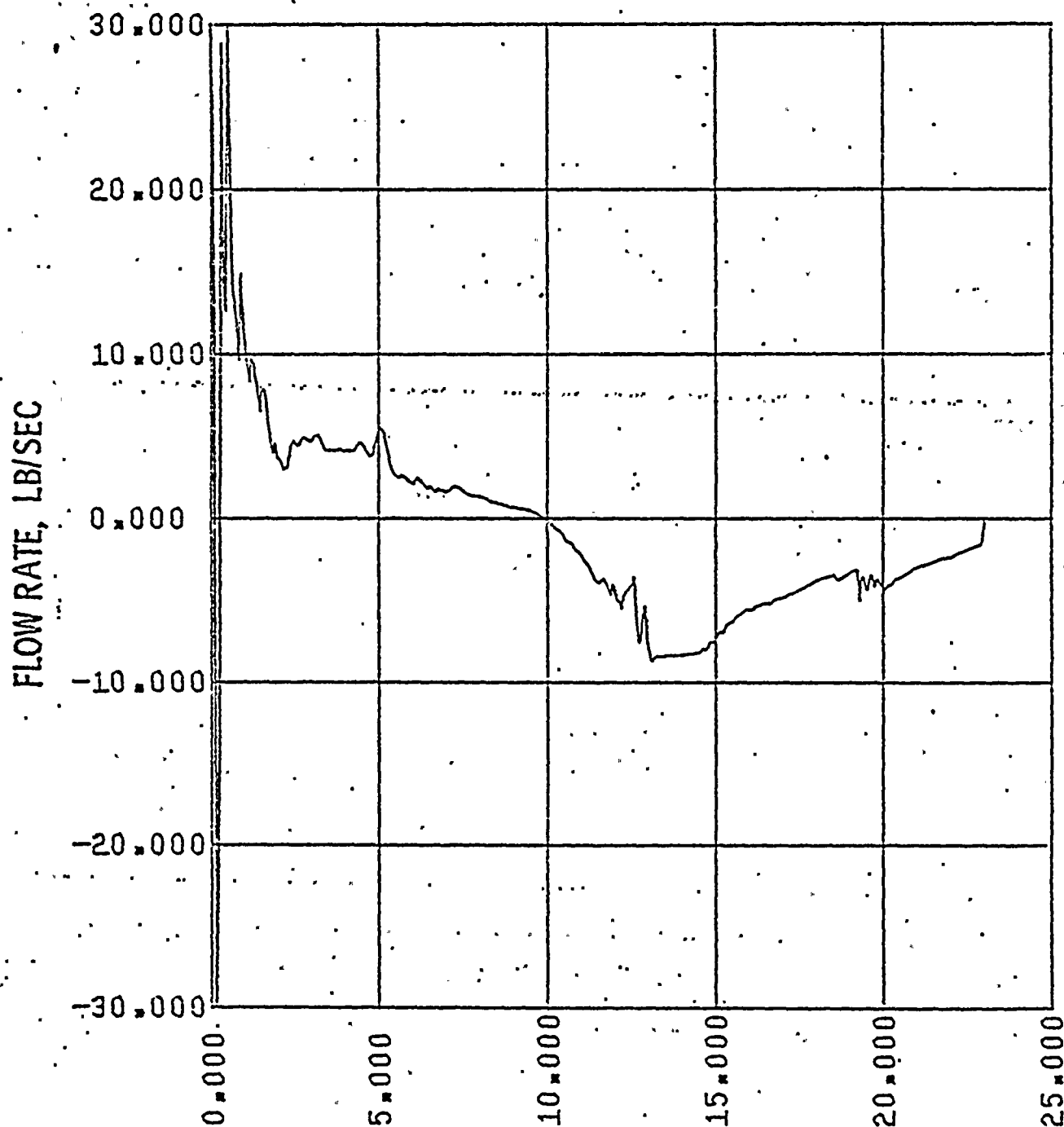


Figure II.3-D.1.

2560 MWt PLANTS

0.6 x DOUBLE ENDED SLOT BREAK IN PUMP DISCHARGE LEG
FLOW IN HOT ASSEMBLY - PATH 16, BELOW HOT SPOT



TIME IN SEC

Figure II.3-D.2

2560 MWt PLANTS

0.6 x DOUBLE ENDED SLOT BREAK IN PUMP DISCHARGE LEG
FLOW IN HOT ASSEMBLY - PATH 17, ABOVE HOT SPOT

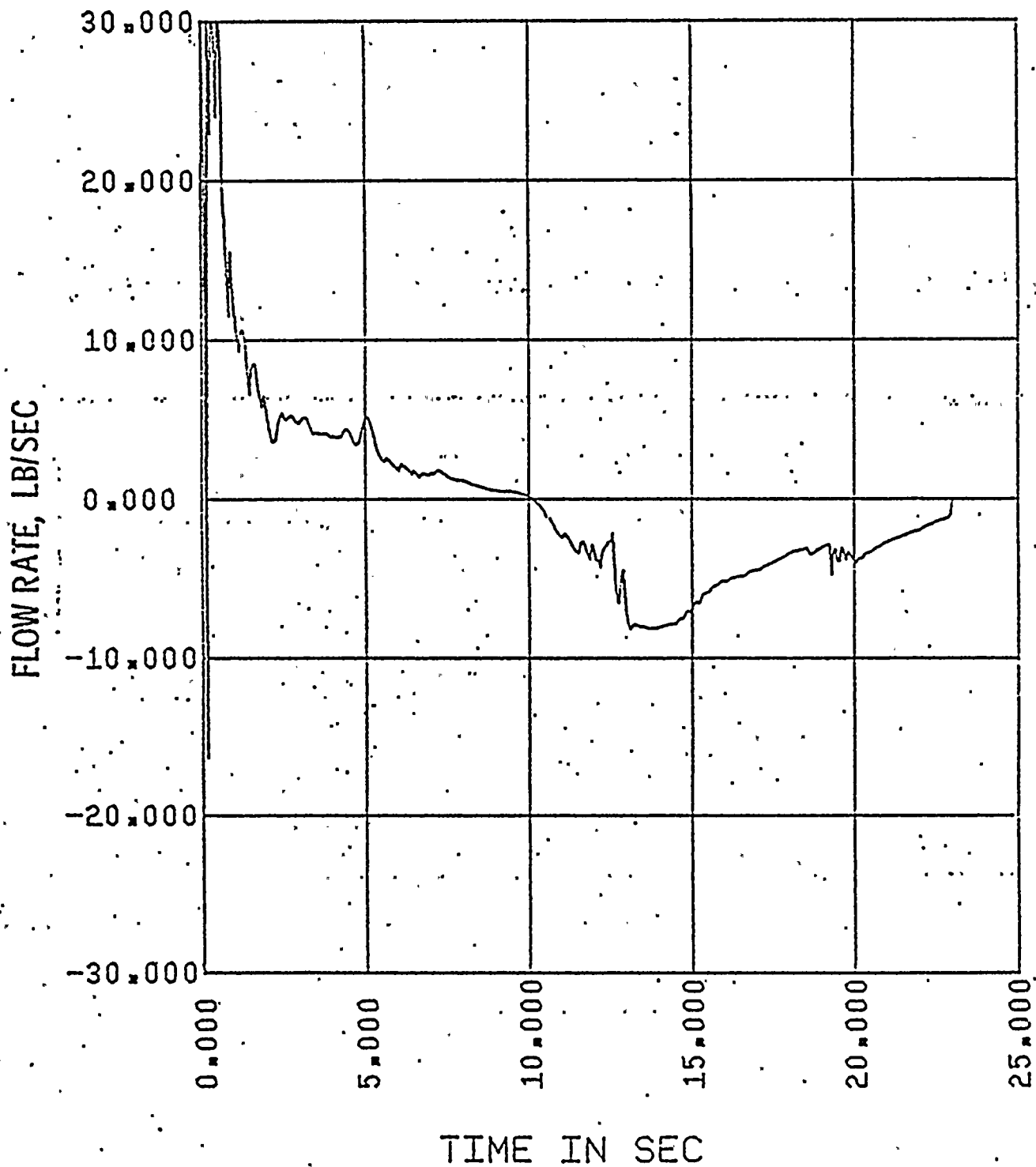




Figure II.3-E

2560 MWt PLANTS
0.6 x DOUBLE ENDED SLOT BREAK IN PUMP DISCHARGE LEG
HOT ASSEMBLY QUALITY

— NODE 13, BELOW HOTTEST REGION
- - - NODE 14, AT HOTTEST REGION
- · - · - NODE 15, ABOVE HOTTEST REGION

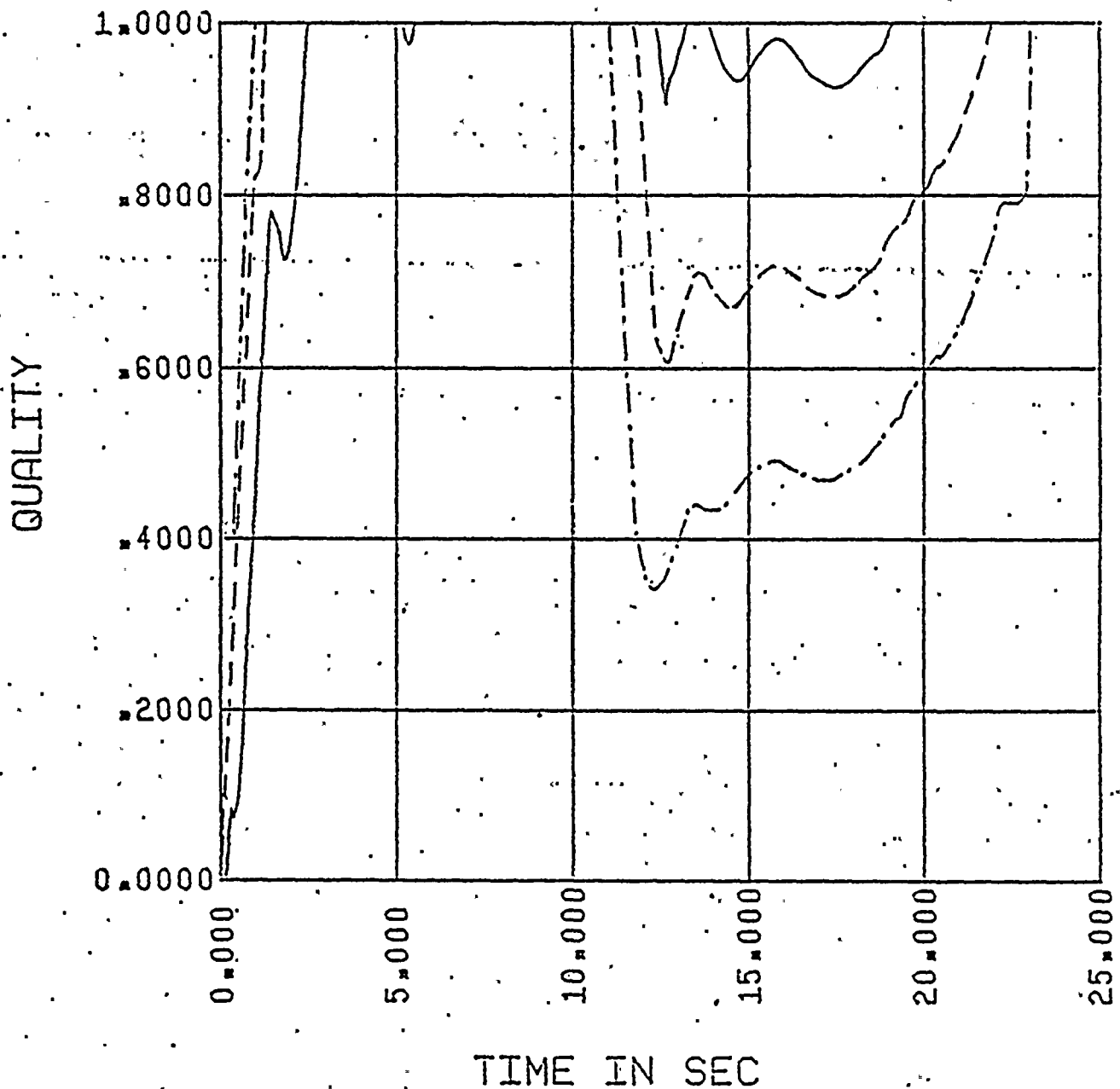




FIGURE II.3-F
ST. LUCIE UNIT I
0.6 x DOUBLE ENDED SLOT BREAK IN PUMP DISCHARGE LEG
CONTAINMENT PRESSURE

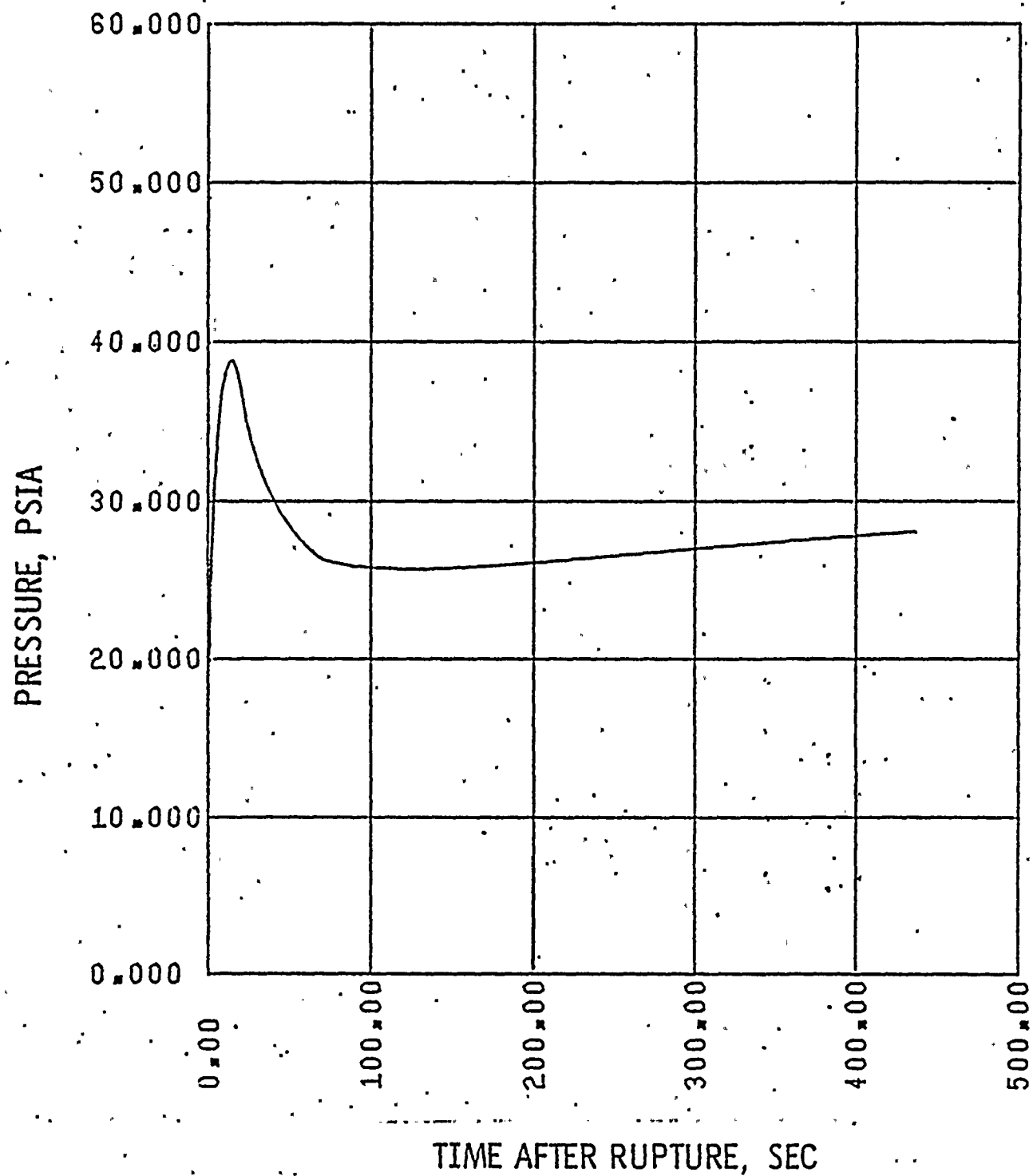


FIGURE II.3-G

ST. LUCIE UNIT I

0.6 x DOUBLE ENDED SLOT BREAK IN PUMP DISCHARGE LEG
MASS ADDED TO CORE DURING REFLOOD

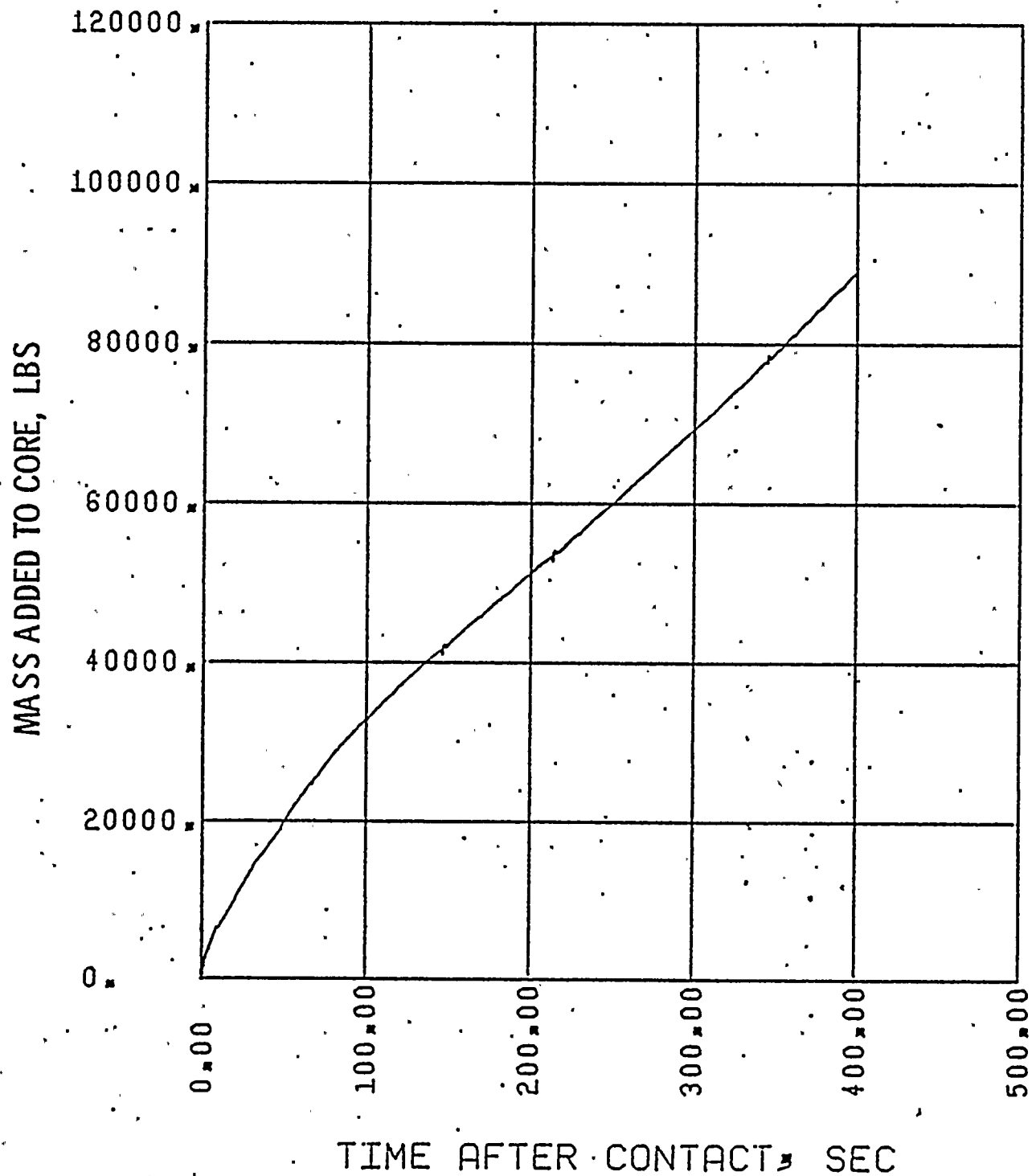




FIGURE II.3-H

ST. LUCIE UNIT I
0.6 x DOUBLE ENDED SLOT BREAK IN PUMP DISCHARGE LEG
PEAK CLAD TEMPERATURE

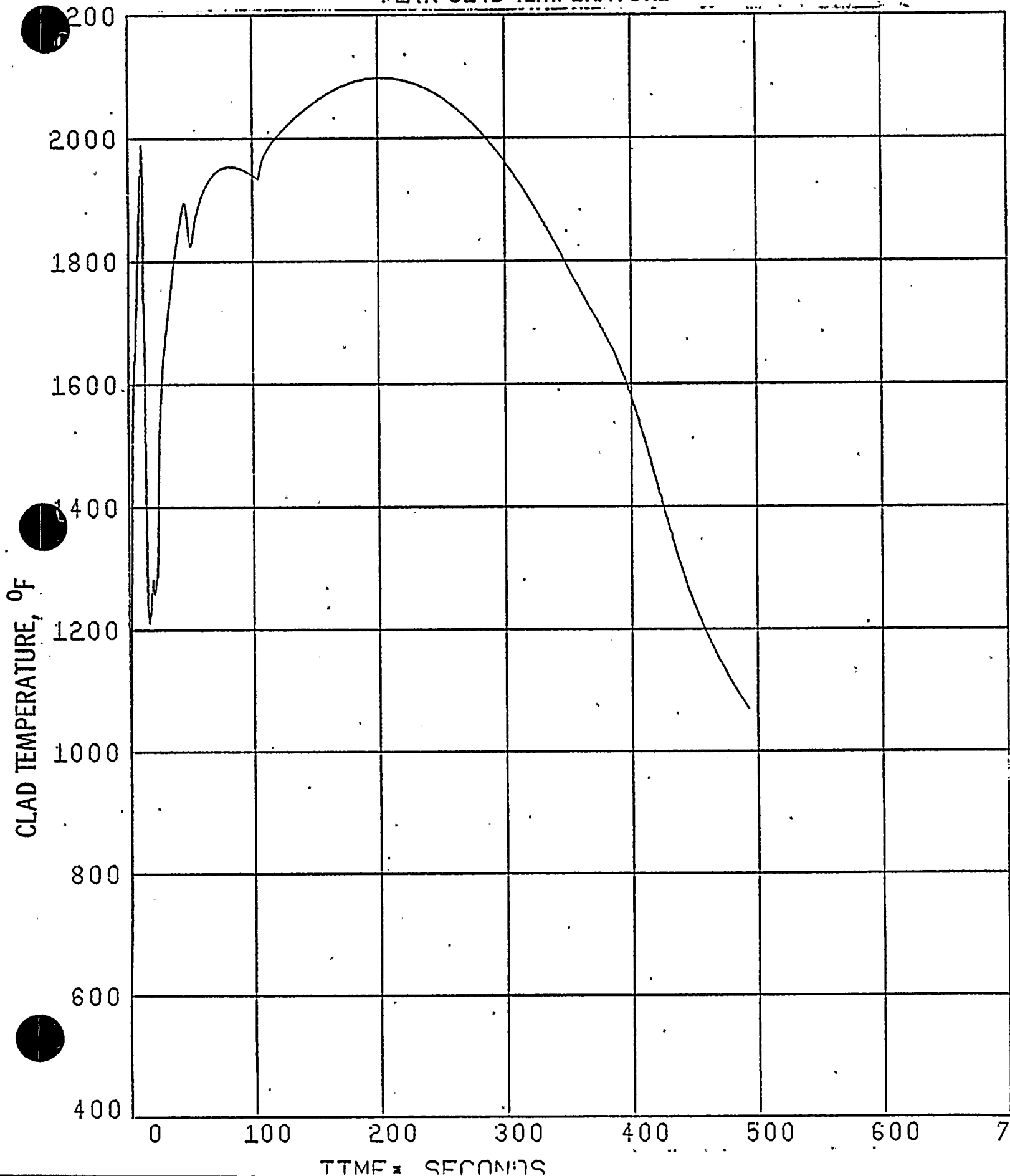




Figure II.4-A
2560 MWt PLANTS
0.5 FT² SLOT BREAK IN PUMP DISCHARGE LEG
CORE POWER

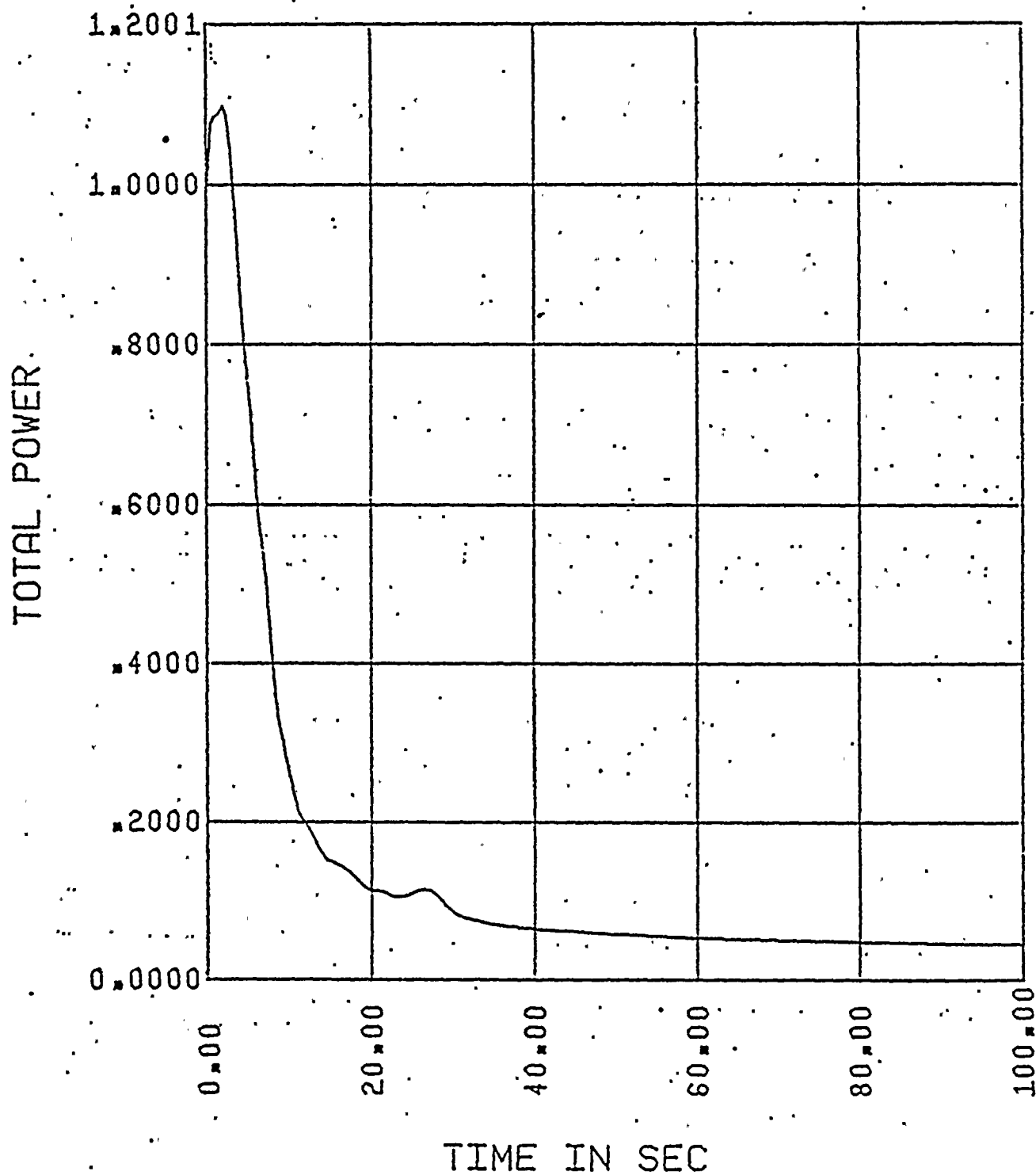




Figure II.4-B
2560 MWt PLANTS
0.5 FT² SLOT BREAK IN PUMP DISCHARGE LEG
PRESSURE IN CENTER HOT ASSEMBLY NODE

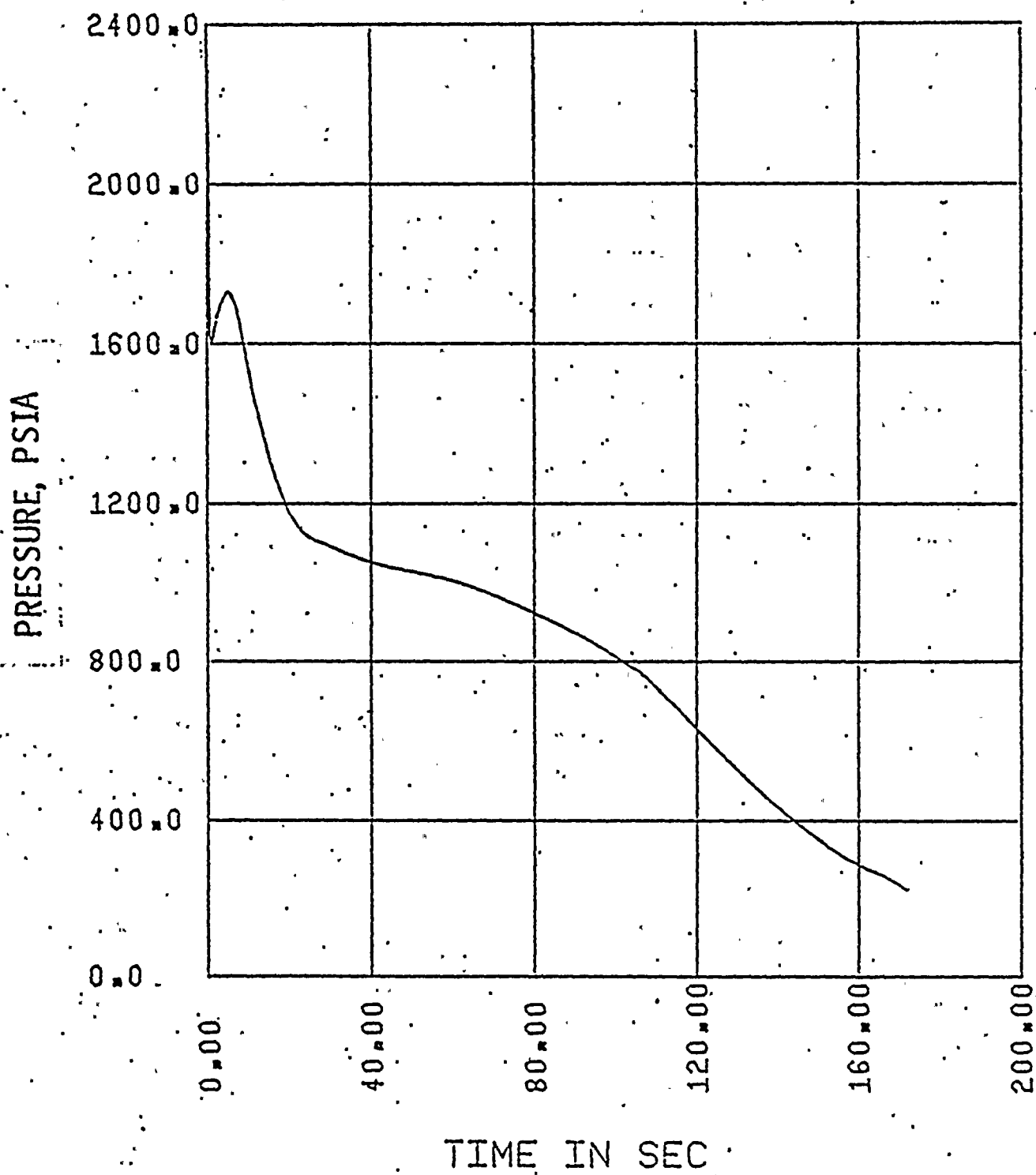


Figure II.4-C
2560 MWt PLANTS
0.5 FT² SLOT BREAK IN PUMP DISCHARGE LEG
LEAK FLOW

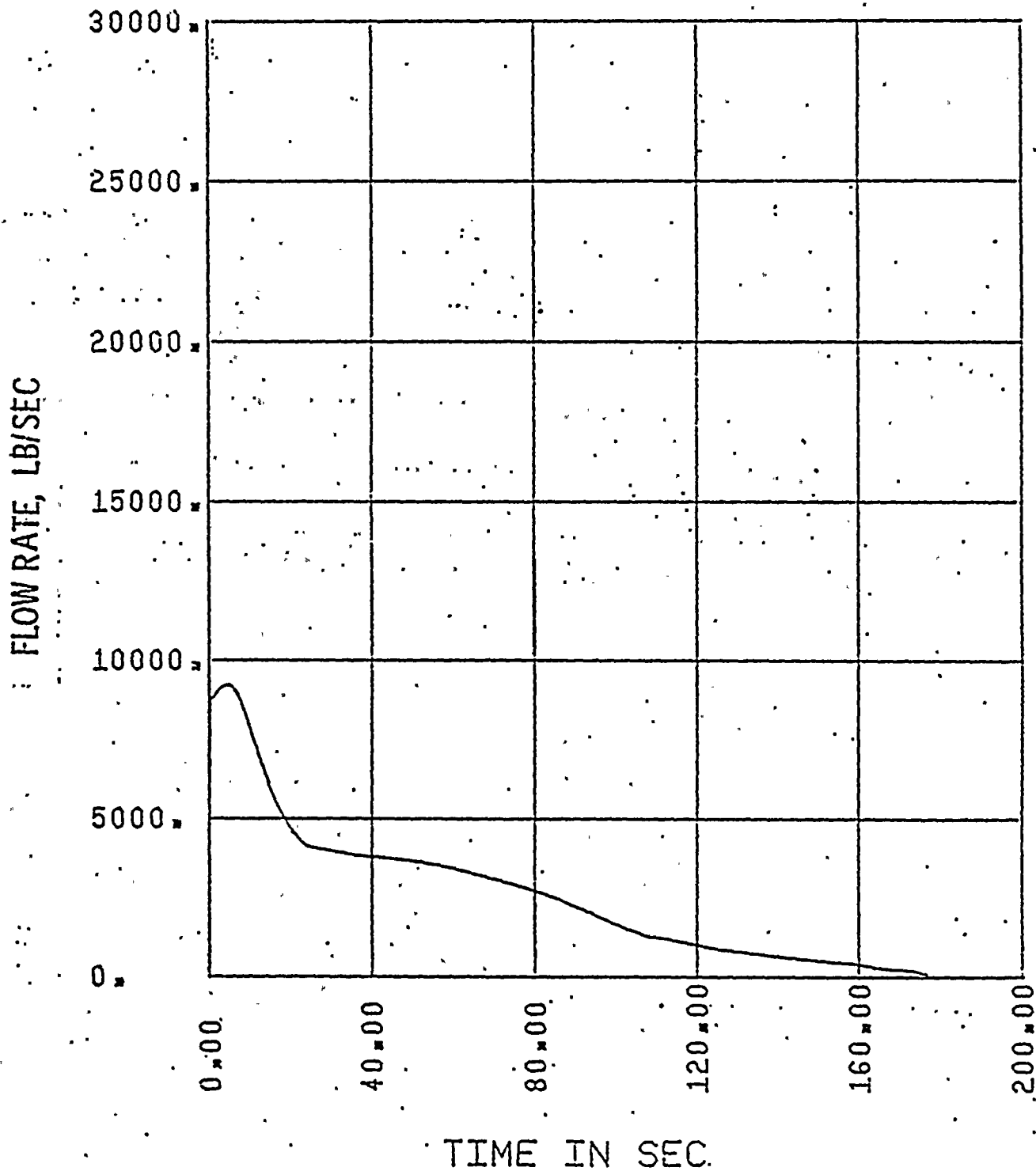
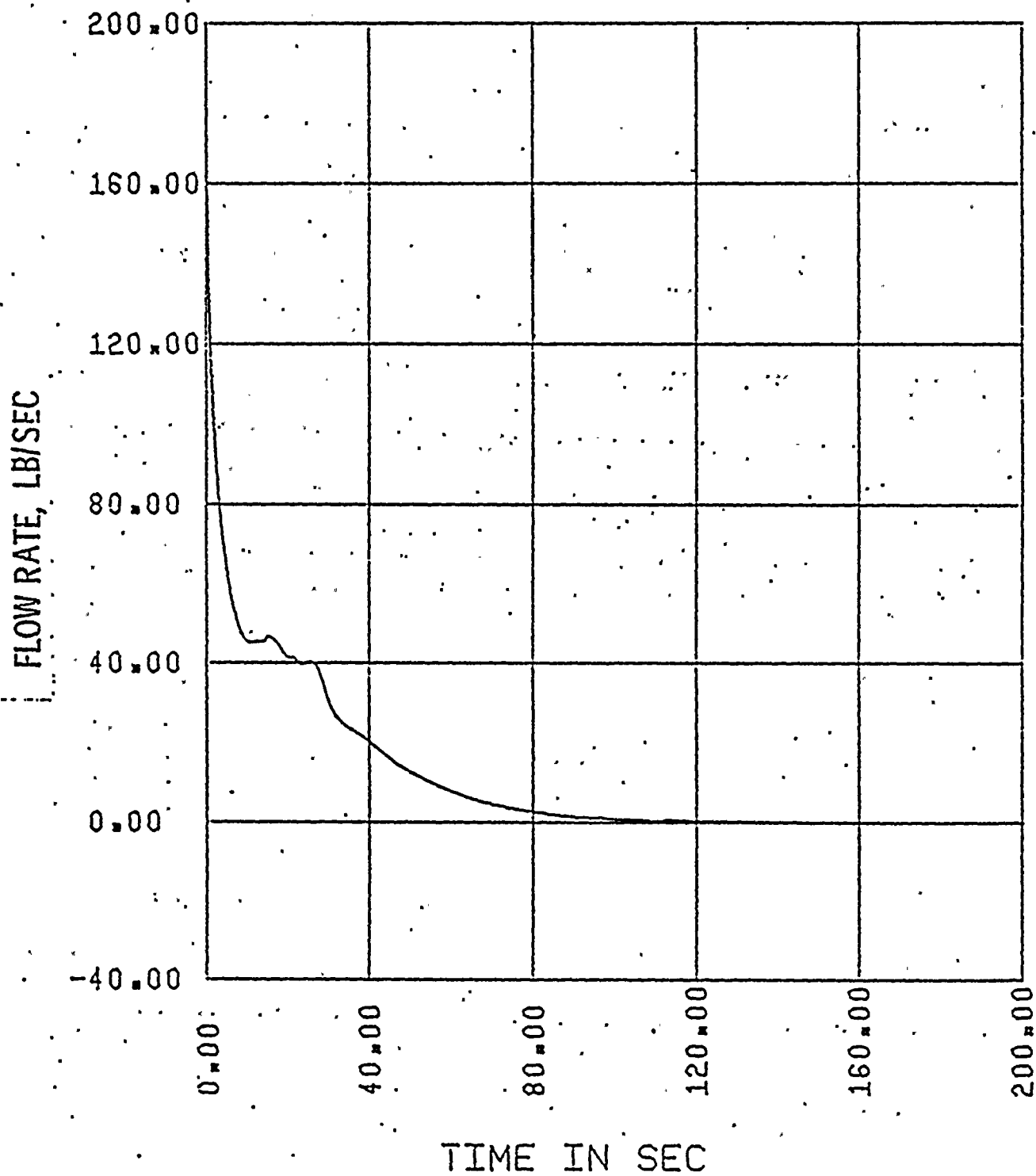




Figure II.4-D.1
2560 MWt PLANTS
0.5 FT² SLOT BREAK IN PUMP DISCHARGE LEG
FLOW IN HOT ASSEMBLY - PATH 16, BELOW HOT SPOT



)



Figure II.4-D.2

2560 MWt PLANTS
0.5 FT² SLOT BREAK IN PUMP DISCHARGE LEG
FLOW IN HOT ASSEMBLY - PATH 17, ABOVE HOT SPOT

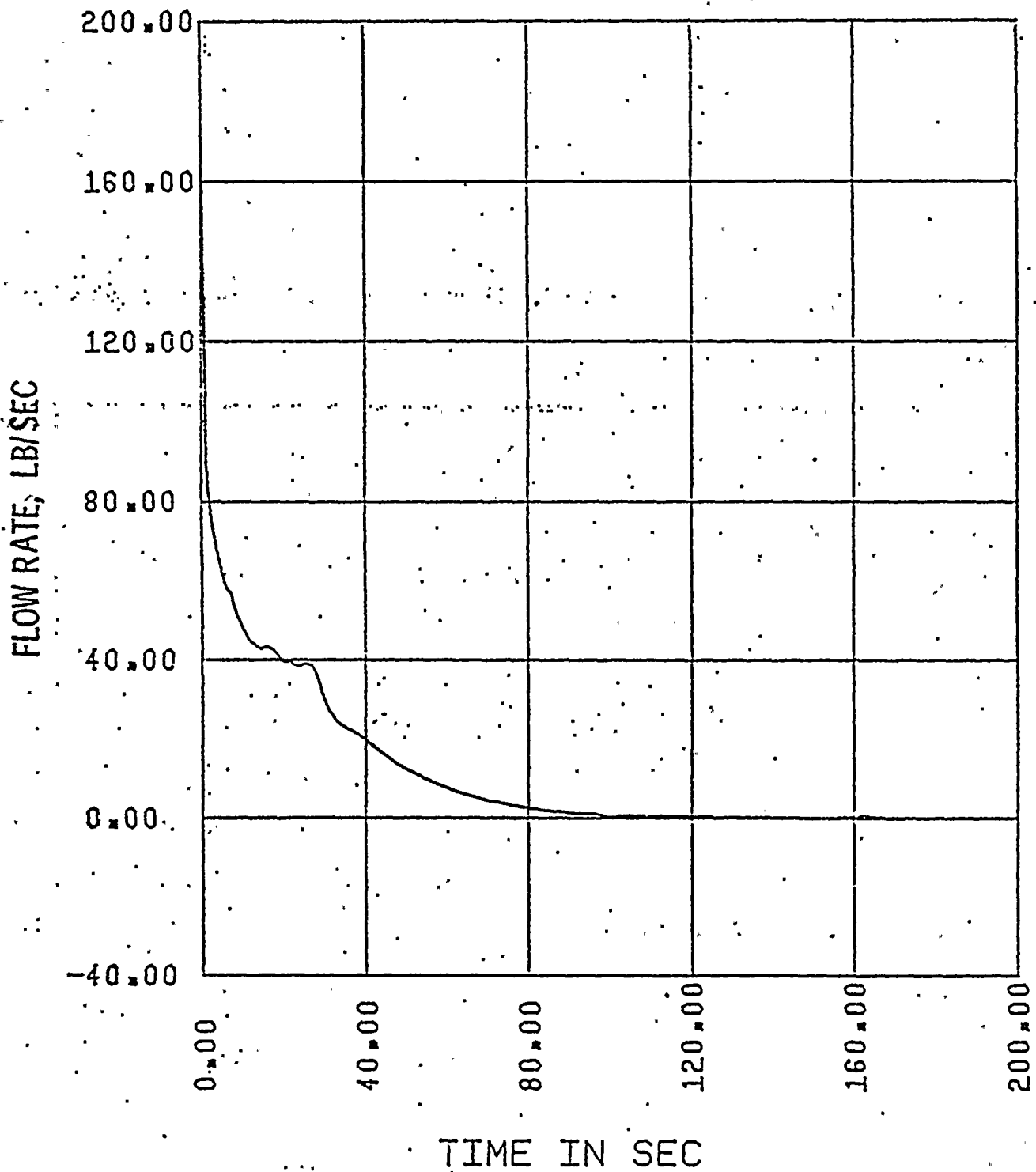


Figure II.4-E
2560 MWt PLANTS
0.5 FT² SLOT BREAK IN PUMP DISCHARGE LEG
HOT ASSEMBLY QUALITY

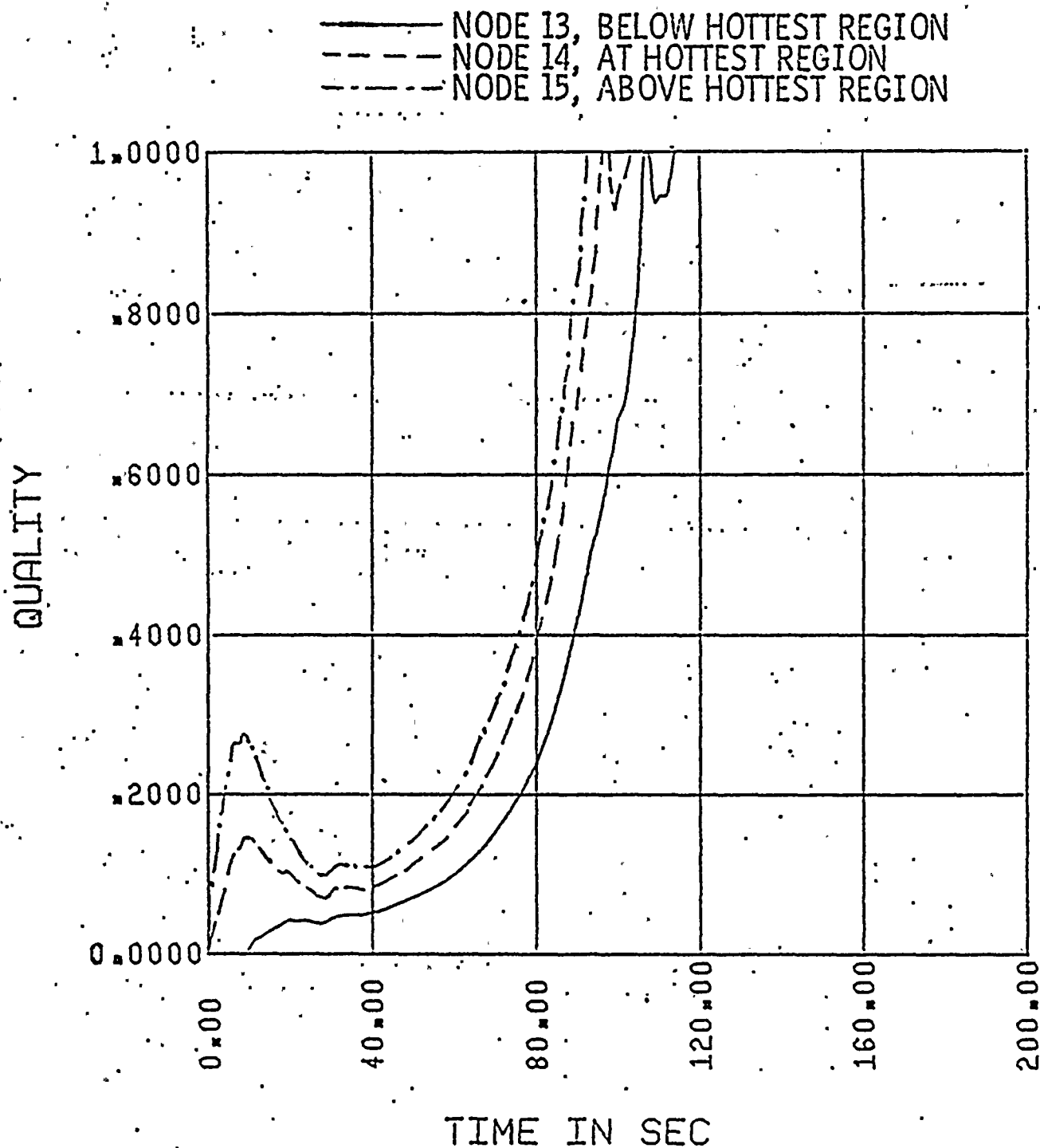




FIGURE II.4-F
ST. LUCIE UNIT I
0.5 FT² SLOT BREAK IN PUMP DISCHARGE LEG
CONTAINMENT PRESSURE

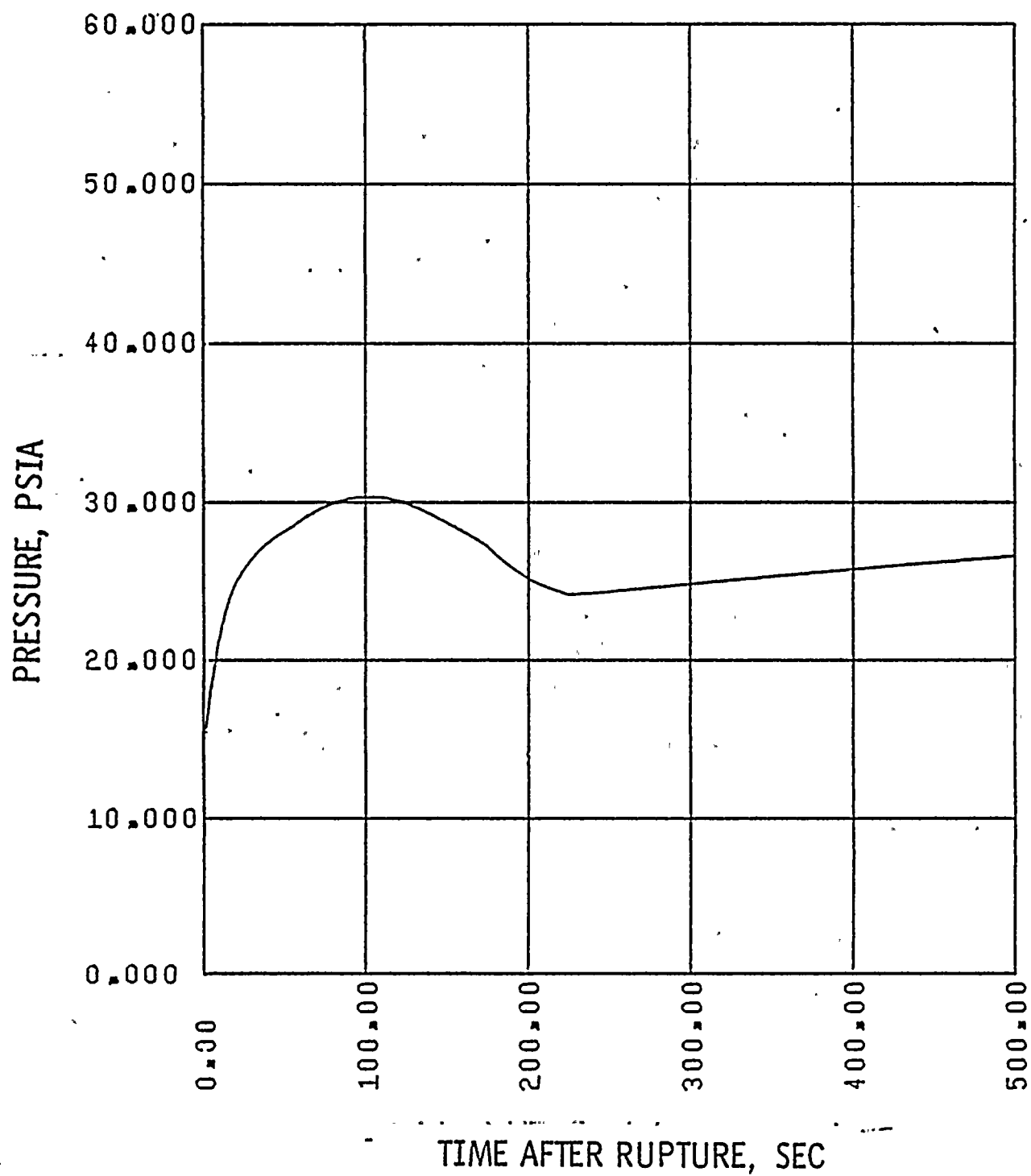
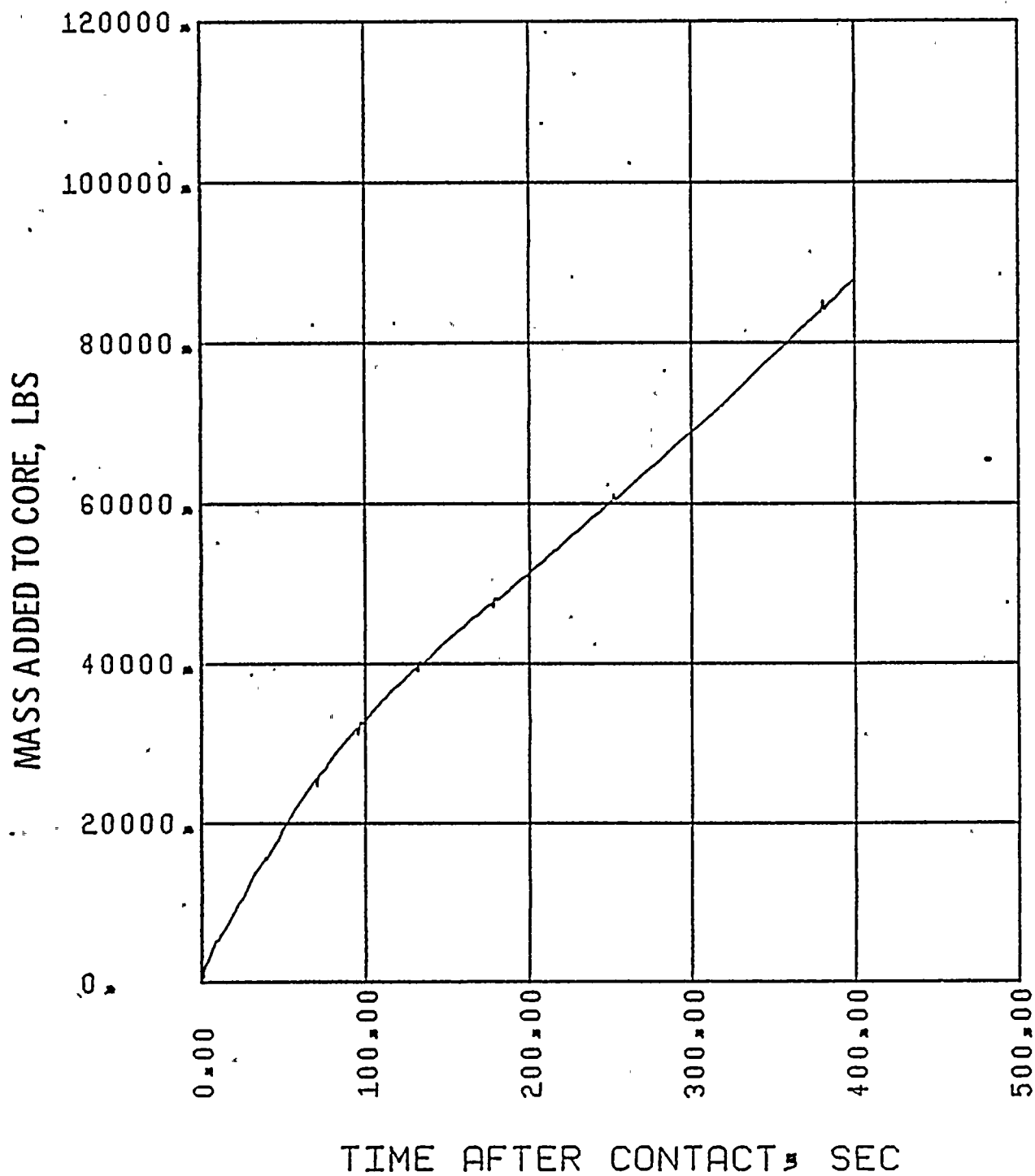


FIGURE II.4-G
ST. LUCIE UNIT I
0.5 FT² SLOT BREAK IN PUMP DISCHARGE LEG
MASS ADDED TO CORE DURING REFLOOD





ST. LUCIE UNIT I
0.5 FT² SLOT BREAK IN PUMP DISCHARGE LEG
PEAK CLAD TEMPERATURE

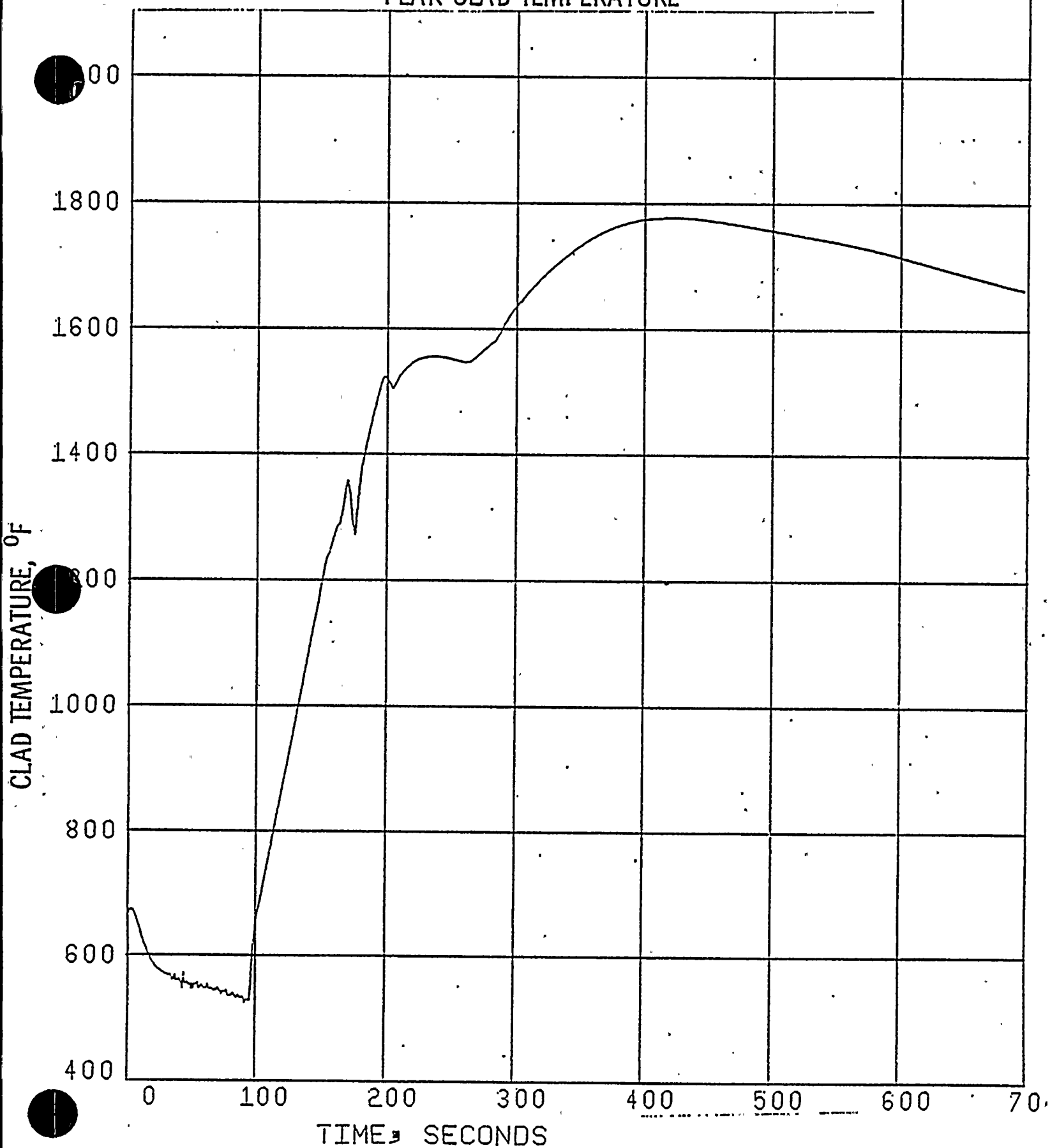




Figure II.5-A
2560 MWt PLANTS
1.0 x DOUBLE ENDED GUILLOTINE BREAK IN PUMP DISCHARGE LEG
CORE POWER

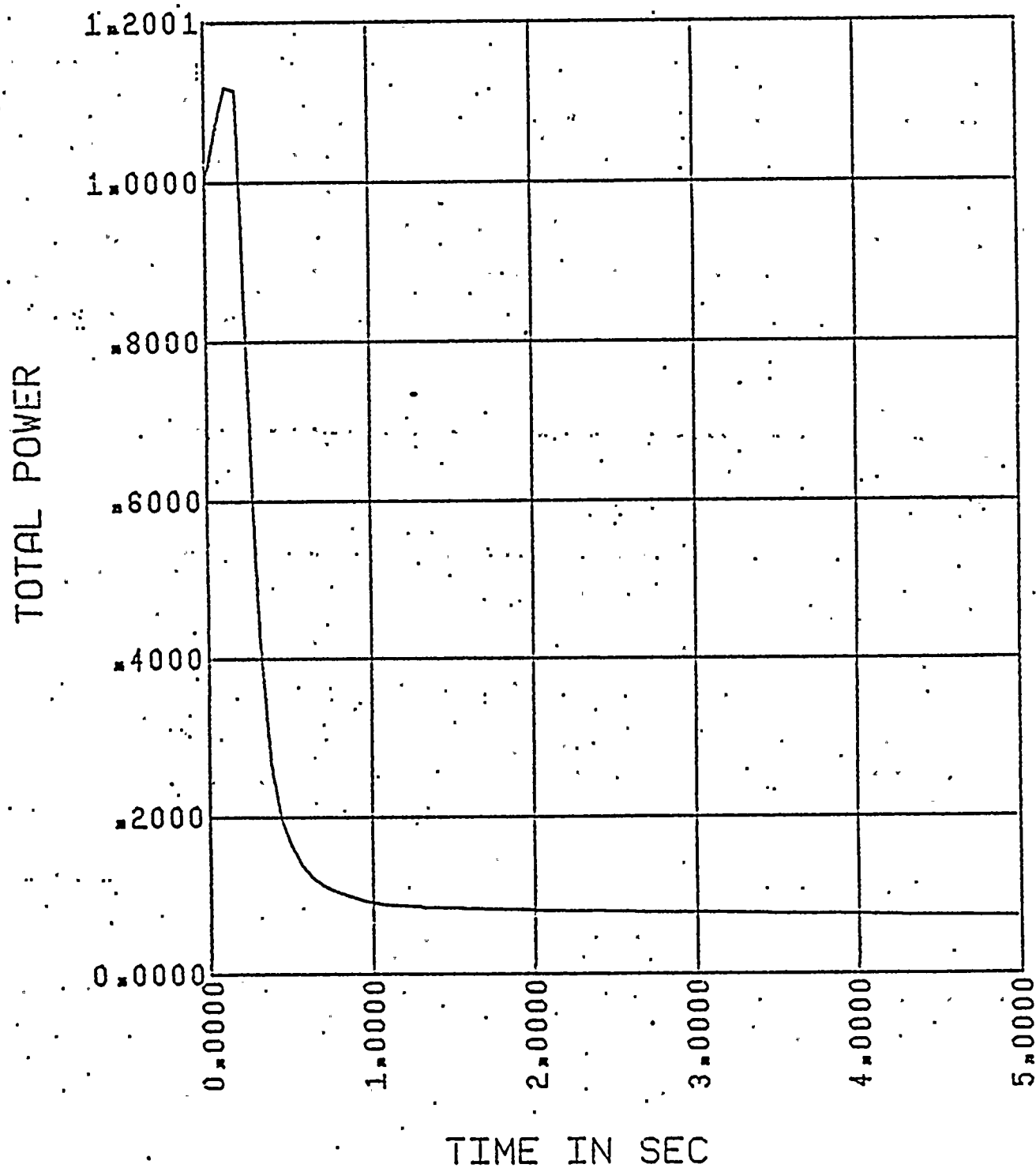


Figure II.5-B

2560 MWt PLANTS

1.0 x DOUBLE ENDED GUILLOTINE BREAK IN PUMP DISCHARGE LEG
PRESSURE IN CENTER HOT ASSEMBLY NODE

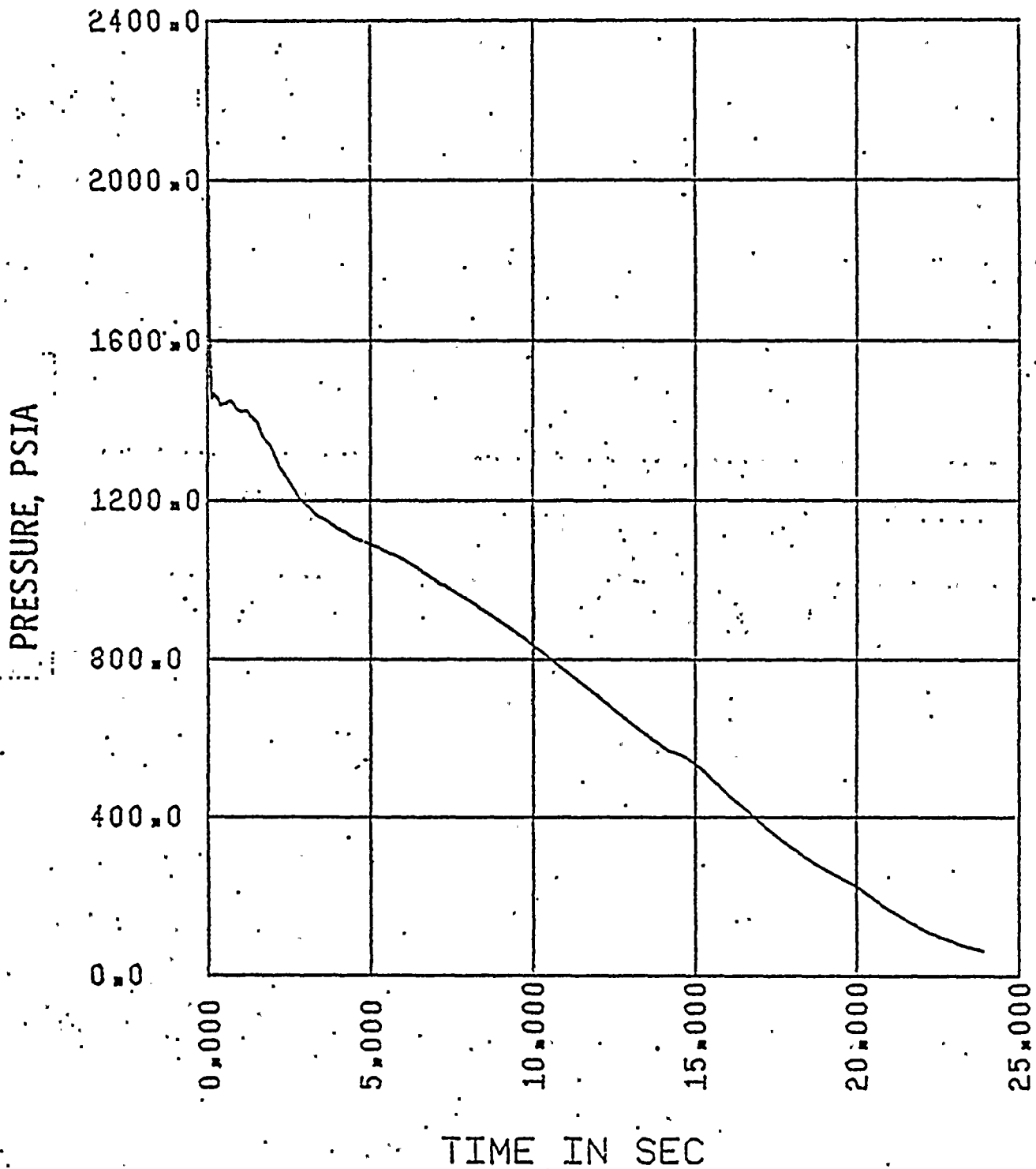




Figure II.5-C
2560 MWt PLANTS
1.0 x DOUBLE ENDED GUILLOTINE BREAK IN PUMP DISCHARGE LEG
LEAK FLOW

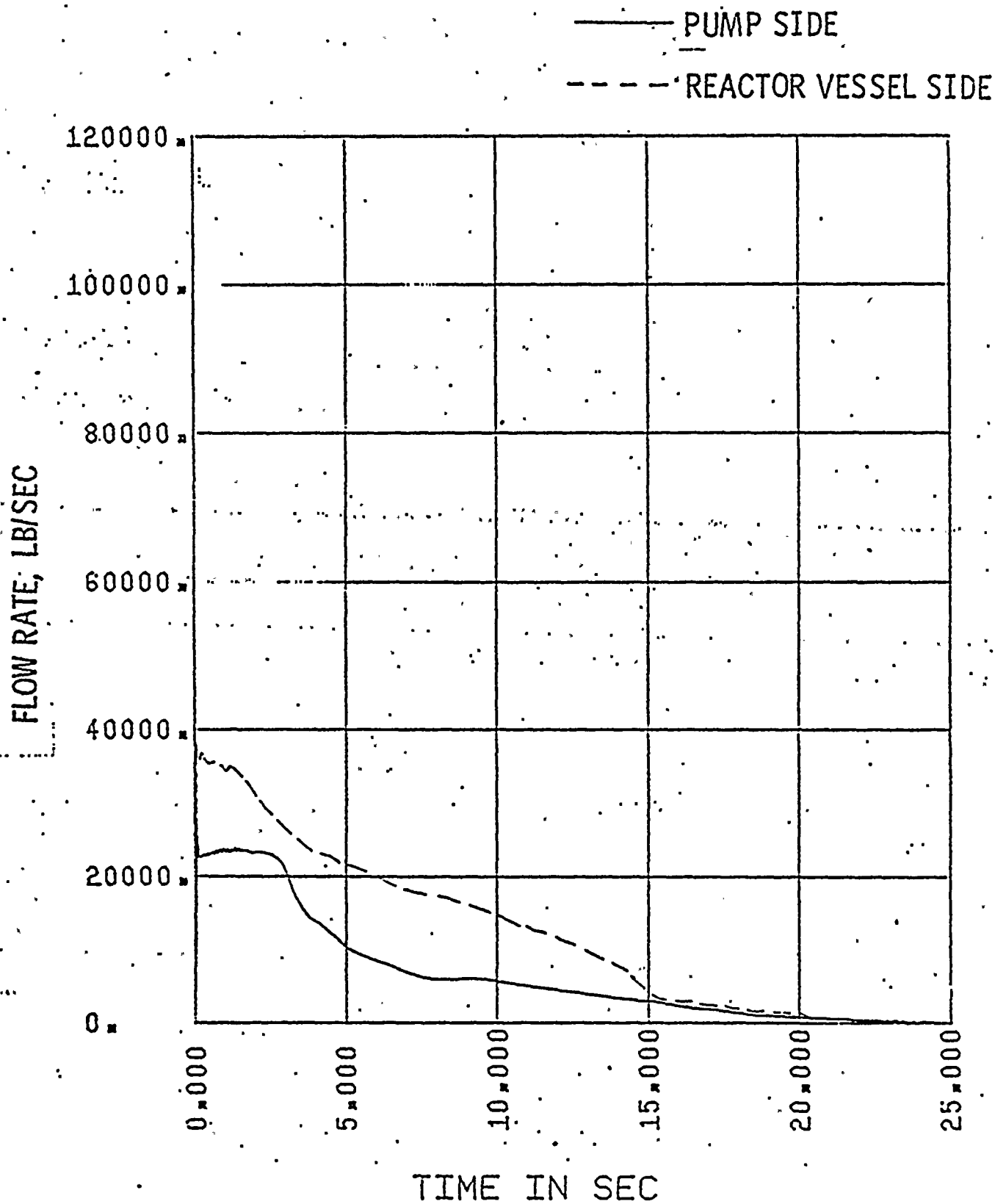


Figure II.5-D.1

2560 MWt PLANTS

1.0 x DOUBLE ENDED GUILLOTINE BREAK IN PUMP DISCHARGE LEG
FLOW IN HOT ASSEMBLY - PATH 16, BELOW HOT SPOT

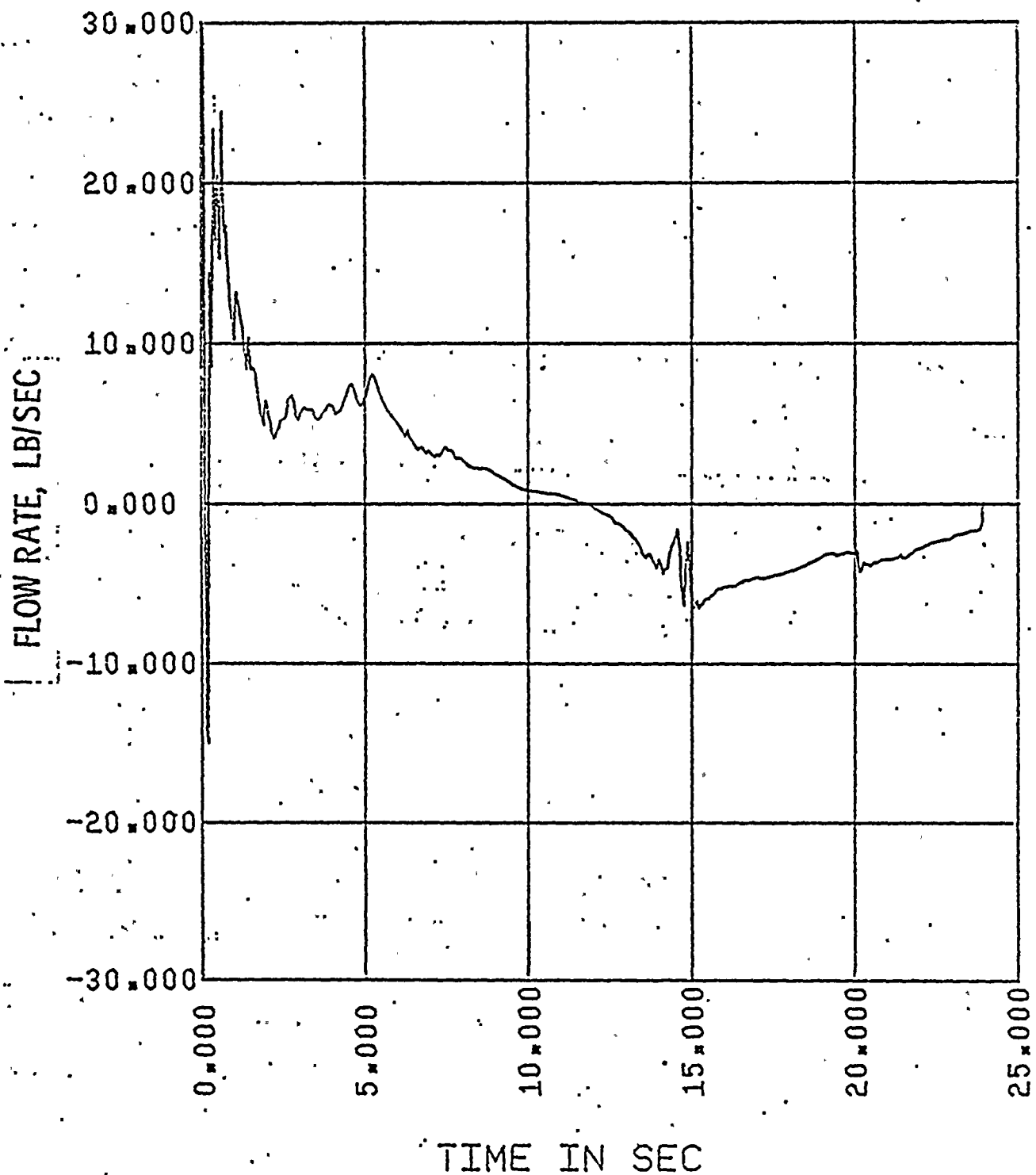


Figure II.5-D.2

2560 MWt PLANTS
1.0 x DOUBLE ENDED GUILLOTINE BREAK IN PUMP DISCHARGE LEG
FLOW IN HOT ASSEMBLY - PATH 17, ABOVE HOT SPOT

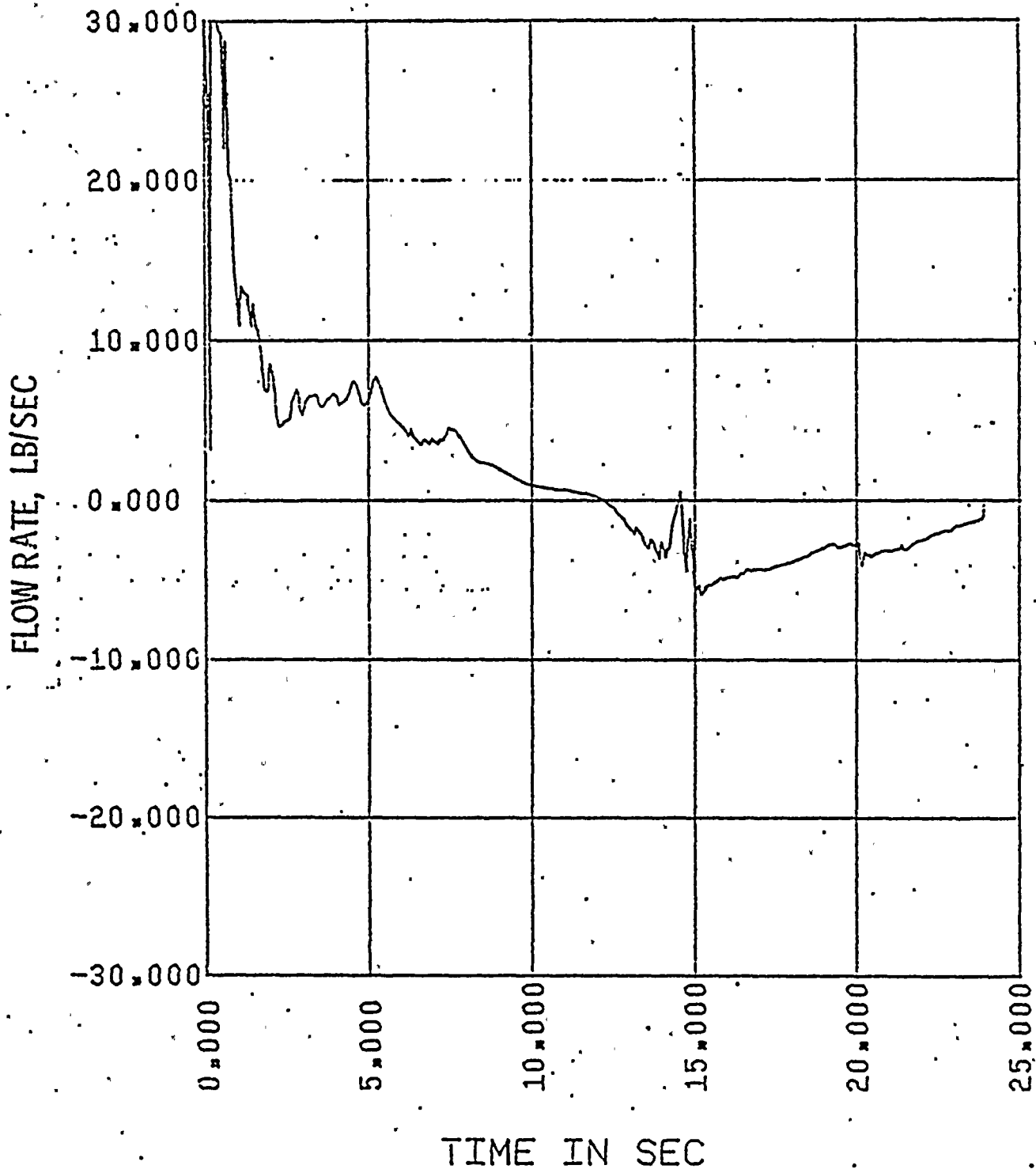


Figure II.5-E

2560 MWt PLANTS
1.0 x DOUBLE ENDED GUILLOTINE BREAK IN PUMP DISCHARGE LEG
HOT ASSEMBLY QUALITY

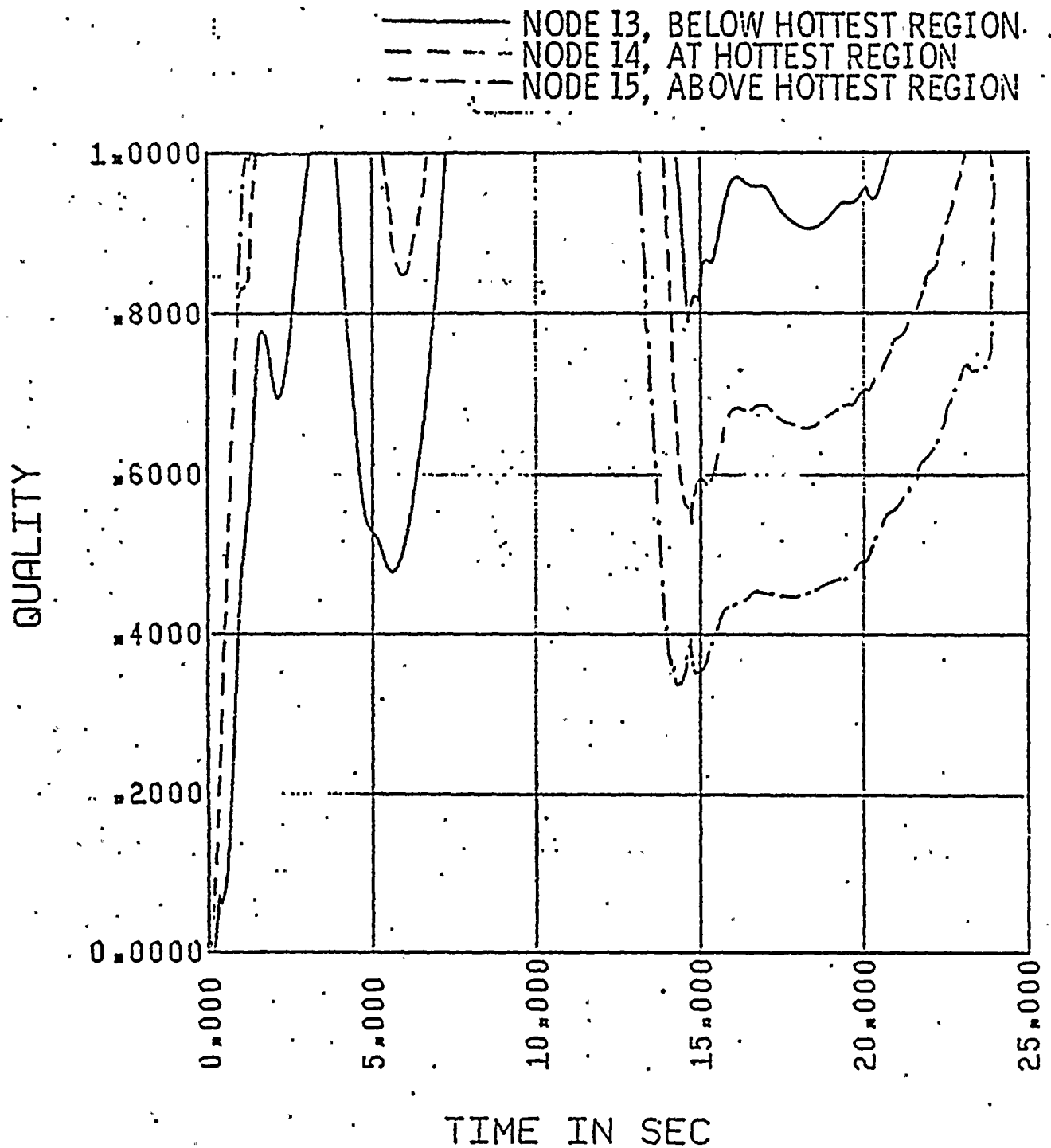


FIGURE II.5-F
ST. LUCIE UNIT I
1.0 x DOUBLE ENDED GUILLOTINE BREAK IN PUMP DISCHARGE LEG
CONTAINMENT PRESSURE

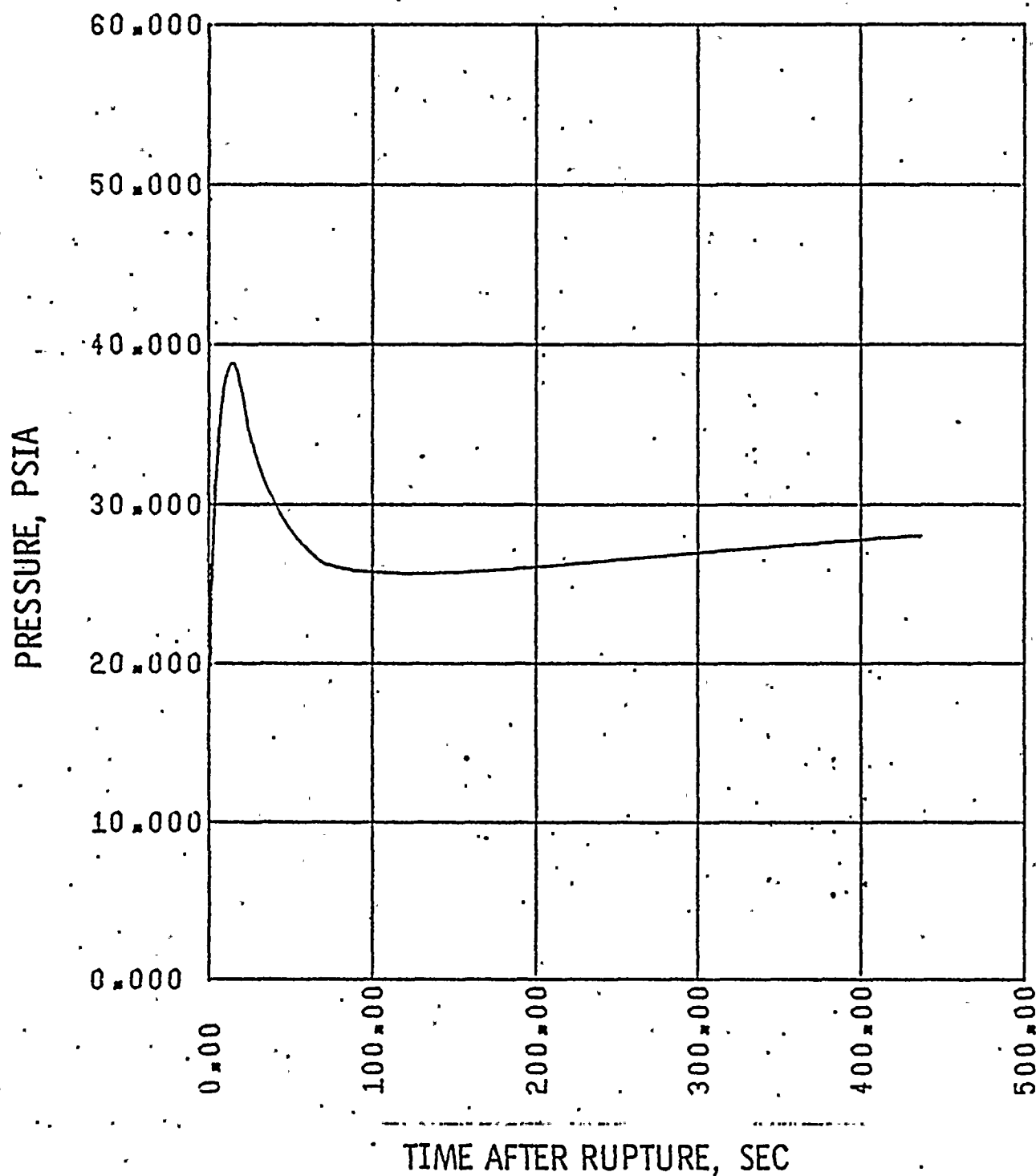


FIGURE II.5-G
ST. LUCIE UNIT I
1.0 x DOUBLE ENDED GUILLOTINE BREAK IN PUMP DISCHARGE LEG
MASS ADDED TO CORE DURING REFLOOD

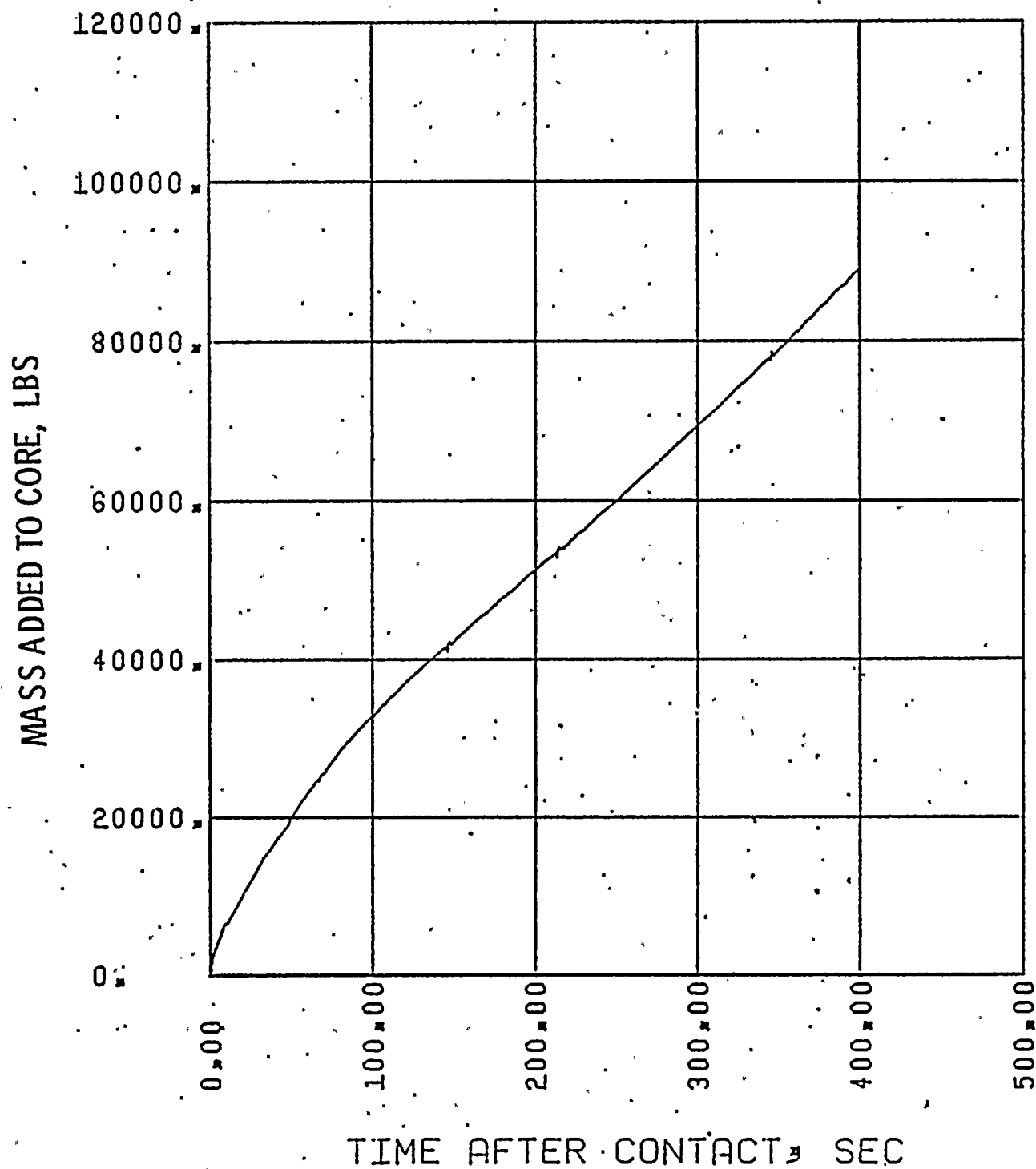




FIGURE 11.5-H

ST. LUCIE UNIT I

1.0 x DOUBLE ENDED GUILLLOTINE BREAK IN PUMP DISCHARGE LEG

PEAK CLAD TEMPERATURE

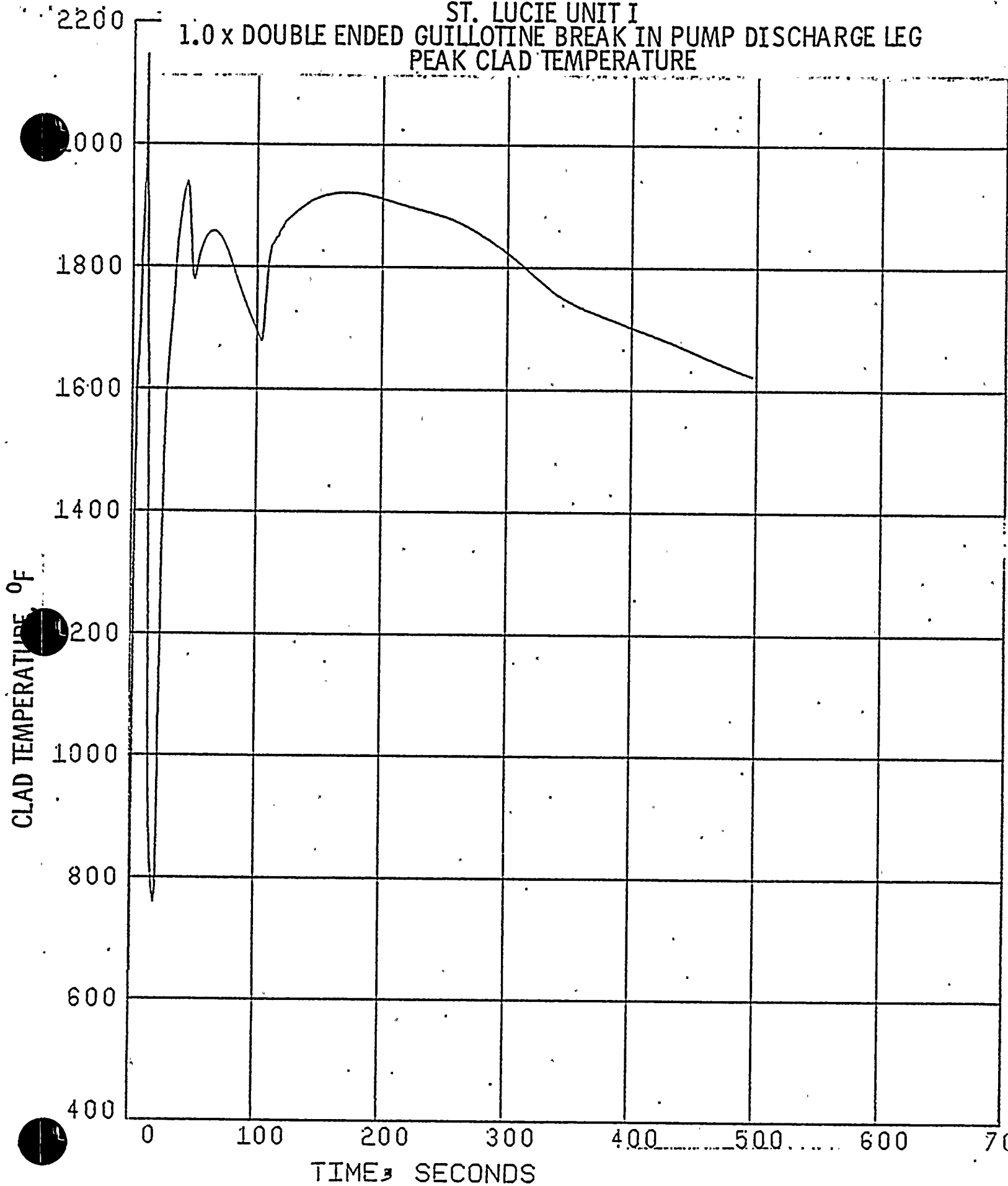


Figure II.6-A
2560 MWt PLANTS
0.8 x DOUBLE ENDED GUILLOTINE BREAK-IN-PUMP DISCHARGE LEG
CORE POWER

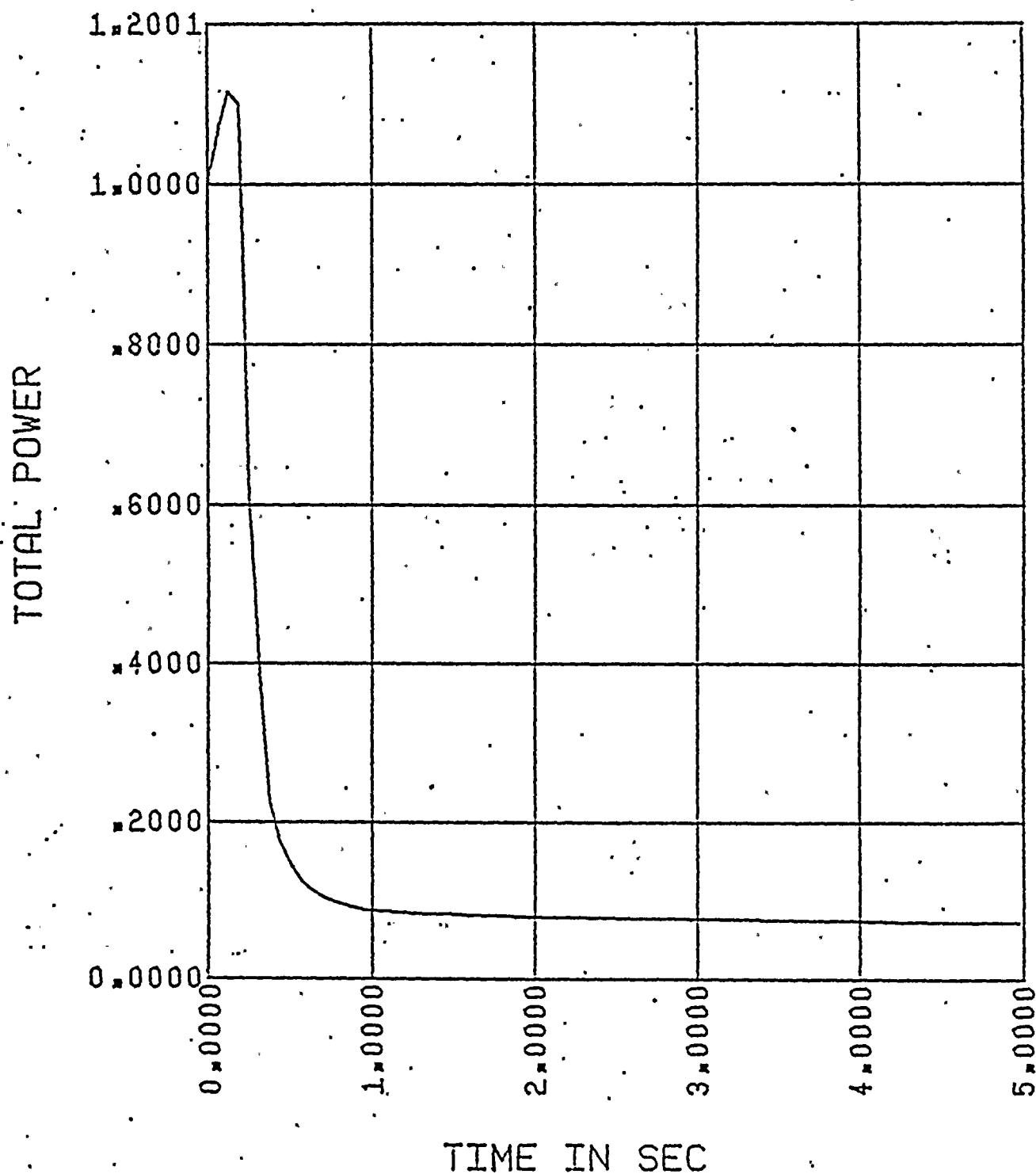


Figure II.6-B
2560 MWt FLANTS
0.8 x DOUBLE ENDED GUILLLOTINE BREAK IN PUMP DISCHARGE LEG
PRESSURE IN CENTER HOT ASSEMBLY NODE

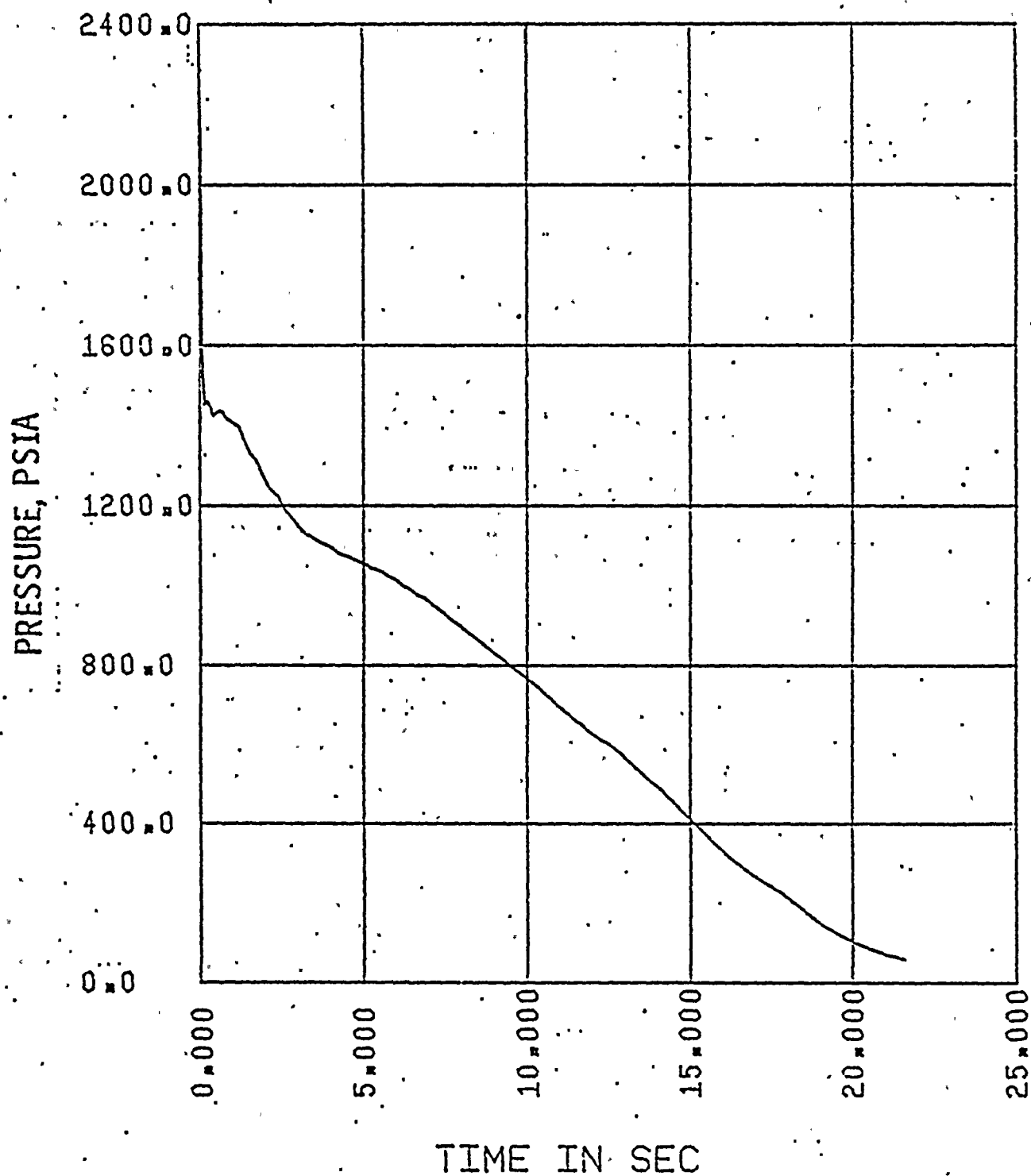


Figure II.6-C
2560 MWt PLANTS
0.8 x DOUBLE ENDED GUILLOTINE BREAK IN PUMP DISCHARGE LEG
LEAK FLOW

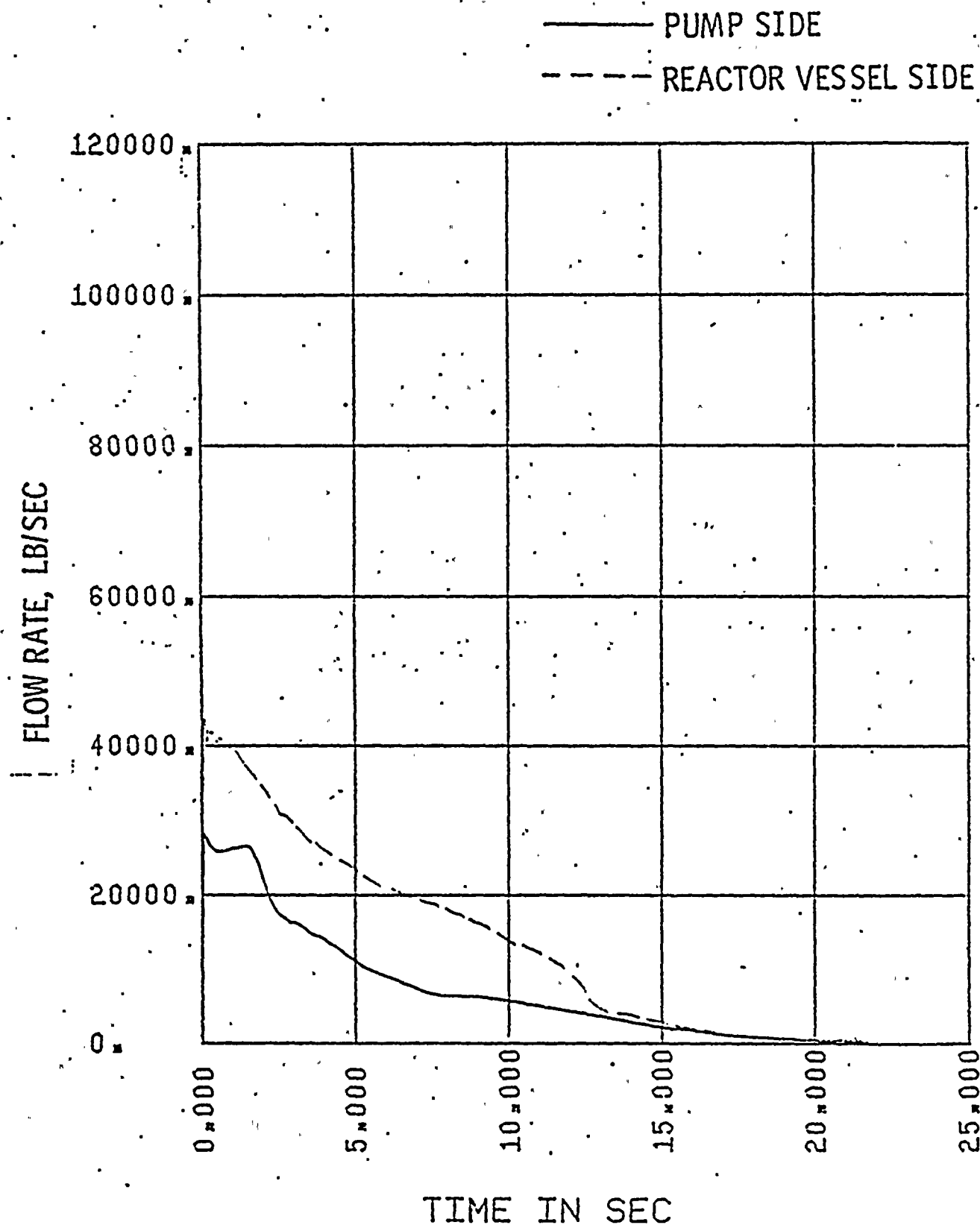


Figure II.6-D.1

2560 MWt PLANTS

0.8 x DOUBLE ENDED GUILLOTINE BREAK IN PUMP DISCHARGE LEG
FLOW IN HOT ASSEMBLY - PATH 16, BELOW HOT SPOT

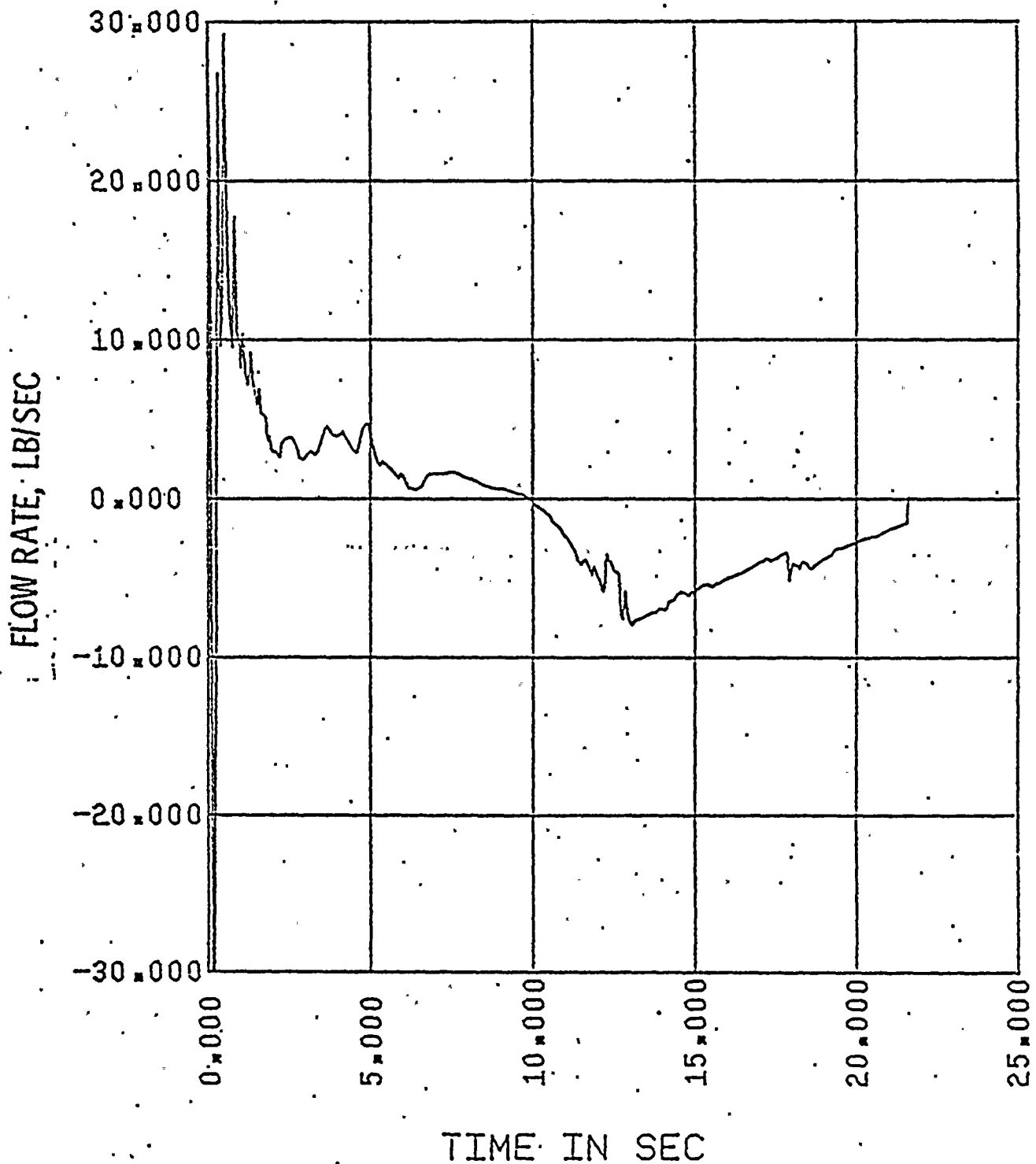
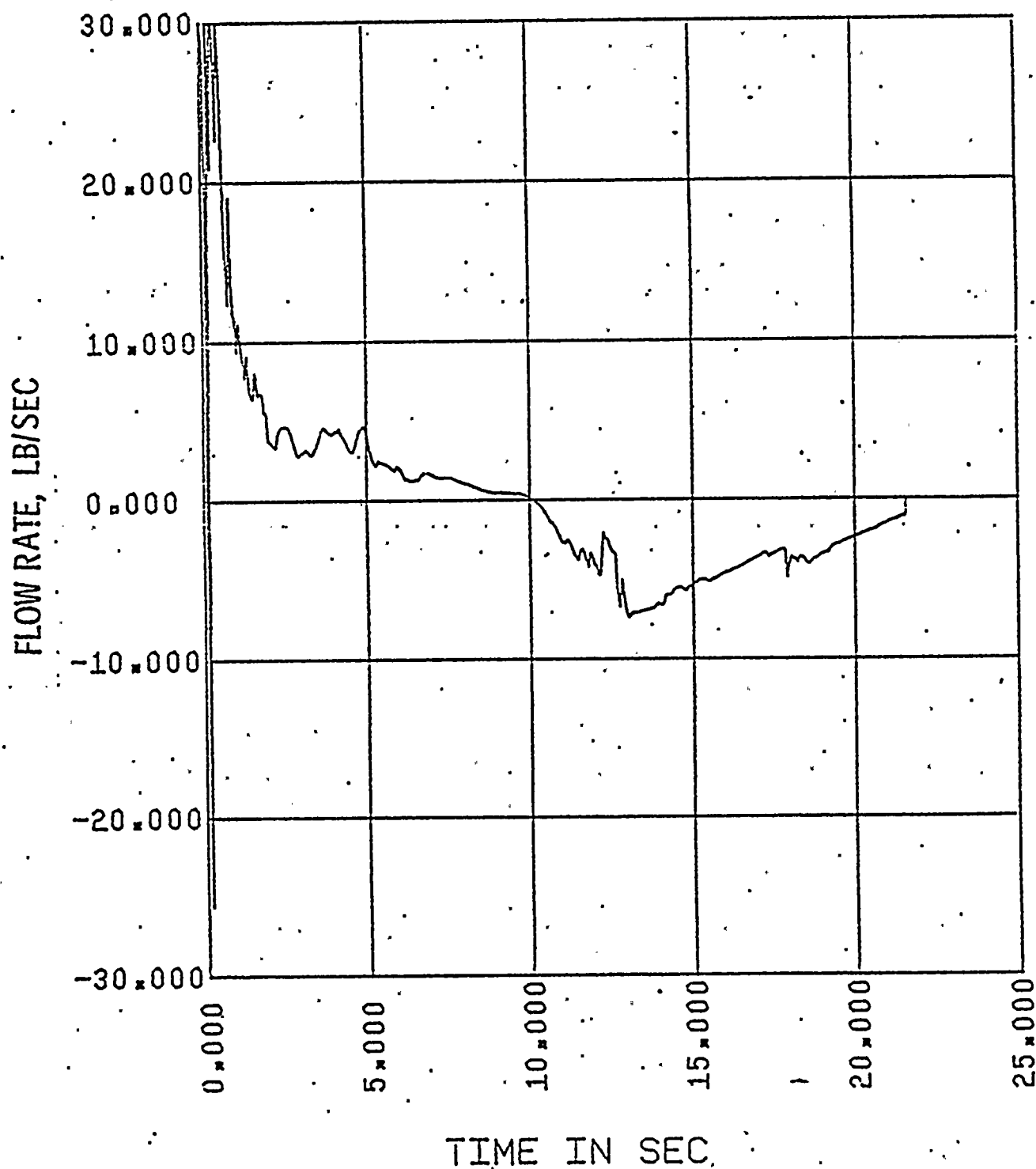


Figure II.6-D.2
2560 MWt PLANTS
0.8 x DOUBLE ENDED GUILLOTINE BREAK IN PUMP DISCHARGE LEG
FLOW IN HOT ASSEMBLY - PATH 17, ABOVE HOT SPOT



(

4 1 1 1



)

Figure II.6-E

2560 MWt PLANTS
0.8 x DOUBLE ENDED GUILLOTINE BREAK IN PUMP DISCHARGE LEG
HOT ASSEMBLY QUALITY

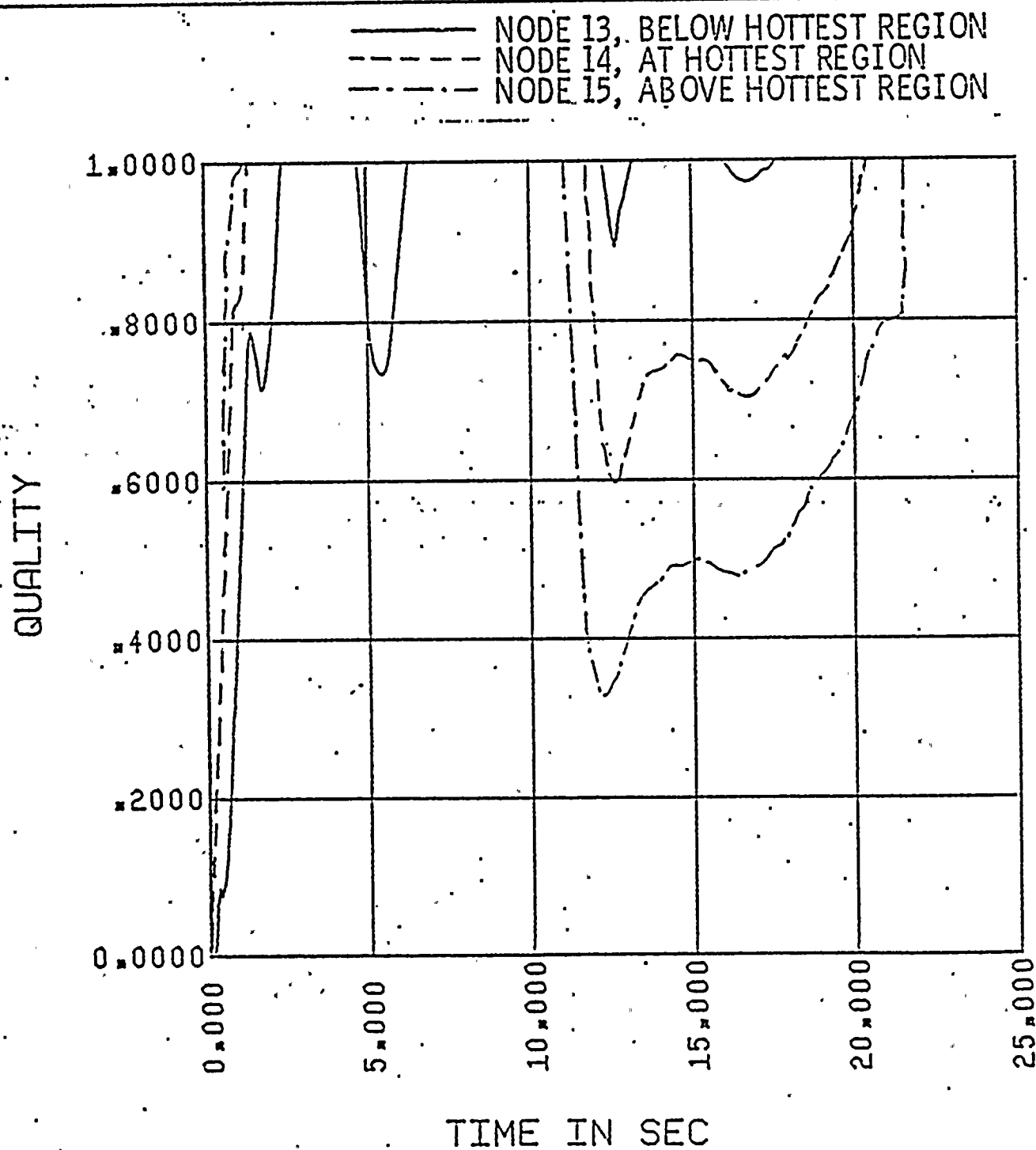


FIGURE II.6-F
ST. LUCIE UNIT I
0.8 x DOUBLE ENDED GUILLOTINE BREAK IN PUMP DISCHARGE LEG
CONTAINMENT PRESSURE

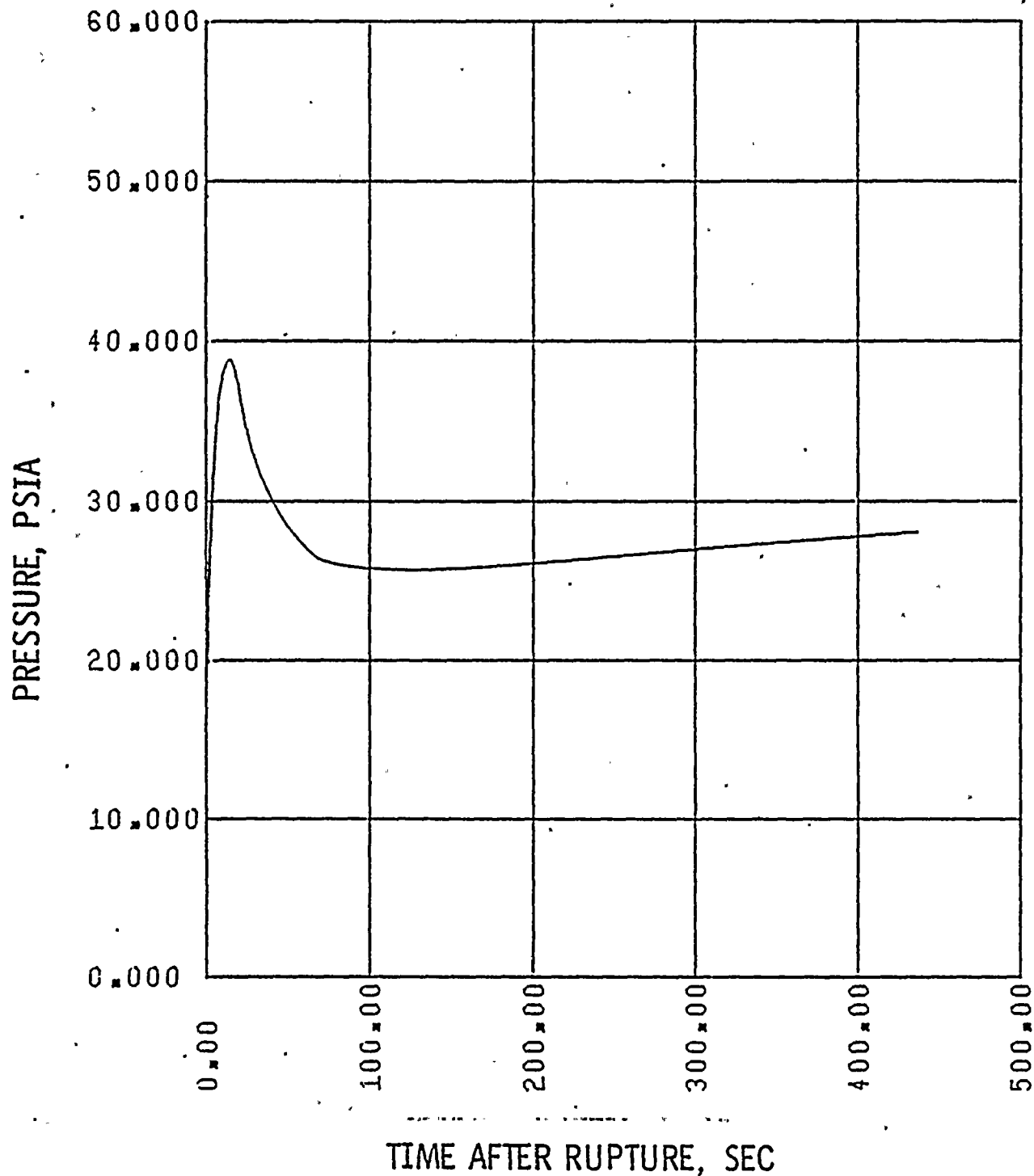




FIGURE II.6-G
 ST. LUCIE UNIT I
 0.8 x DOUBLE ENDED GUILLOTINE BREAK IN PUMP DISCHARGE LEG
 MASS ADDED TO CORE DURING REFLOOD

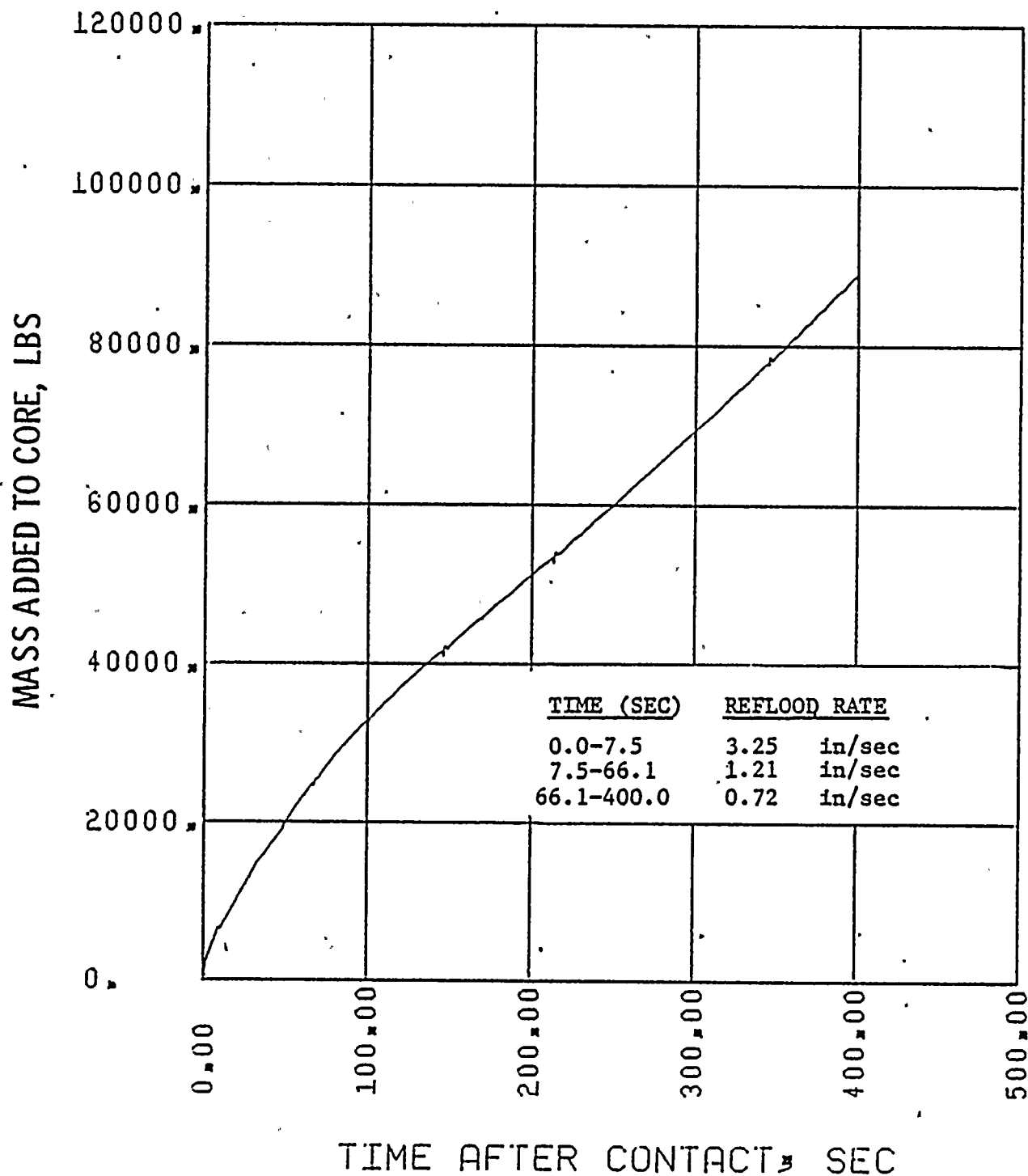


FIGURE 11.6-11

ST. LUCIE UNIT I
0.8 x DOUBLE ENDED GUILLOTINE BREAK IN PUMP DISCHARGE LEG
PEAK CLAD TEMPERATURE

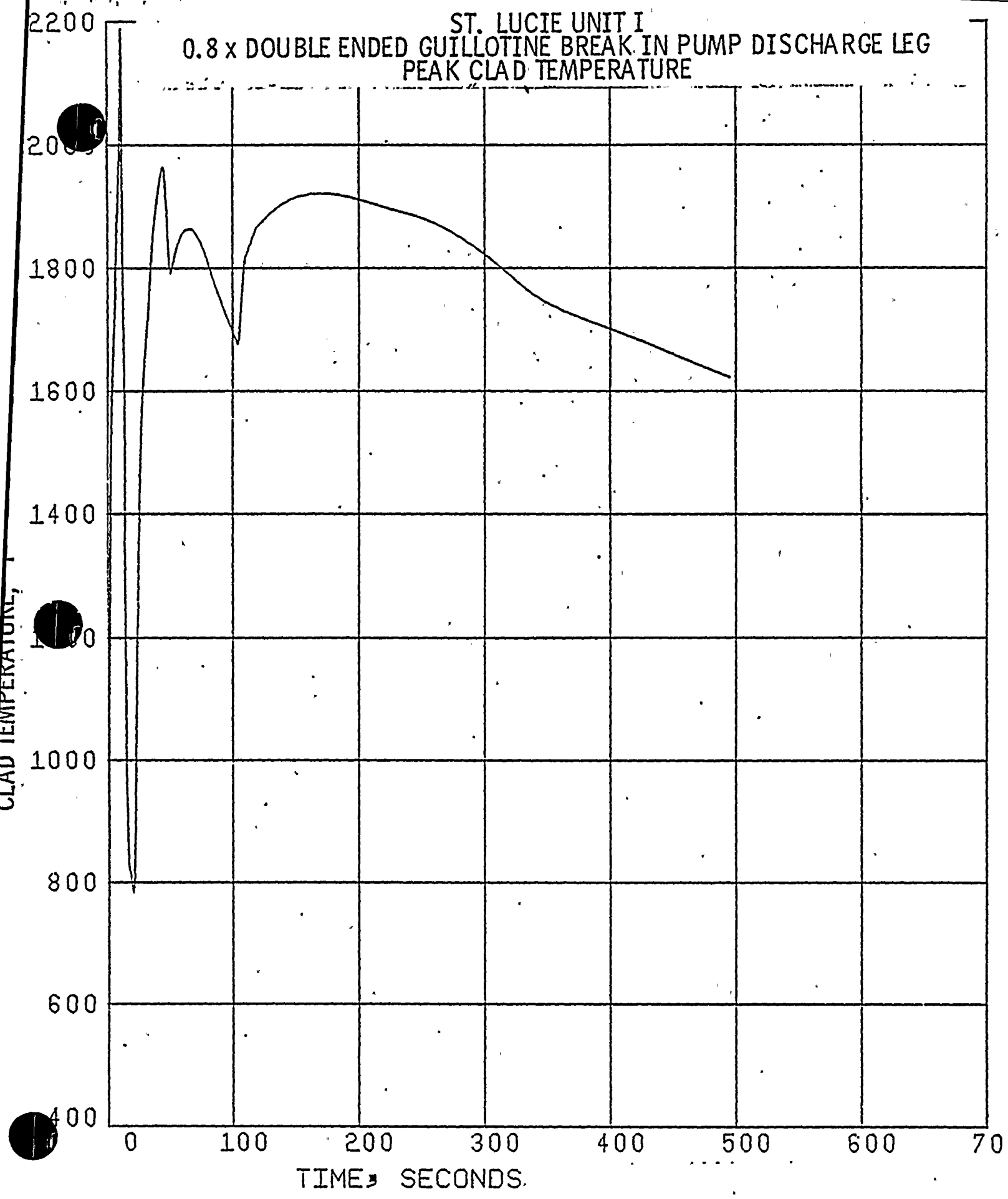


FIGURE II.6-I
ST. LUCIE UNIT I
0.8 x DOUBLE ENDED GUILLOTINE BREAK IN PUMP DISCHARGE LEG
MID-ANNULUS FLOW

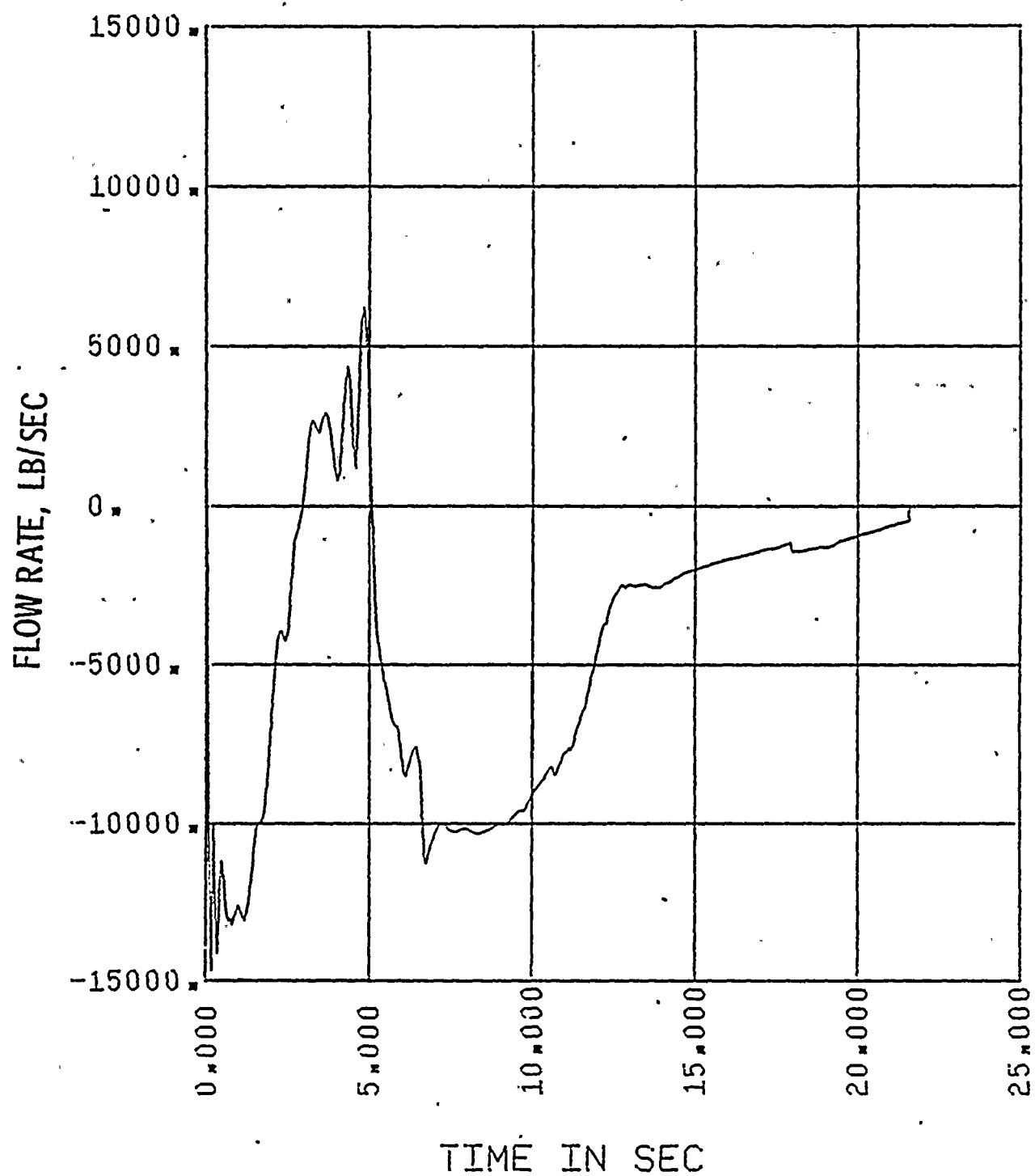


FIGURE II.6-J
ST. LUCIE UNIT I
0.8 x DOUBLE ENDED GUILLOTINE BREAK IN PUMP DISCHARGE LEG
QUALITIES ABOVE AND BELOW THE CORE

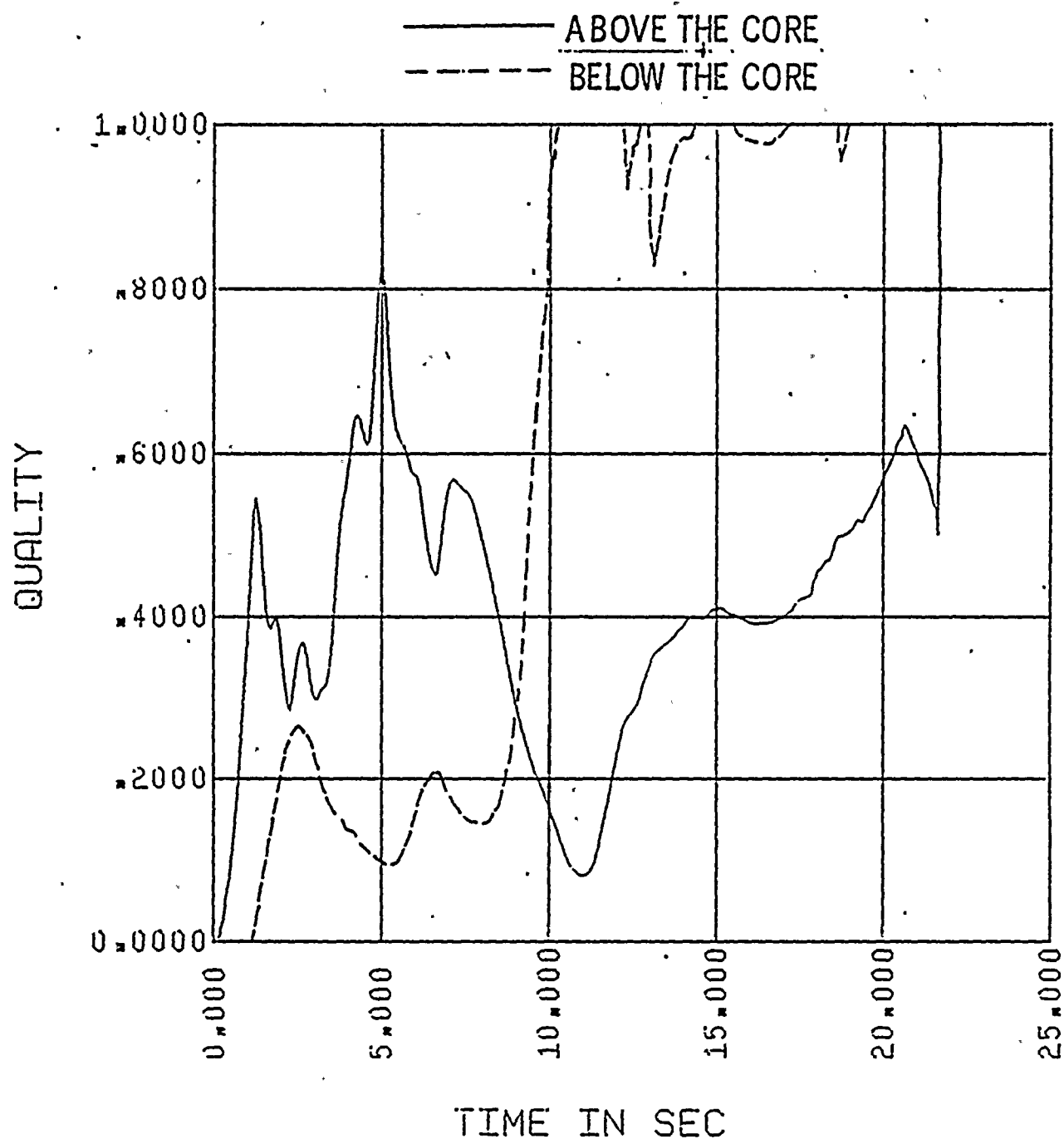




FIGURE II.6-K
ST. LUCIE UNIT I
0.8 x DOUBLE ENDED GUILLOTINE BREAK IN PUMP DISCHARGE LEG
CORE PRESSURE DROP

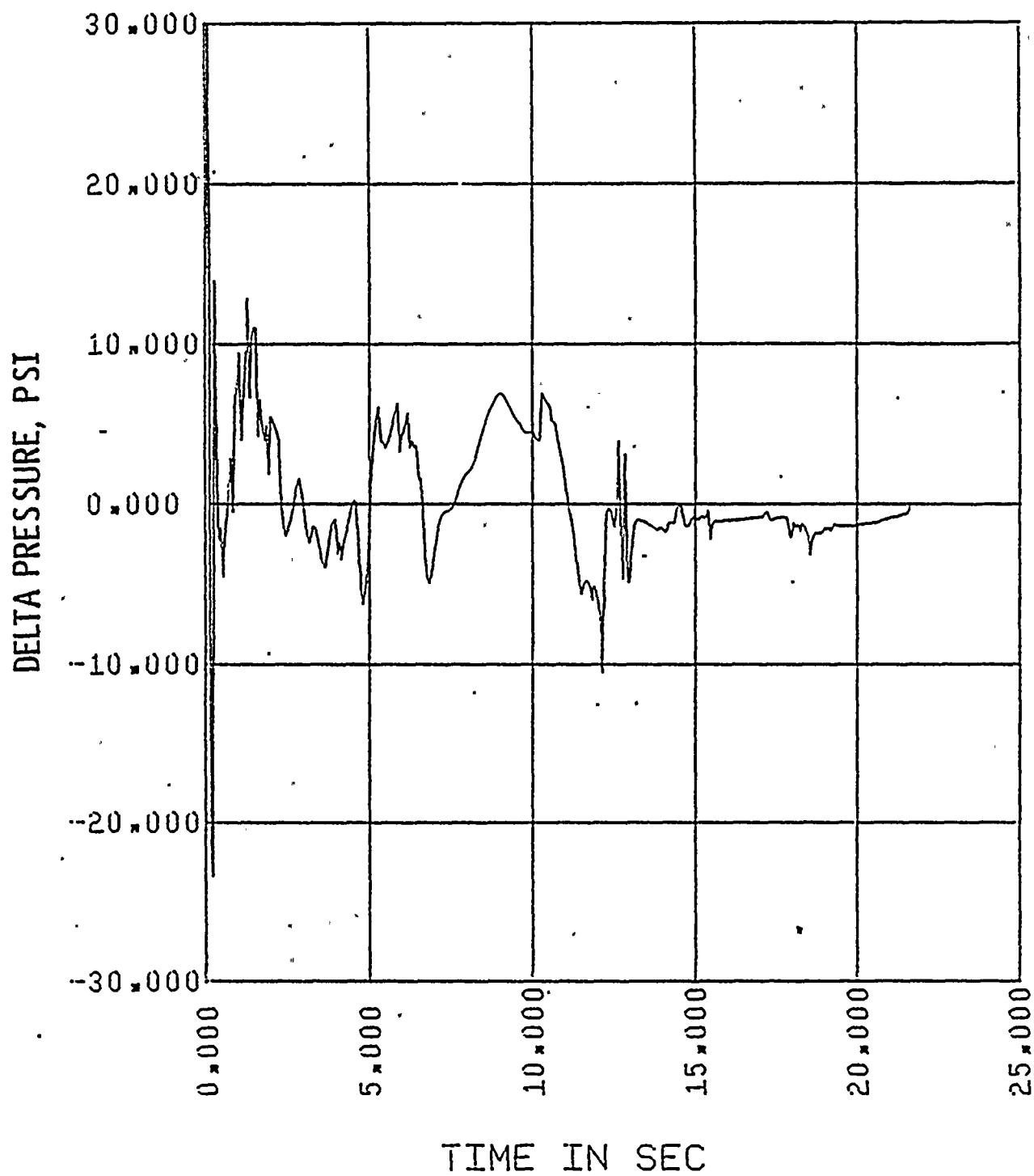


FIGURE II.6-L

ST. LUCIE UNIT I
0.8 x DOUBLE ENDED GUILLOTINE BREAK IN PUMP DISCHARGE LEG
SAFETY INJECTION FLOW INTO INTACT DISCHARGE LEGS

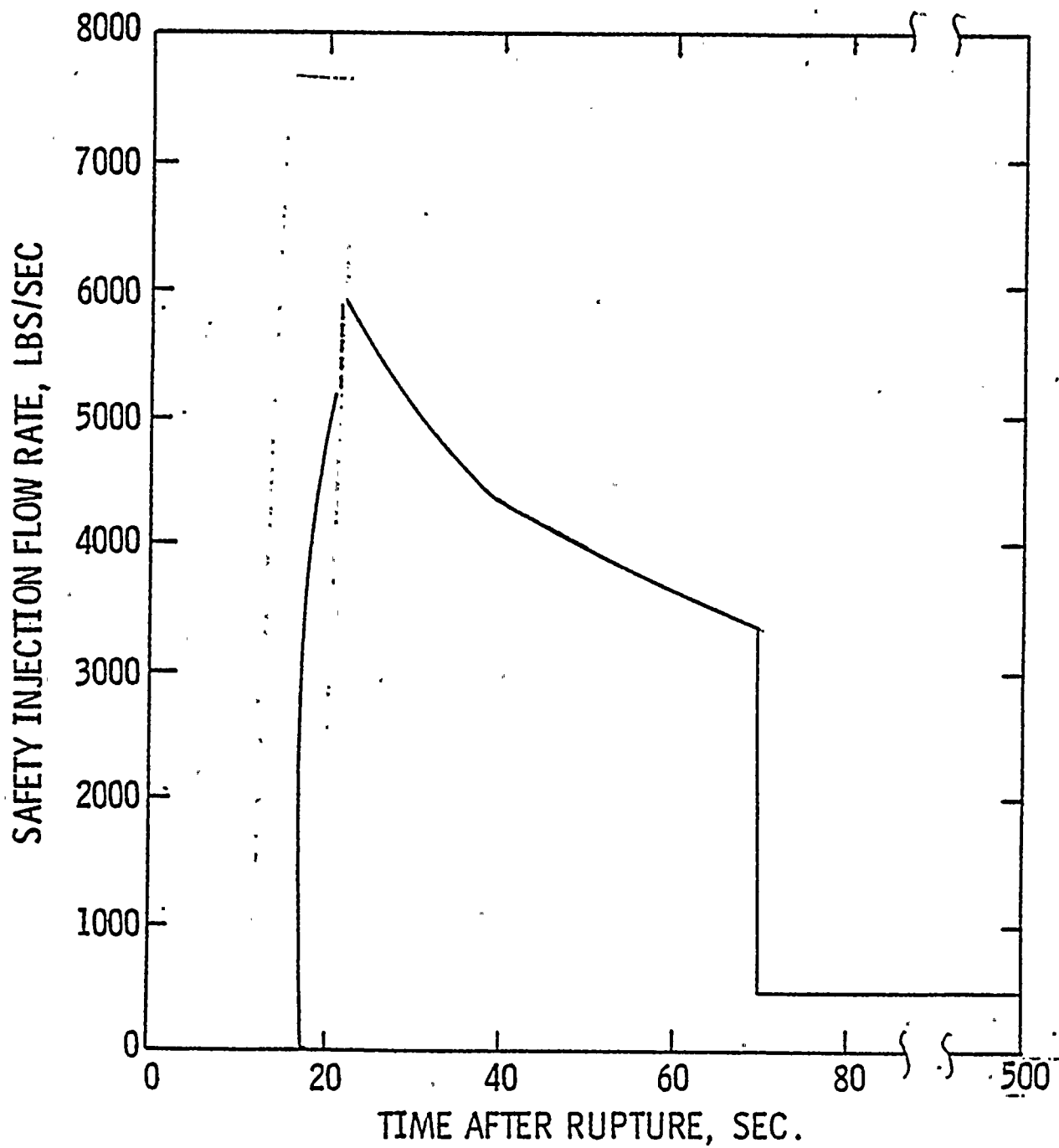
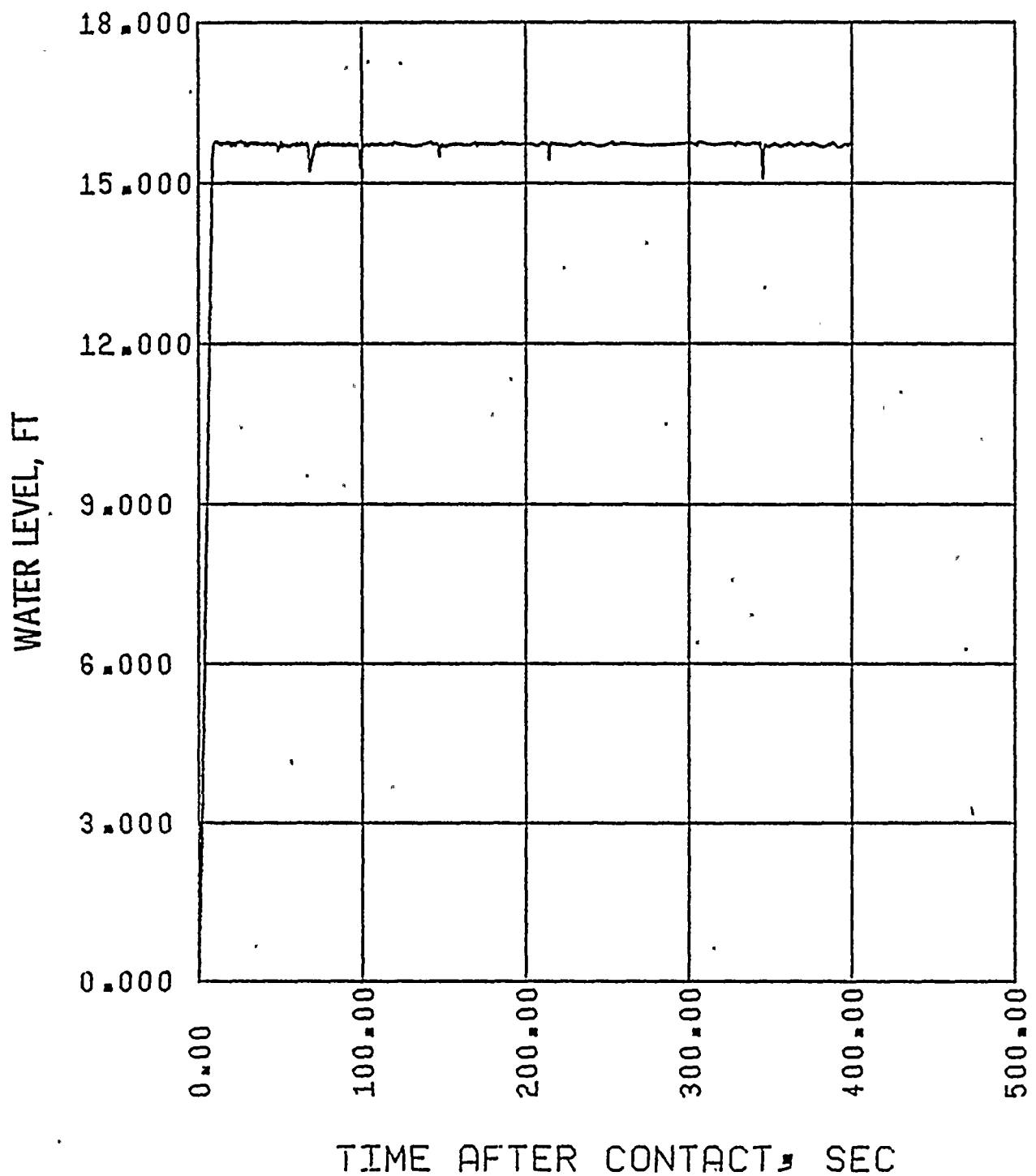


FIGURE II.6-M
ST. LUCIE UNIT I
0.8 x DOUBLE ENDED GUILLOTINE BREAK IN PUMP DISCHARGE LEG
WATER LEVEL IN DOWNCOMER DURING REFLOOD



ST. LUCIE UNIT I

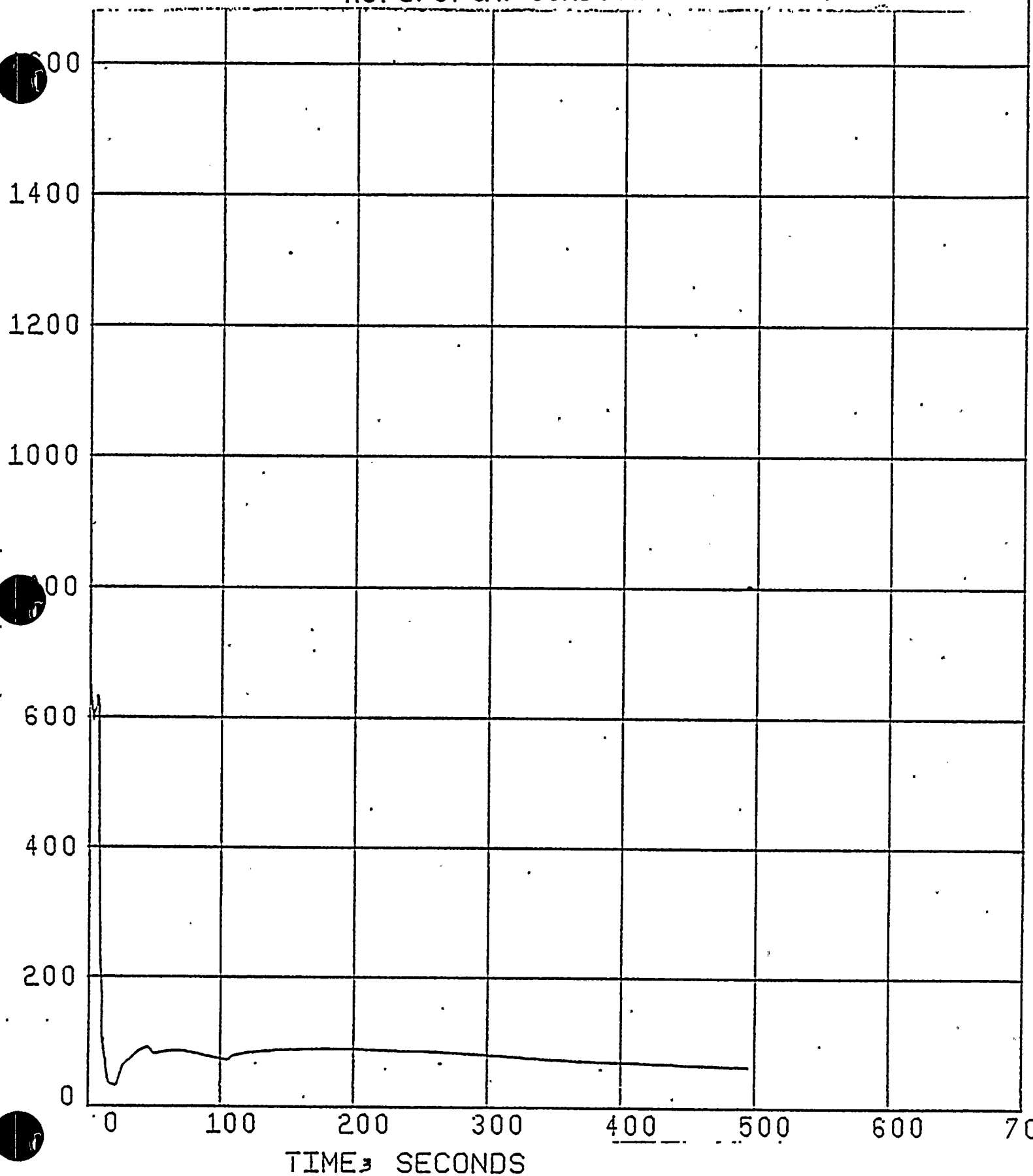
0.8 x DOUBLE ENDED GUILLOTINE BREAK IN PUMP DISCHARGE LEG
HOT SPOT GAP CONDUCTANCEGAP CONDUCTANCE, BTU/HR-FT²-°F

FIGURE II.6-0

ST. LUCIE UNIT I

0.8x DOUBLE ENDED GUILLOTINE BREAK IN PUMP DISCHARGE LEG
PEAK LOCAL CLAD OXIDATION

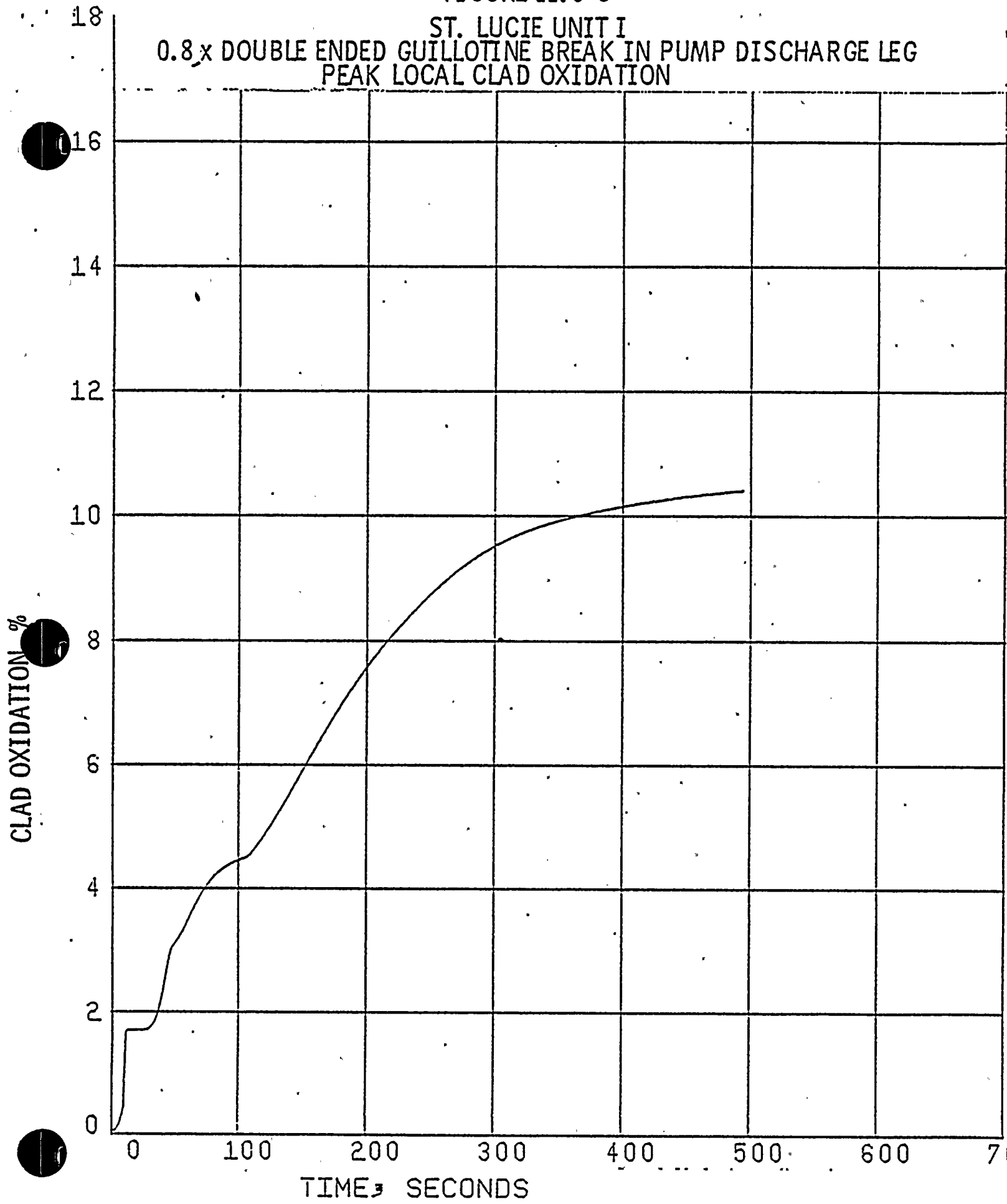
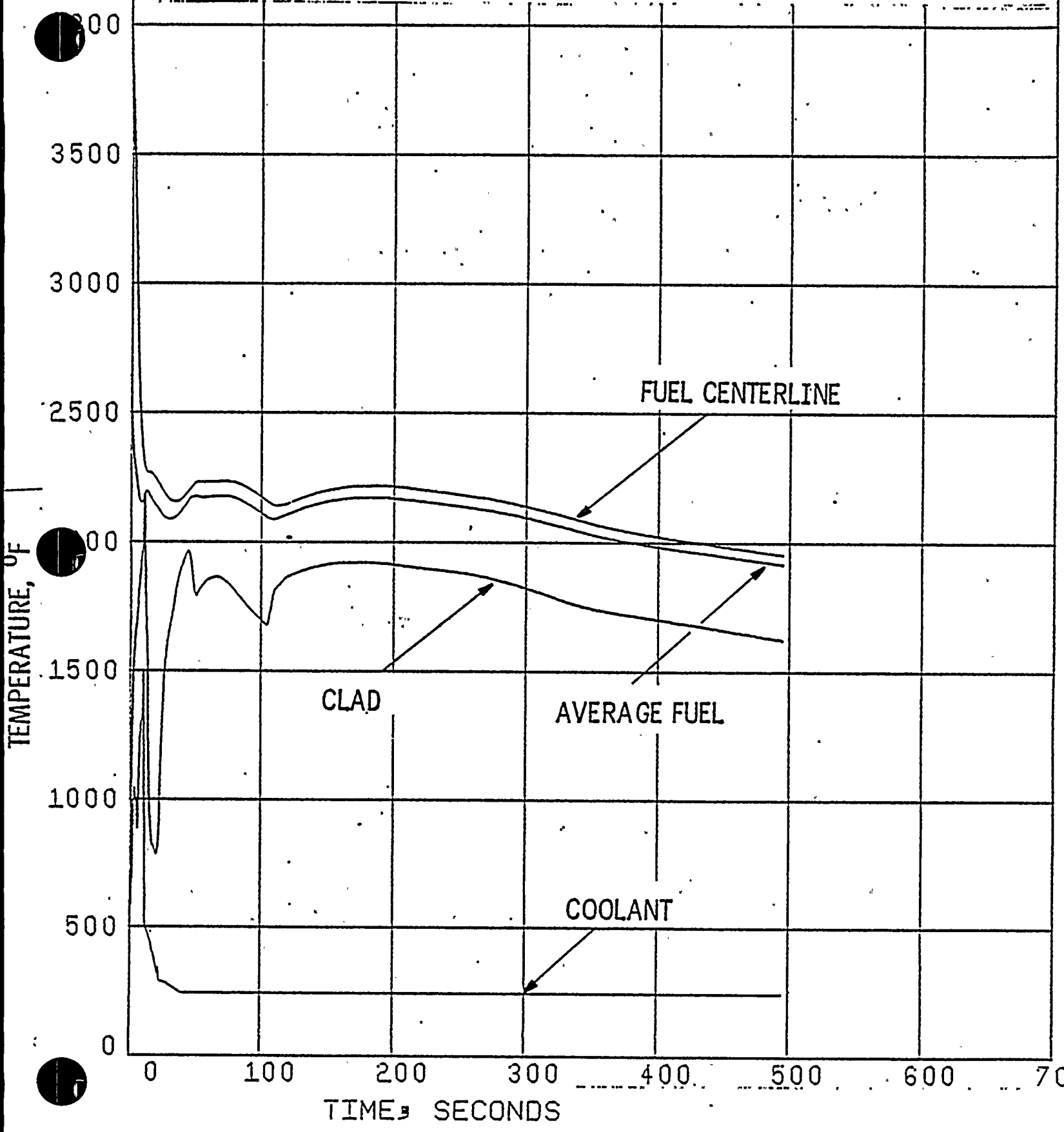


FIGURE 11.6-P

ST. LUCIE UNIT I

0.8 x DOUBLE ENDED GUILLOTINE BREAK IN PUMP DISCHARGE LEG
CLAD TEMPERATURE, CENTERLINE FUEL TEMPERATURE, AVERAGE
FUEL TEMPERATURE AND COOLANT TEMPERATURE FOR HOTTEST NODE



ST. LUCIE UNIT I

0.8 x DOUBLE ENDED GUILLOTINE BREAK IN PUMP DISCHARGE LEG
HOT SPOT HEAT TRANSFER COEFFICIENT

HEAT TRANSFER COEFFICIENT, BTU/HR-FT²-°F

180

160

140

120

100

80

60

40

20

0

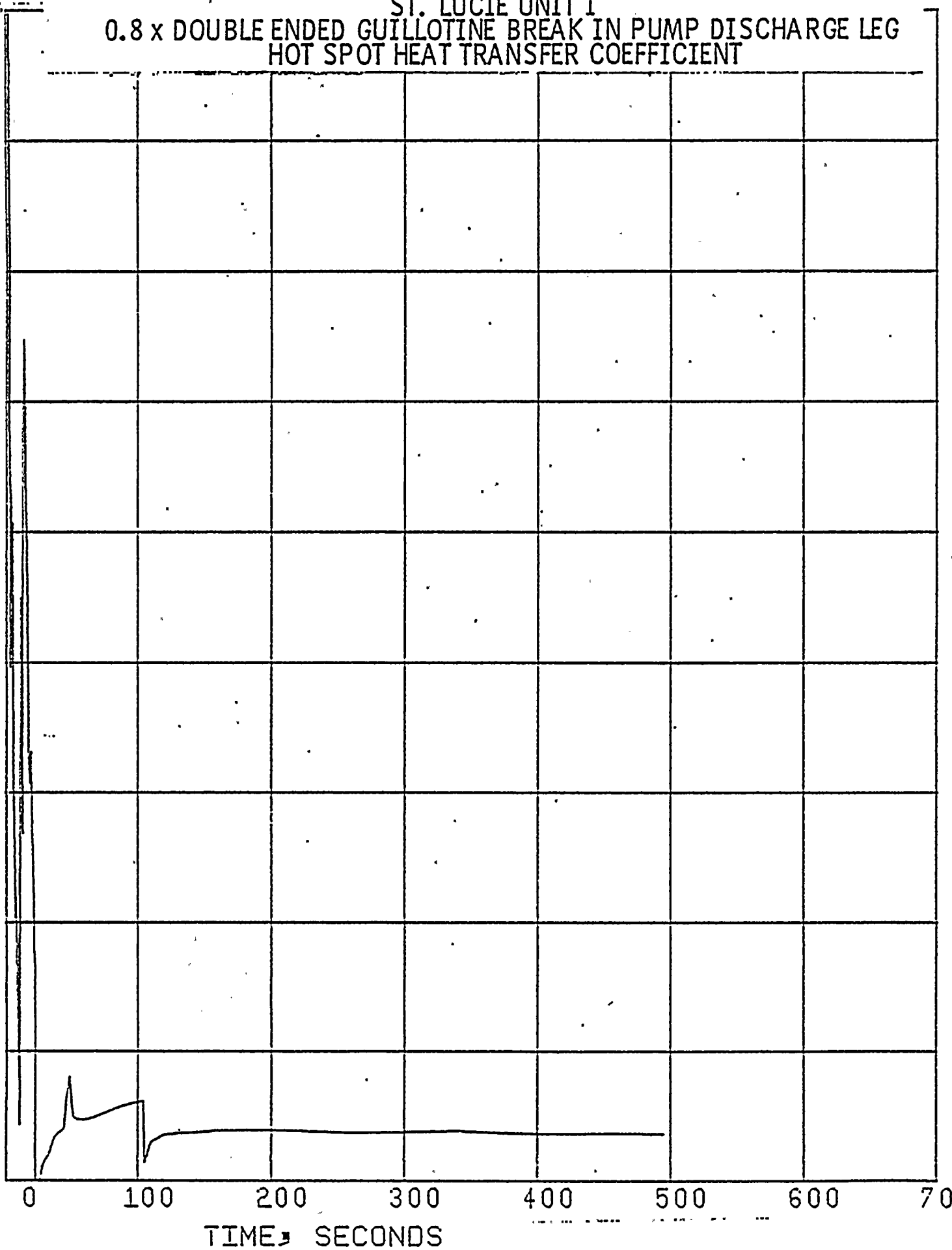




FIGURE II.6-R

ST. LUCIE UNIT I

0.8 x DOUBLE ENDED GUILLOTINE BREAK IN PUMP DISCHARGE LEG
HOT SPOT HEAT TRANSFER COEFFICIENT DURING REFLOOD

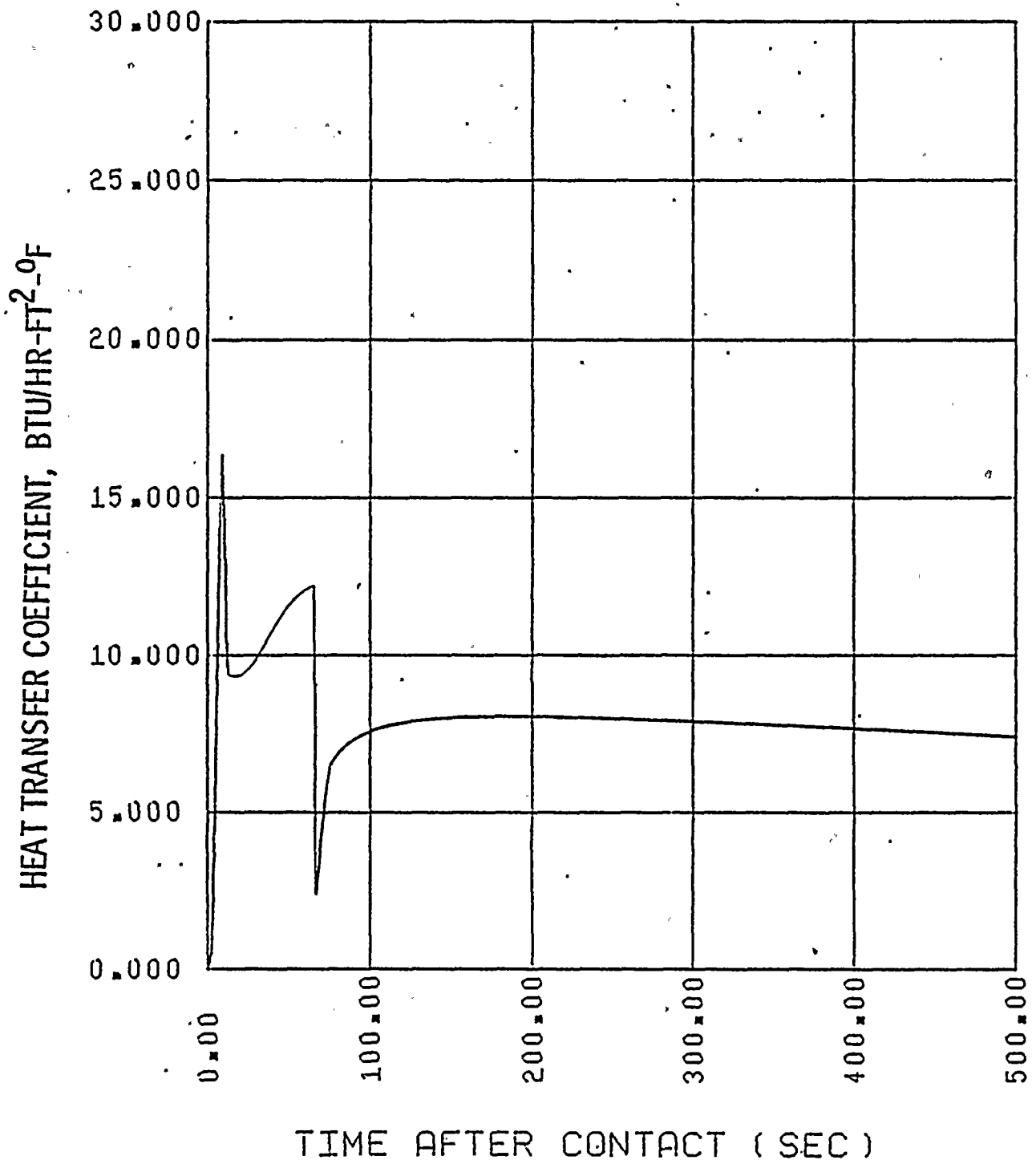




FIGURE II.6-S
ST. LUCIE UNIT I
0.8 x DOUBLE ENDED GUILLOTINE BREAK IN PUMP DISCHARGE LEG
CONTAINMENT TEMPERATURE

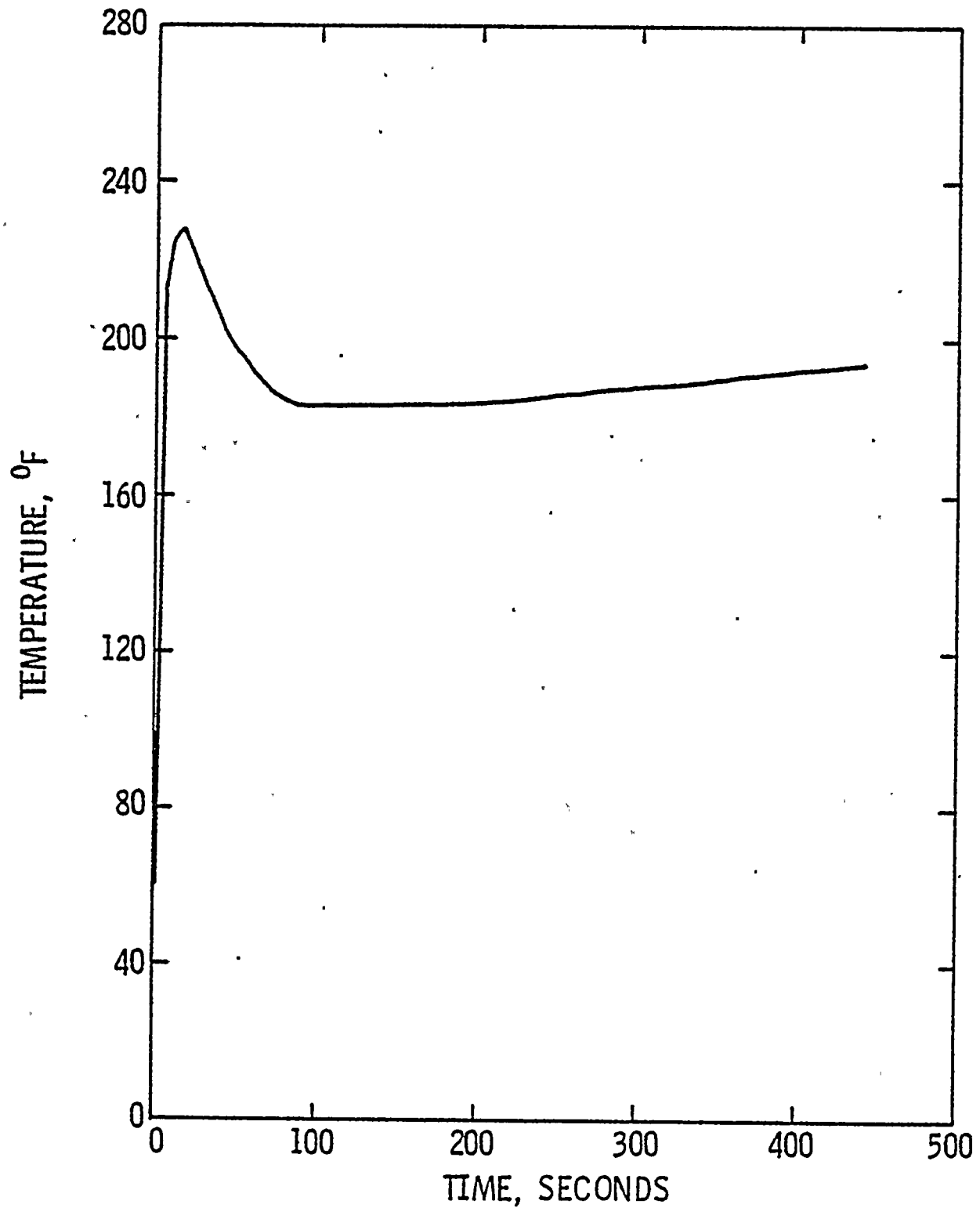




FIGURE II.6-T
ST. LUCIE UNIT I
0.8 x DOUBLE ENDED GUILLOTINE BREAK IN PUMP DISCHARGE LEG
SUMP TEMPERATURE

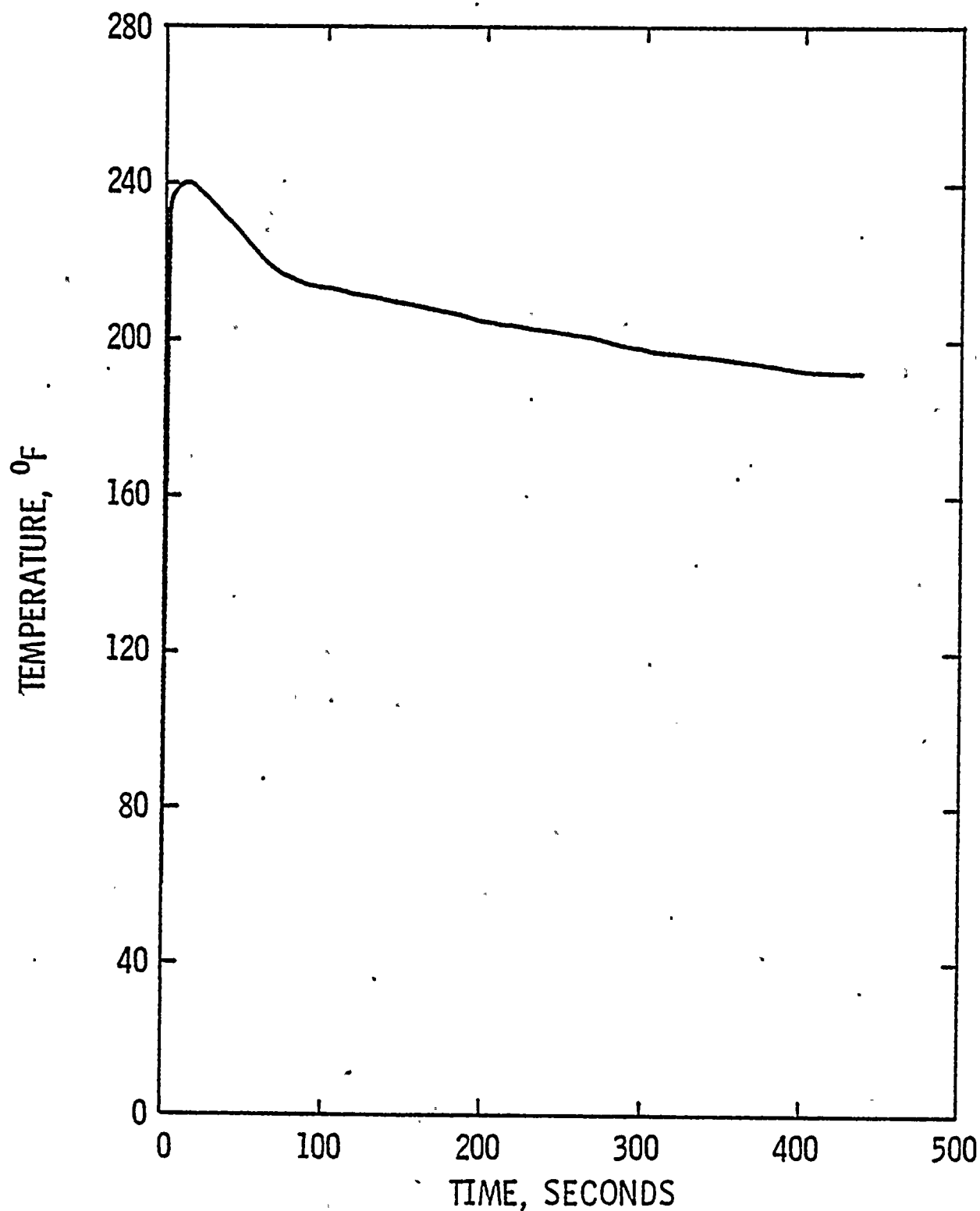




FIGURE II.6-U
ST. LUCIE UNIT I
0.8 x DOUBLE ENDED GUILLOTINE BREAK IN PUMP DISCHARGE LEG
HOT ROD INTERNAL GAS PRESSURE

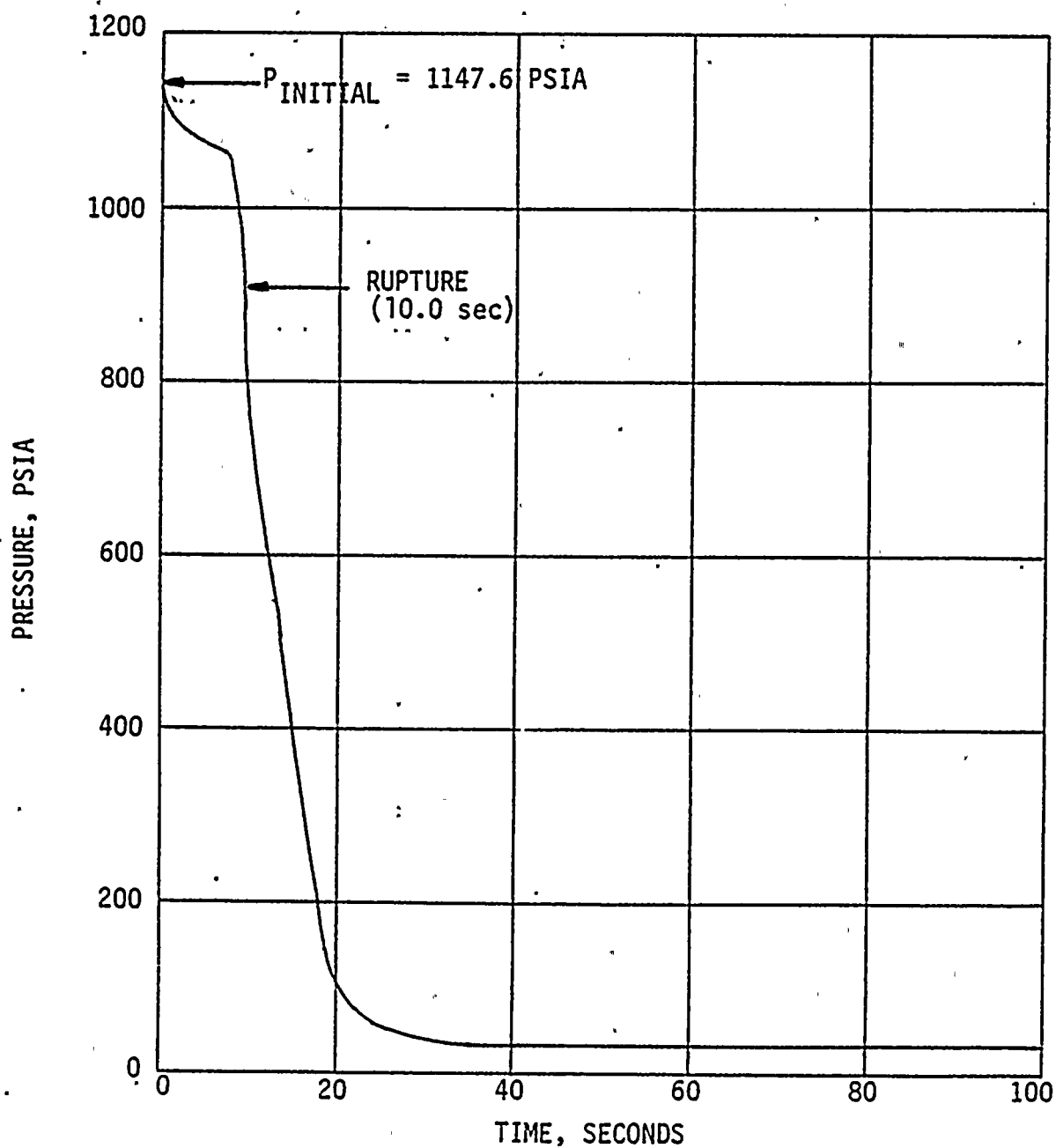




FIGURE II.6-V
ST. LUCIE UNIT I
0.8 x DOUBLE ENDED GUILLOTINE BREAK IN PUMP DISCHARGE LEG
CORE BULK CHANNEL FLOW RATE

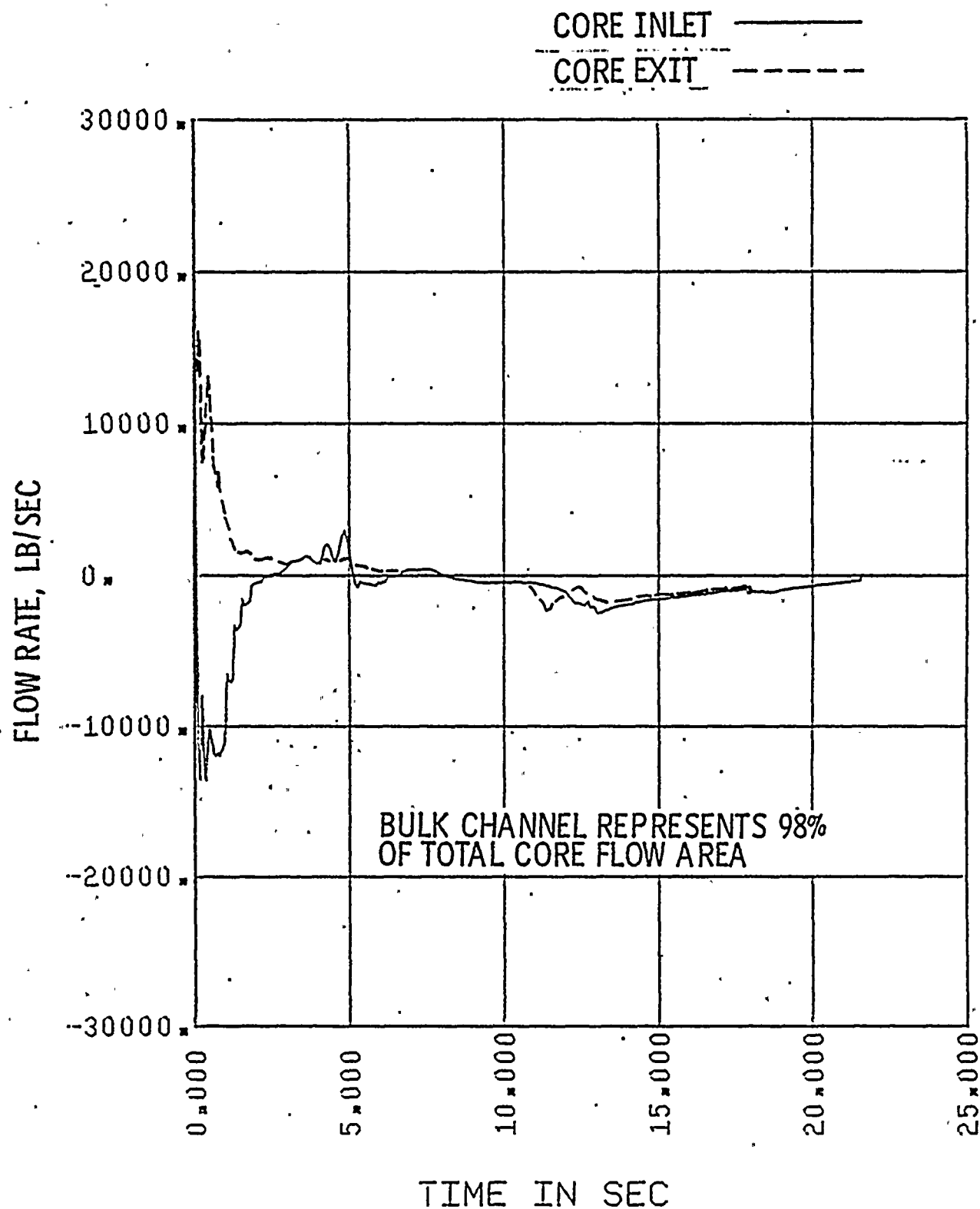
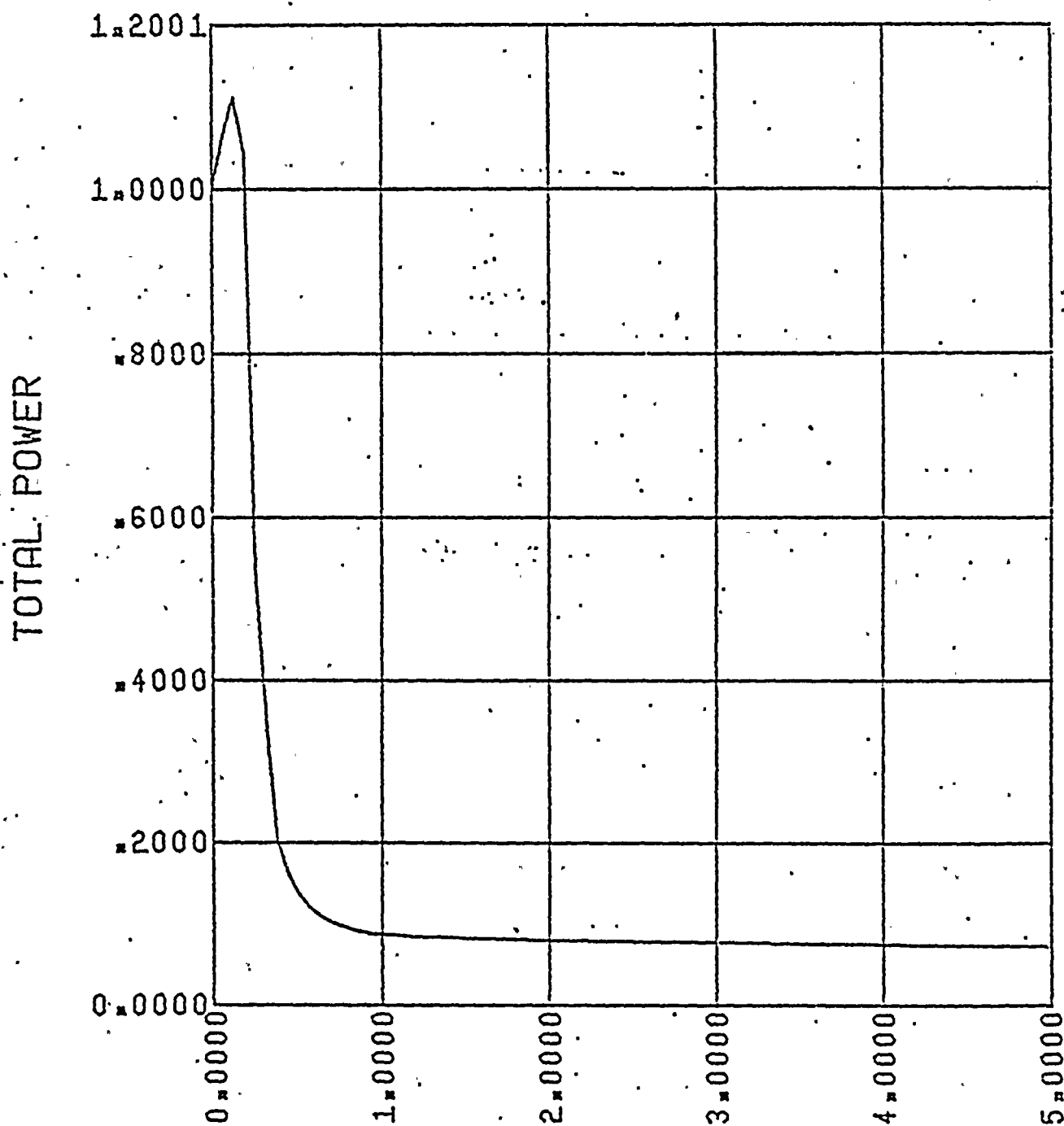


Figure II.7-A
2560 MWt PLANTS
0.6 x DOUBLE ENDED GUILLOTINE BREAK IN PUMP DISCHARGE LEG
CORE POWER



TIME IN SEC

Figure II.7-B

2560 MWt PLANTS

0.6 x DOUBLE ENDED GUILLOTINE BREAK IN PUMP DISCHARGE LEG
PRESSURE IN CENTER HOT ASSEMBLY NODE

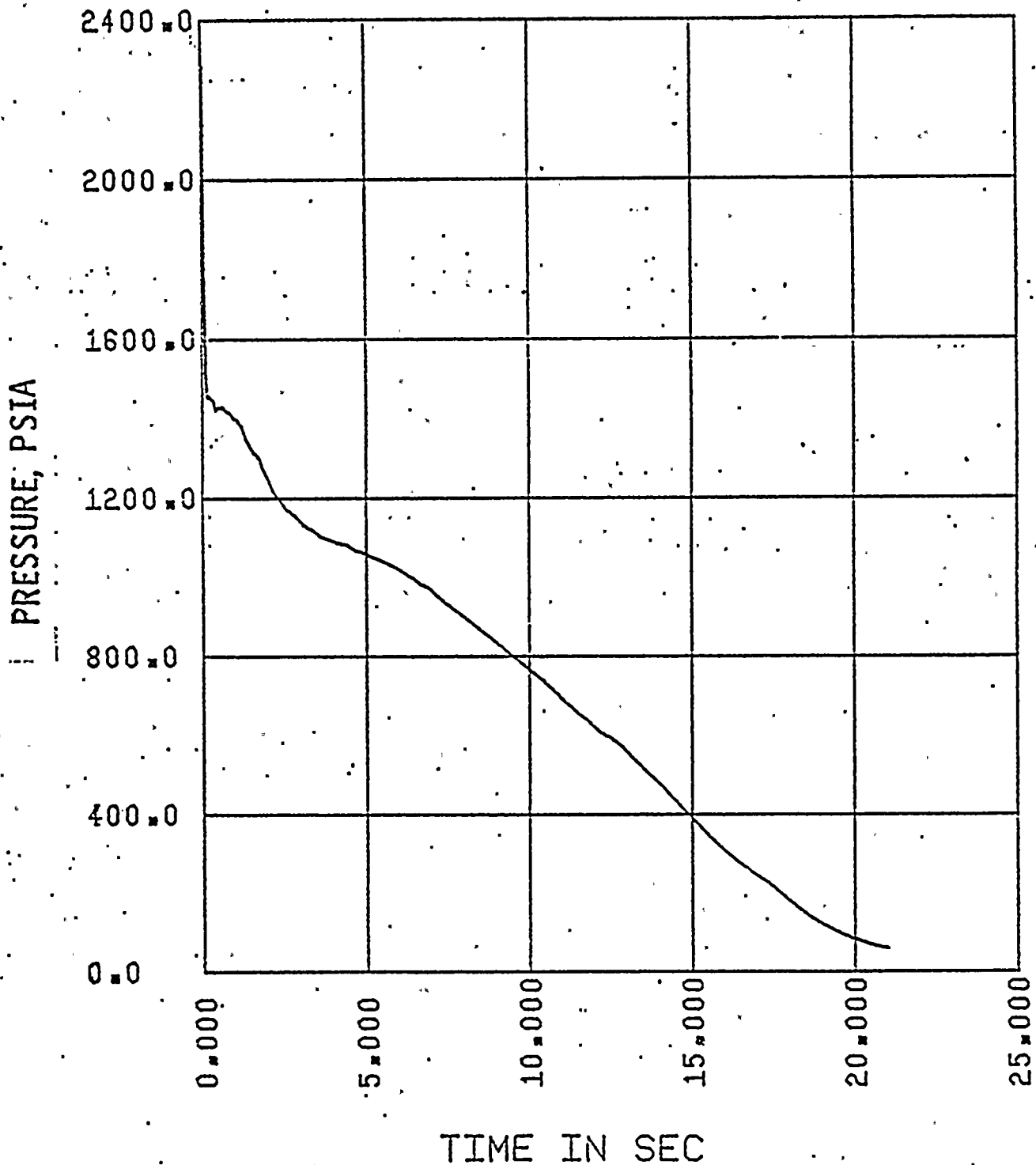




Figure II.7-C
2560 MWt PLANTS
0.6 x DOUBLE ENDED GUILLOTINE BREAK IN PUMP DISCHARGE LEG
LEAK FLOW

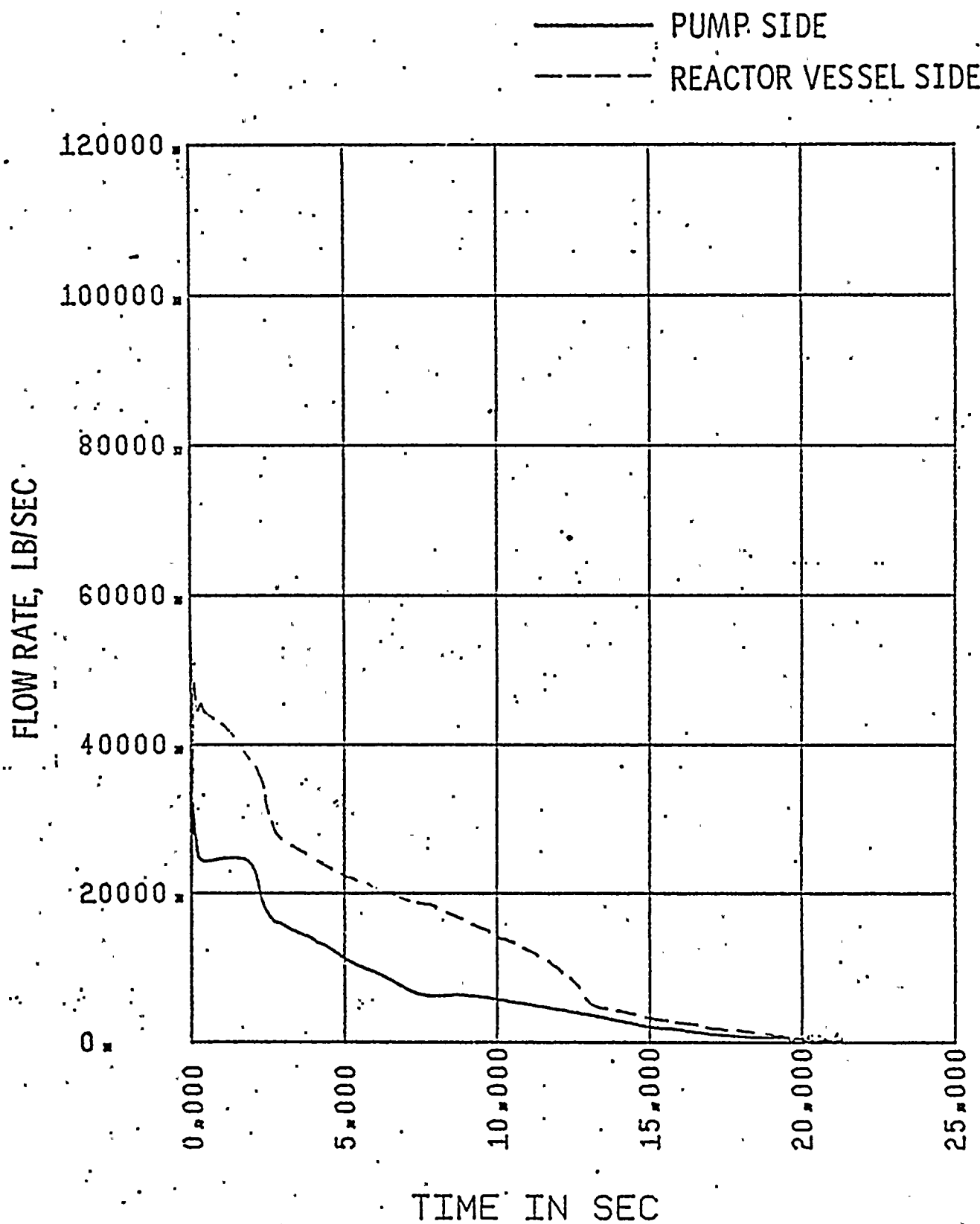
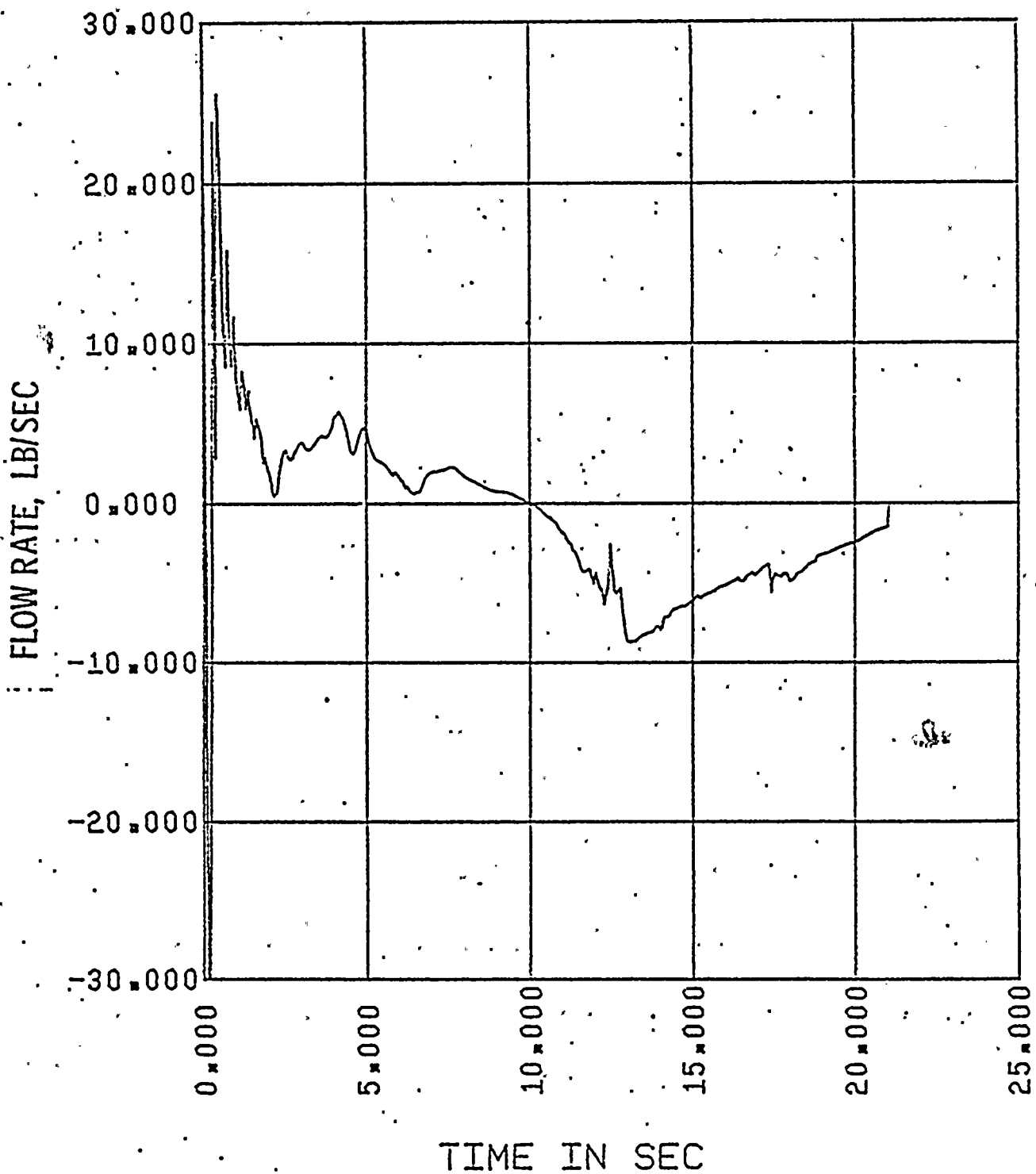




Figure II.7-D.1

2560 MWt PLANTS

0.6 x DOUBLE ENDED GUILLOTINE BREAK IN PUMP DISCHARGE LEG
FLOW IN HOT ASSEMBLY - PATH 16, BELOW HOT SPOT





22

Figure II.7-D.2

2560 MWt PLANTS

0.6 x DOUBLE ENDED GUILLOTINE BREAK IN PUMP DISCHARGE LEG
FLOW IN HOT ASSEMBLY - PATH 17, ABOVE HOT SPOT

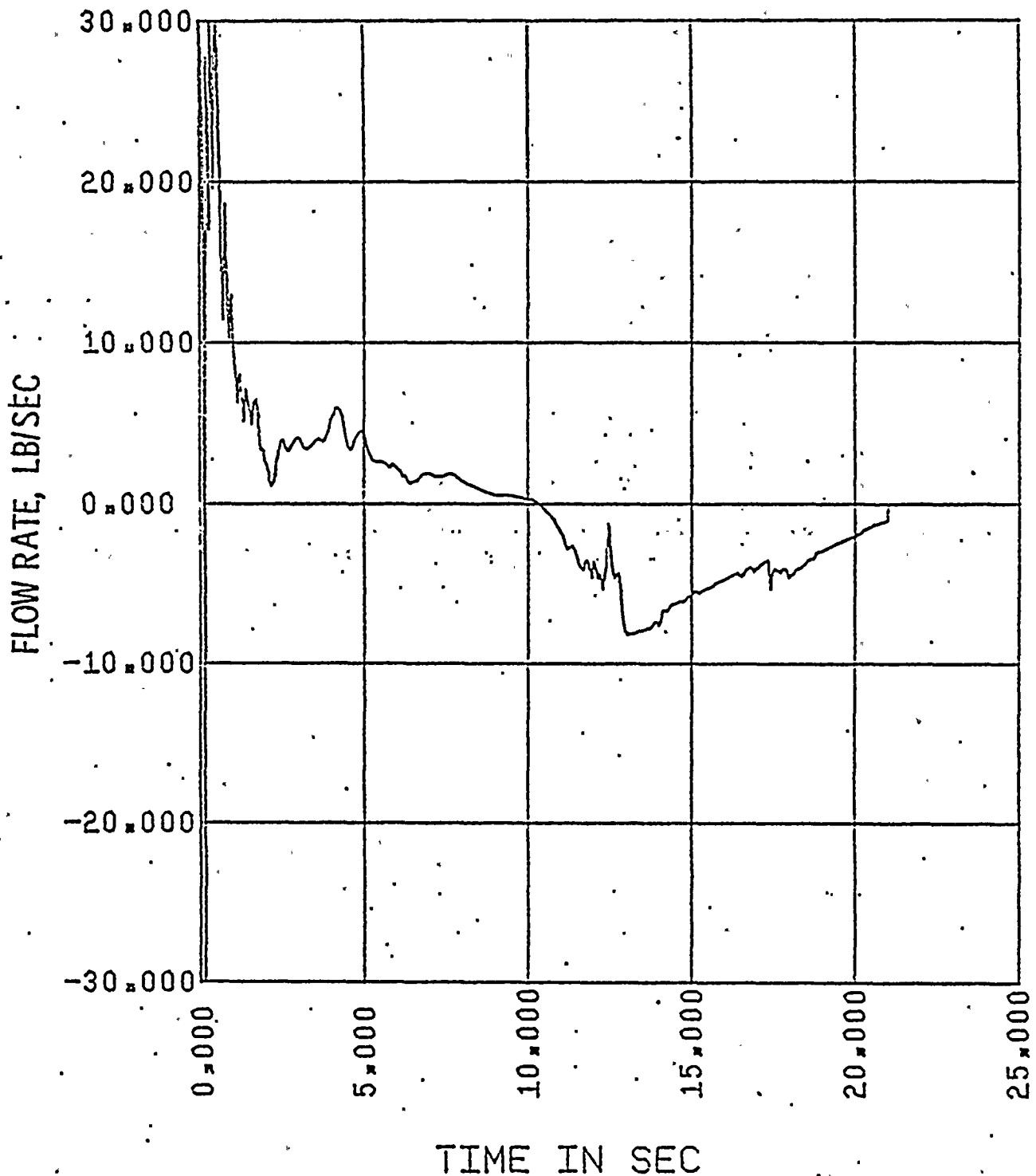


Figure II.7-E

2560 MWt PLANTS

0.6 x DOUBLE ENDED GUILLOTINE BREAK IN PUMP DISCHARGE LEG
HOT ASSEMBLY QUALITY

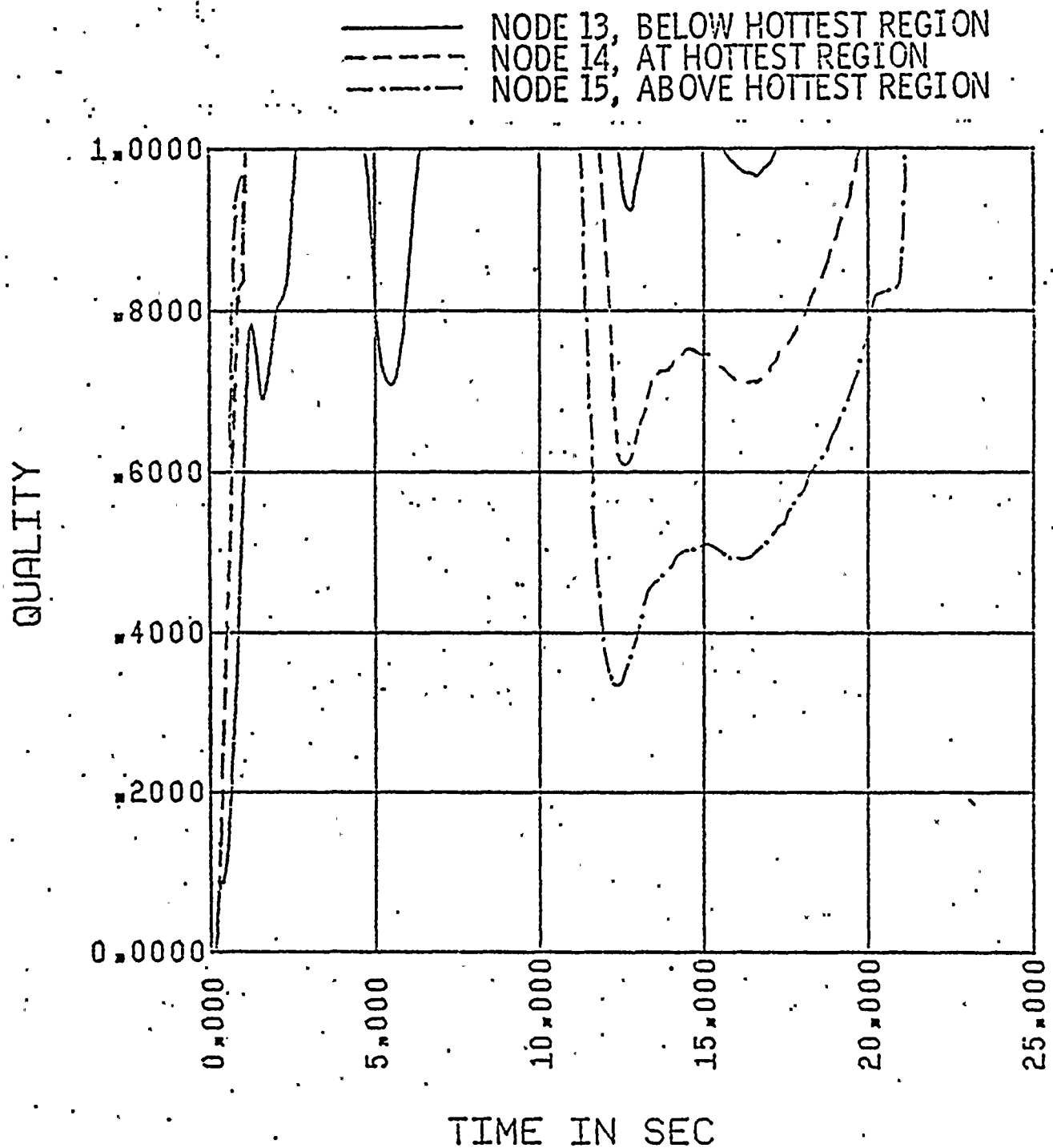




FIGURE II.7-F
ST. LUCIE UNIT I
0.6 x DOUBLE ENDED GUILLOTINE BREAK IN PUMP DISCHARGE LEG
CONTAINMENT PRESSURE

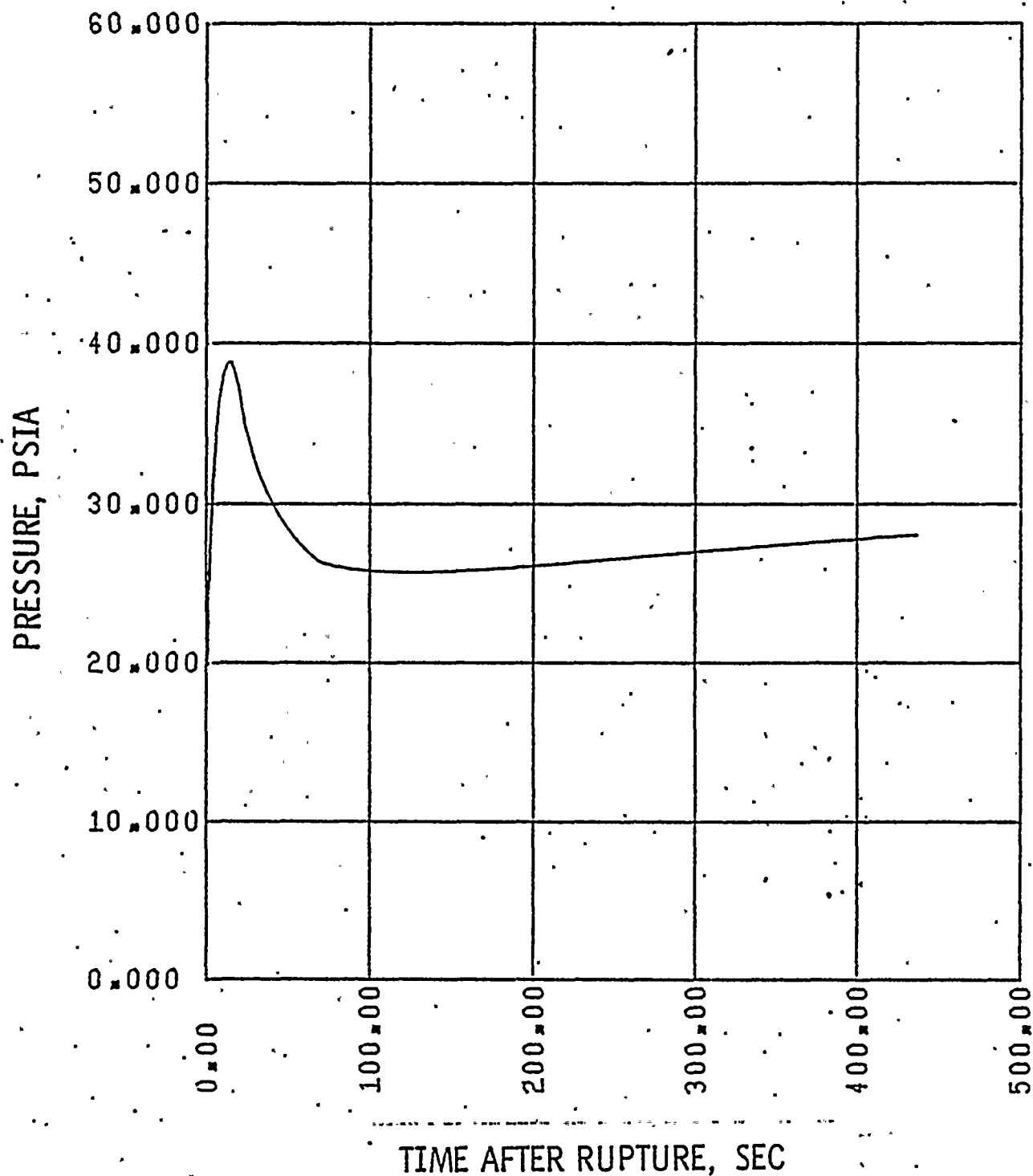




FIGURE II.7-G
ST. LUCIE UNIT I
0.6 x DOUBLE ENDED GUILLOTINE BREAK IN PUMP DISCHARGE LEG
MASS ADDED TO CORE DURING REFLOOD

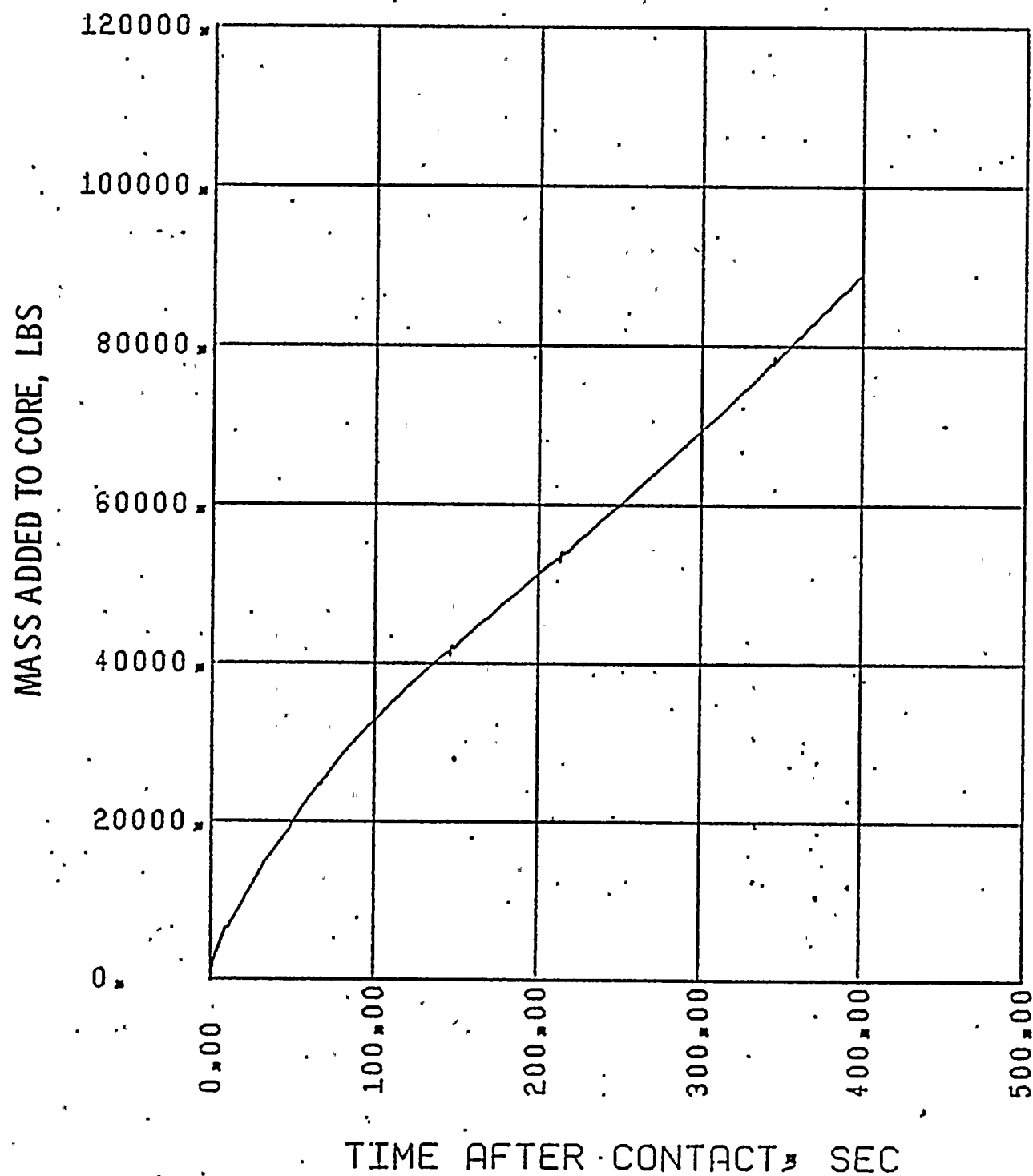




FIGURE II.7-H
ST. LUCIE UNIT I
0.6 x DOUBLE ENDED GUILLOTINE BREAK IN PUMP DISCHARGE LEG
PEAK CLAD TEMPERATURE

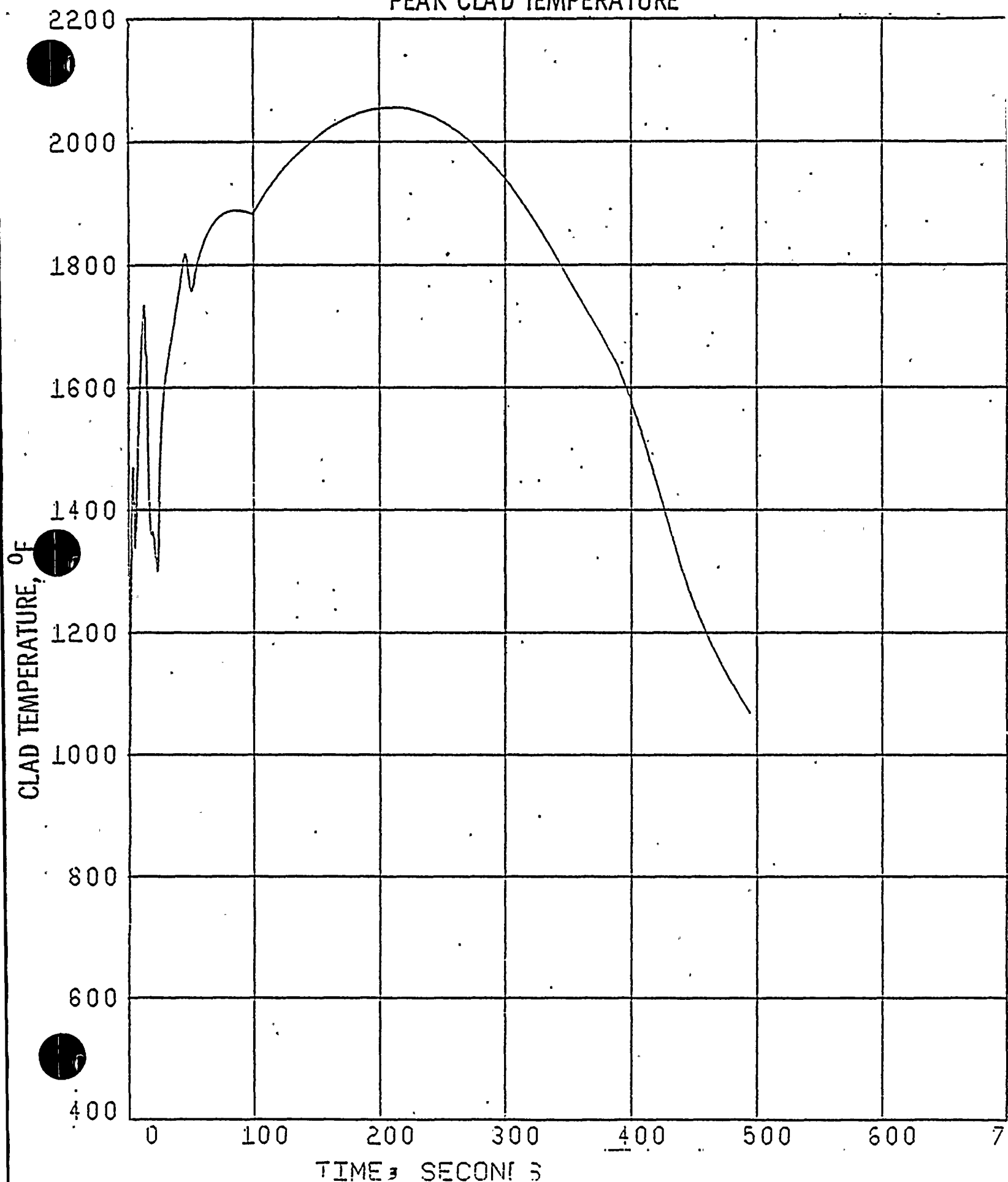


Figure II.8
ST. LUCIE UNIT I
PEAK CLAD TEMPERATURE vs BREAK AREA
(PEAK LHGR = 15.8 KW/FT)

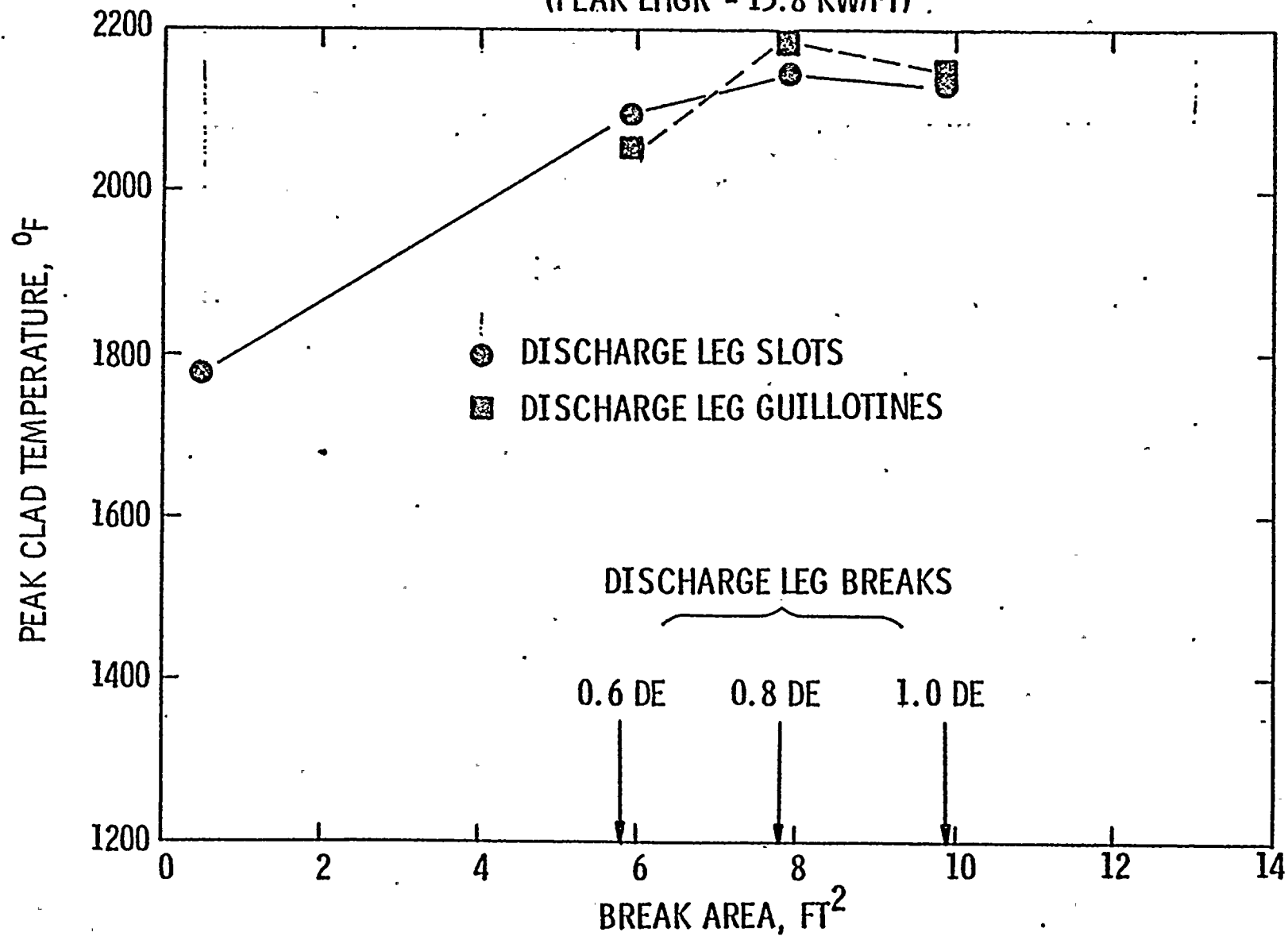


Figure II.9
ST. LUCIE I
COMBINED SPILLAGE AND SPRAY INTO CONTAINMENT

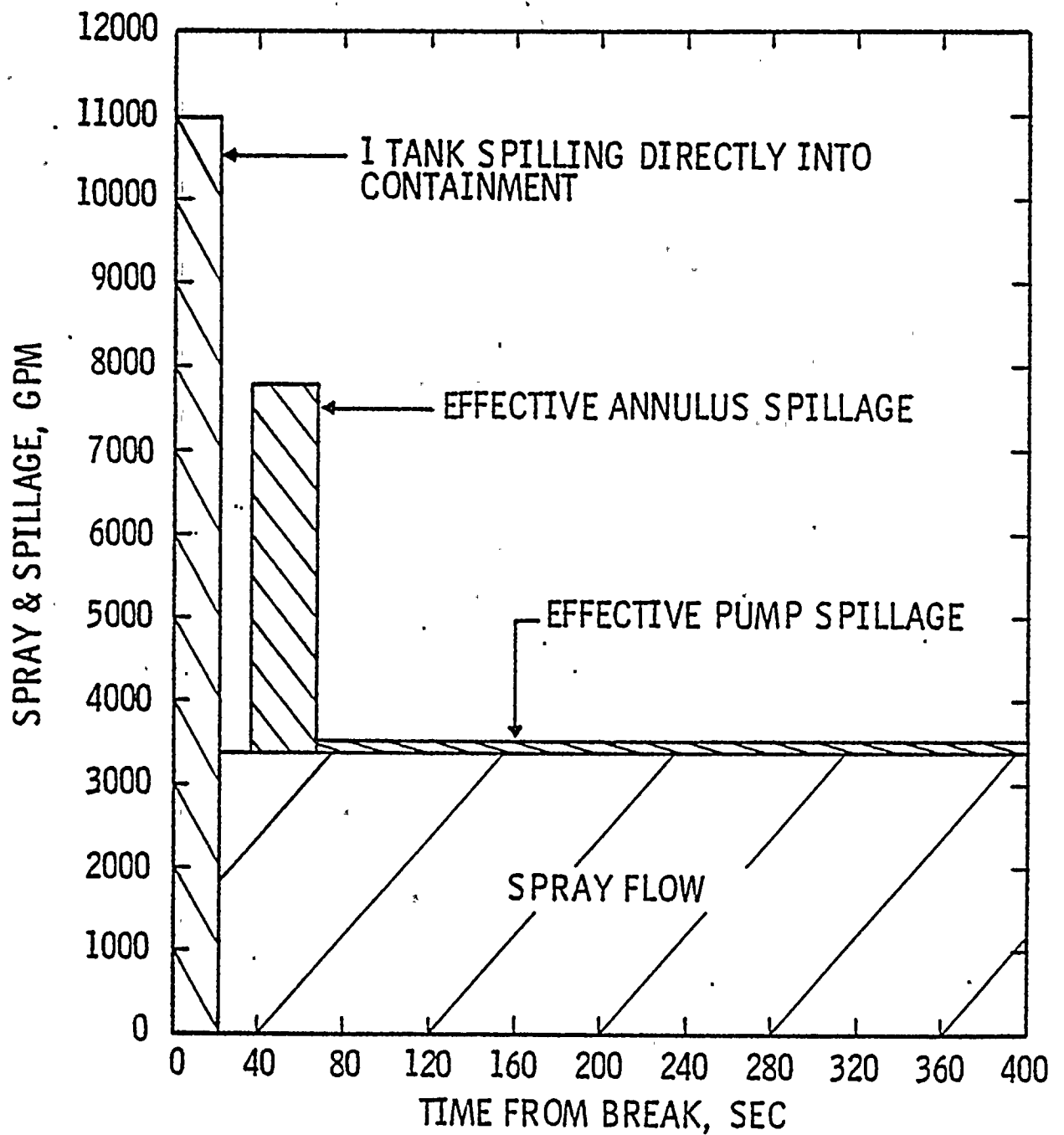


FIGURE III.A
ST. LUCIE UNIT I
ISOLATED SAFETY INJECTION TANK
0.8 x DOUBLE ENDED GUILLOTINE BREAK IN PUMP DISCHARGE LEG
CORE POWER

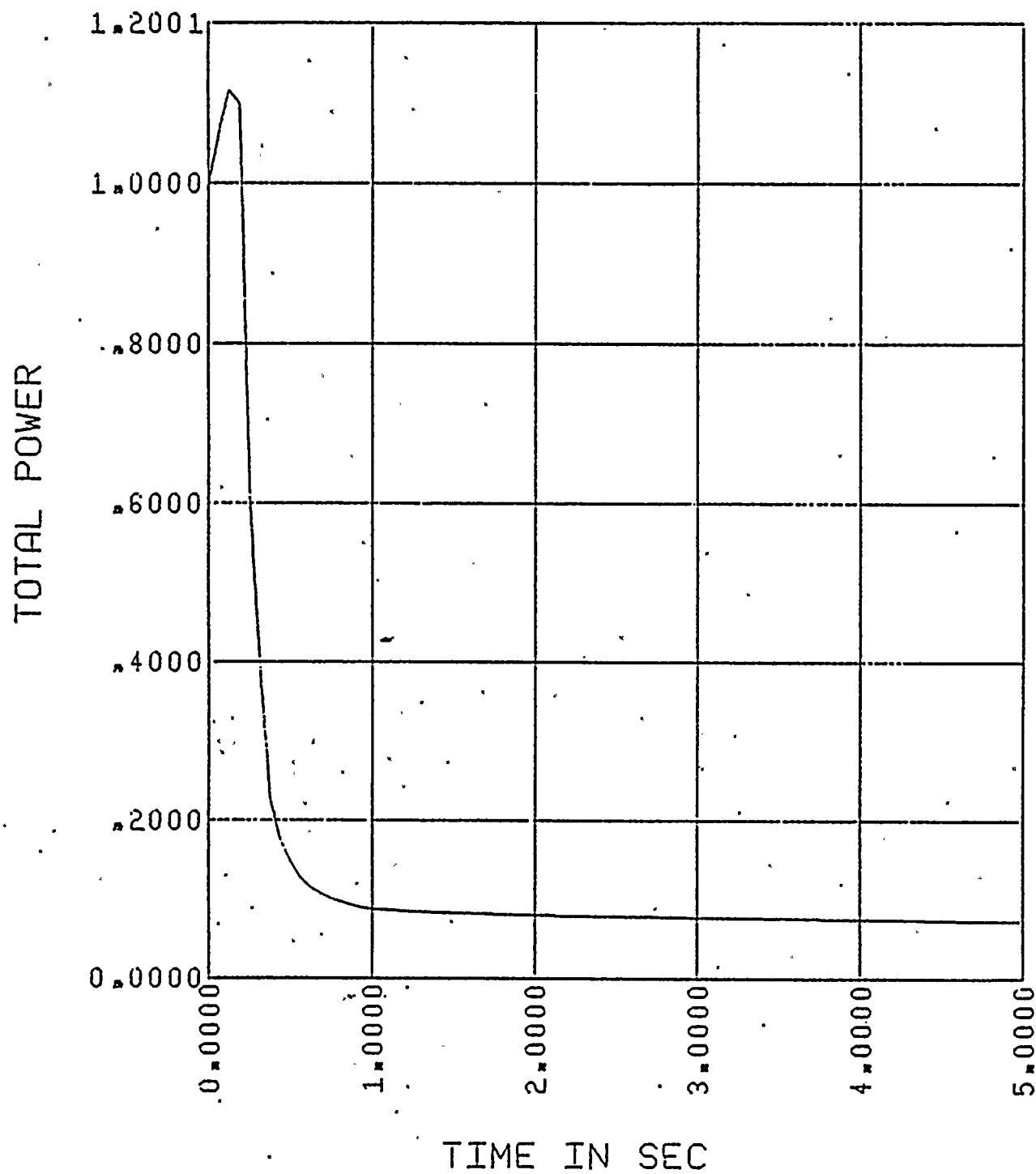


FIGURE III. B
ST. LUCIE UNIT I
ISOLATED SAFETY INJECTION TANK
0.8 x DOUBLE ENDED GUILLOTINE BREAK IN PUMP DISCHARGE LEG
PRESSURE IN CENTER HOT ASSEMBLY NODE

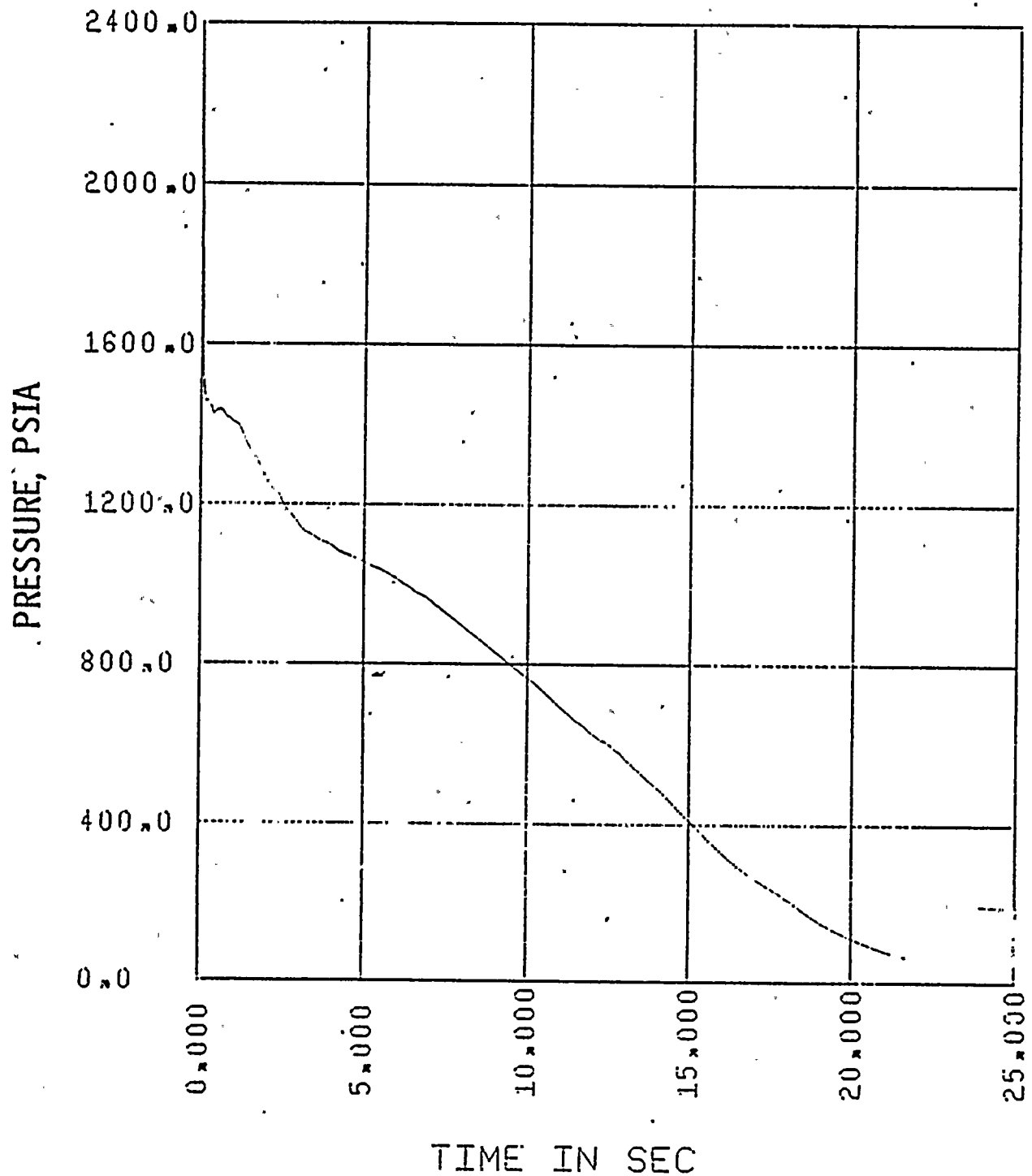


FIGURE III. C
ST. LUCIE UNIT I
ISOLATED SAFETY INJECTION TANK
0.8 x DOUBLE ENDED GUILLOTINE BREAK IN PUMP DISCHARGE LEG
LEAK FLOW

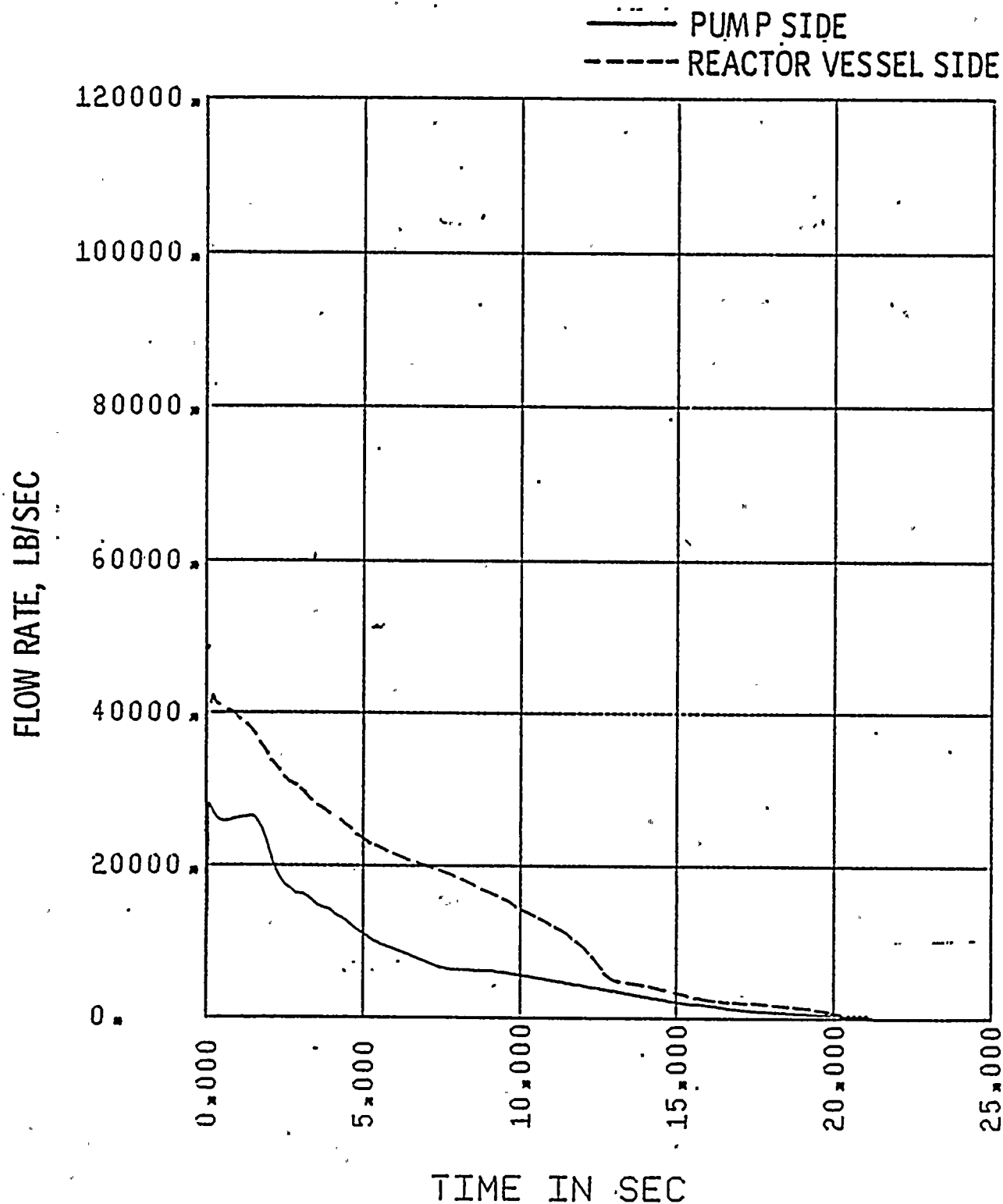




FIGURE III.D.1
ST. LUCIE UNIT I
ISOLATED SAFETY INJECTION TANK
0.8 x DOUBLE ENDED GUILLOTINE BREAK IN PUMP DISCHARGE LEG
FLOW IN HOT ASSEMBLY - PATH 16, BELOW HOT SPOT

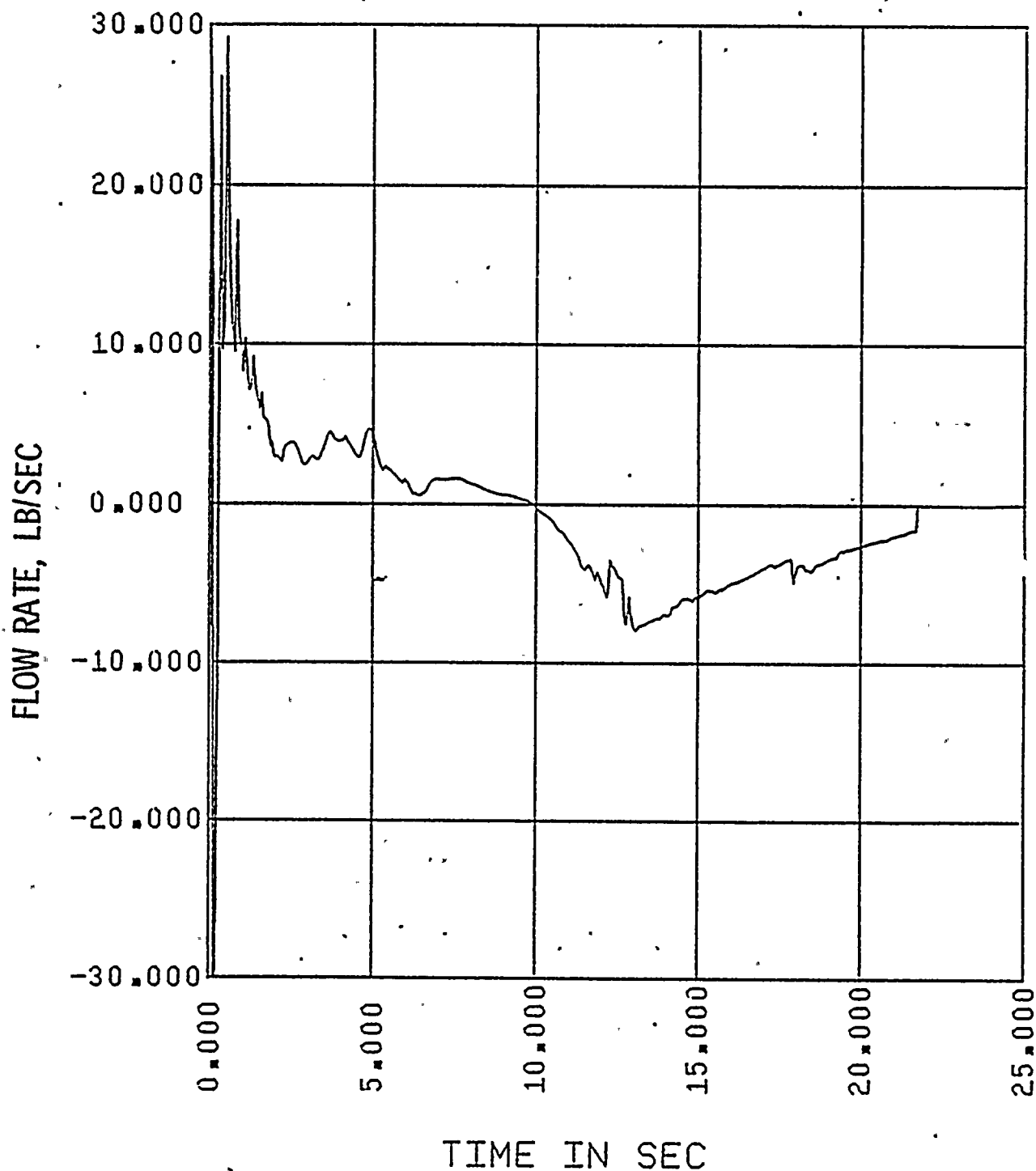




FIGURE III. D. 2
ST. LUCIE UNIT I
ISOLATED SAFETY INJECTION TANK
0.8 x DOUBLE ENDED GUILLOTINE BREAK IN PUMP DISCHARGE LEG
FLOW IN HOT ASSEMBLY - PATH 17, ABOVE HOT SPOT

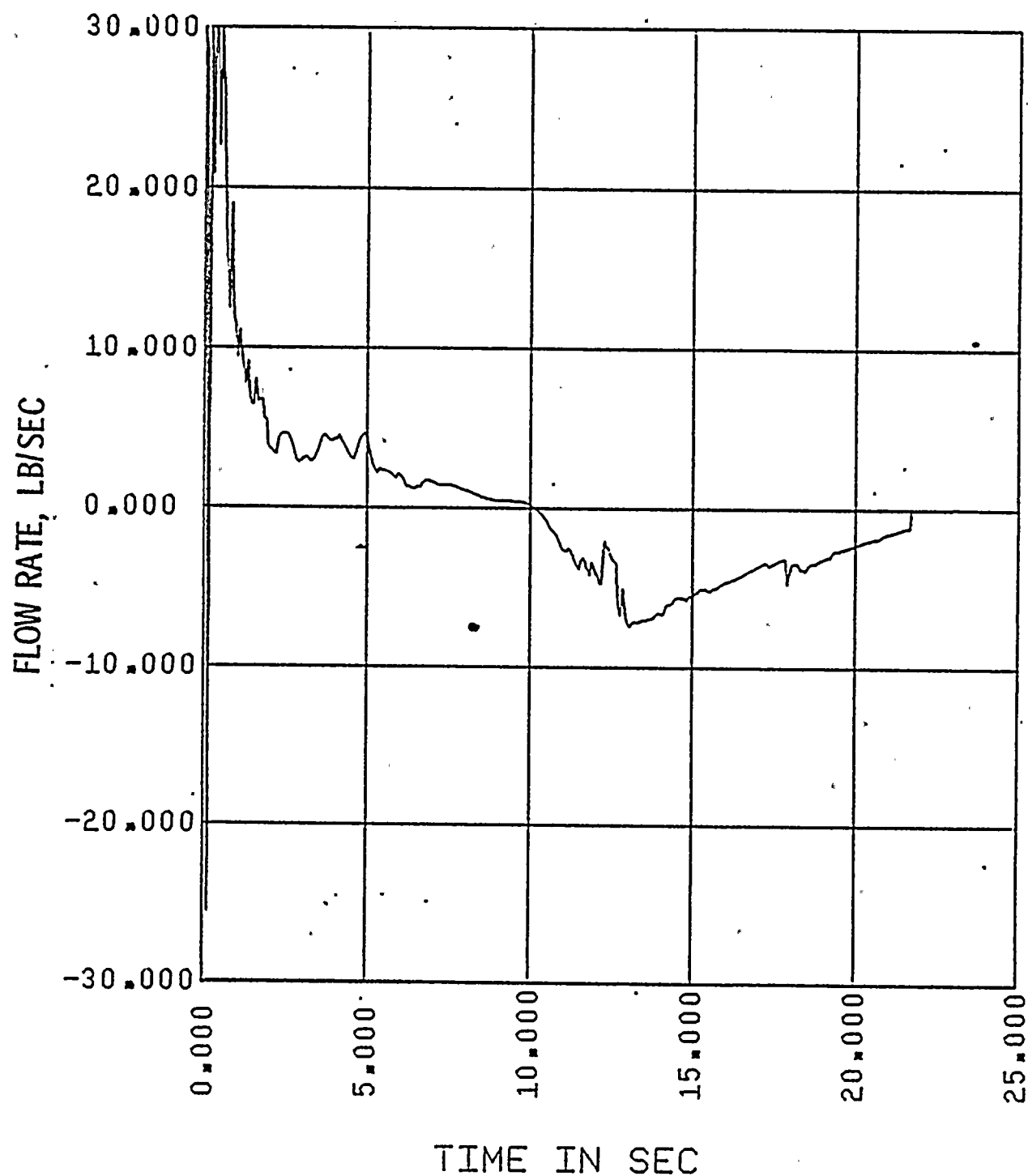


FIGURE III.E
 ST. LUCIE UNIT I
 ISOLATED SAFETY INJECTION TANK
 0.8 x DOUBLE ENDED GUILLOTINE BREAK IN PUMP DISCHARGE LEG
 HOT ASSEMBLY QUALITY

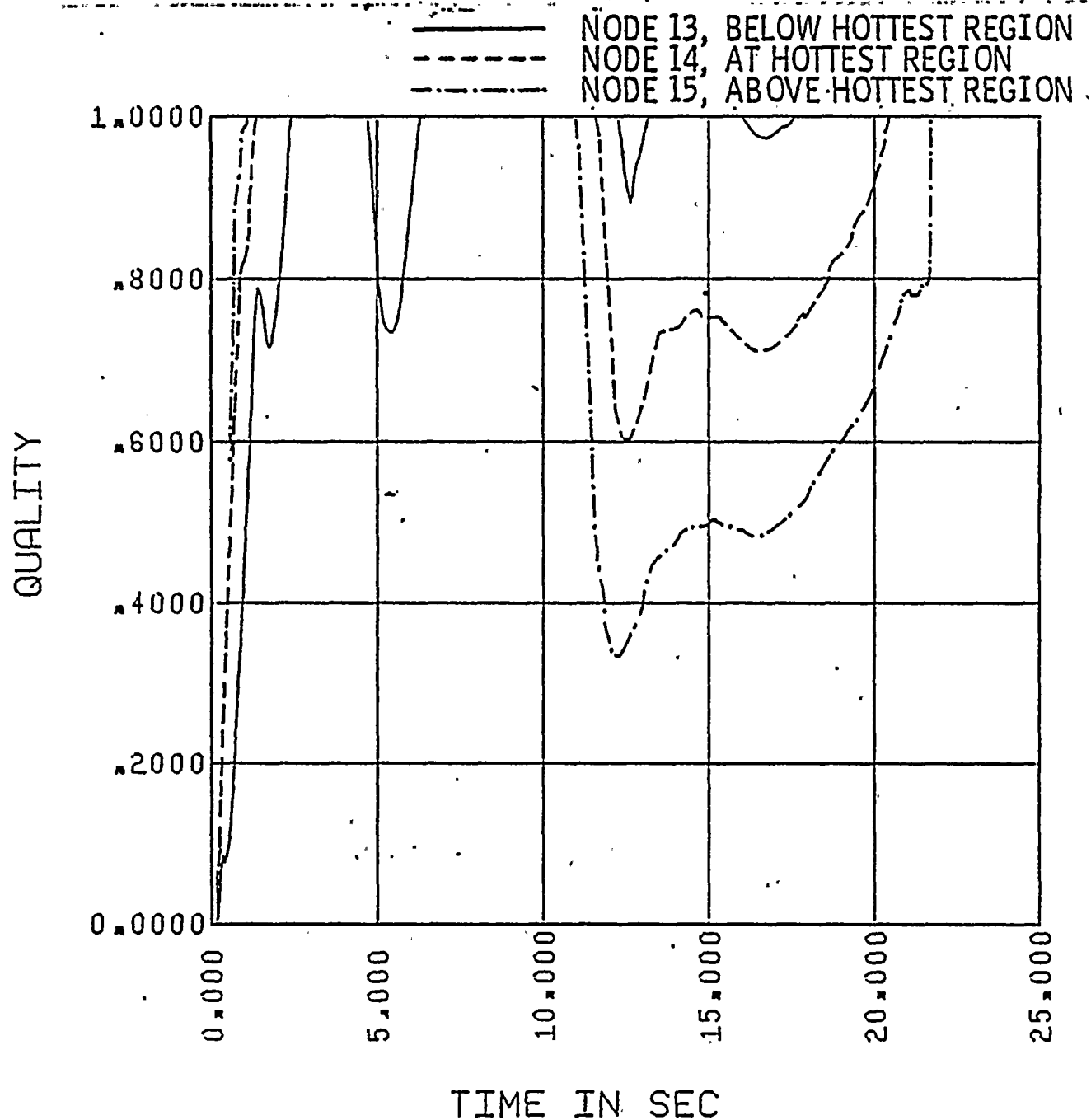


FIGURE III.F
ST. LUCIE UNIT I
ISOLATED SAFETY INJECTION TANK
0.8 x DOUBLE ENDED GUILLOTINE BREAK IN PUMP DISCHARGE LEG
CONTAINMENT PRESSURE

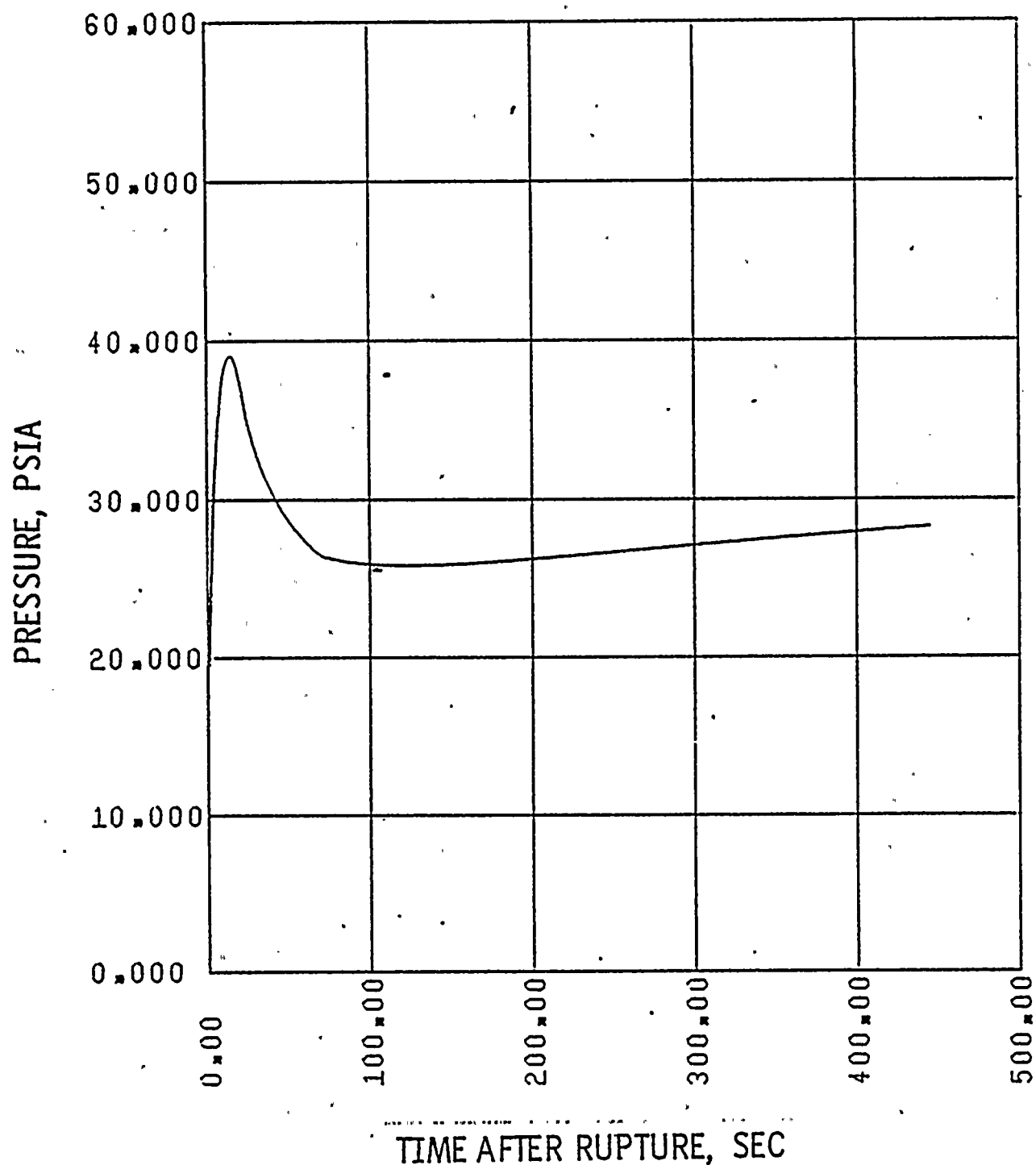




FIGURE III. G
 ST. LUCIE UNIT I
 ISOLATED SAFETY INJECTION TANK
 0.8 x DOUBLE ENDED GUILLOTINE BREAK IN PUMP DISCHARGE LEG
 MASS ADDED TO CORE DURING REFLOOD

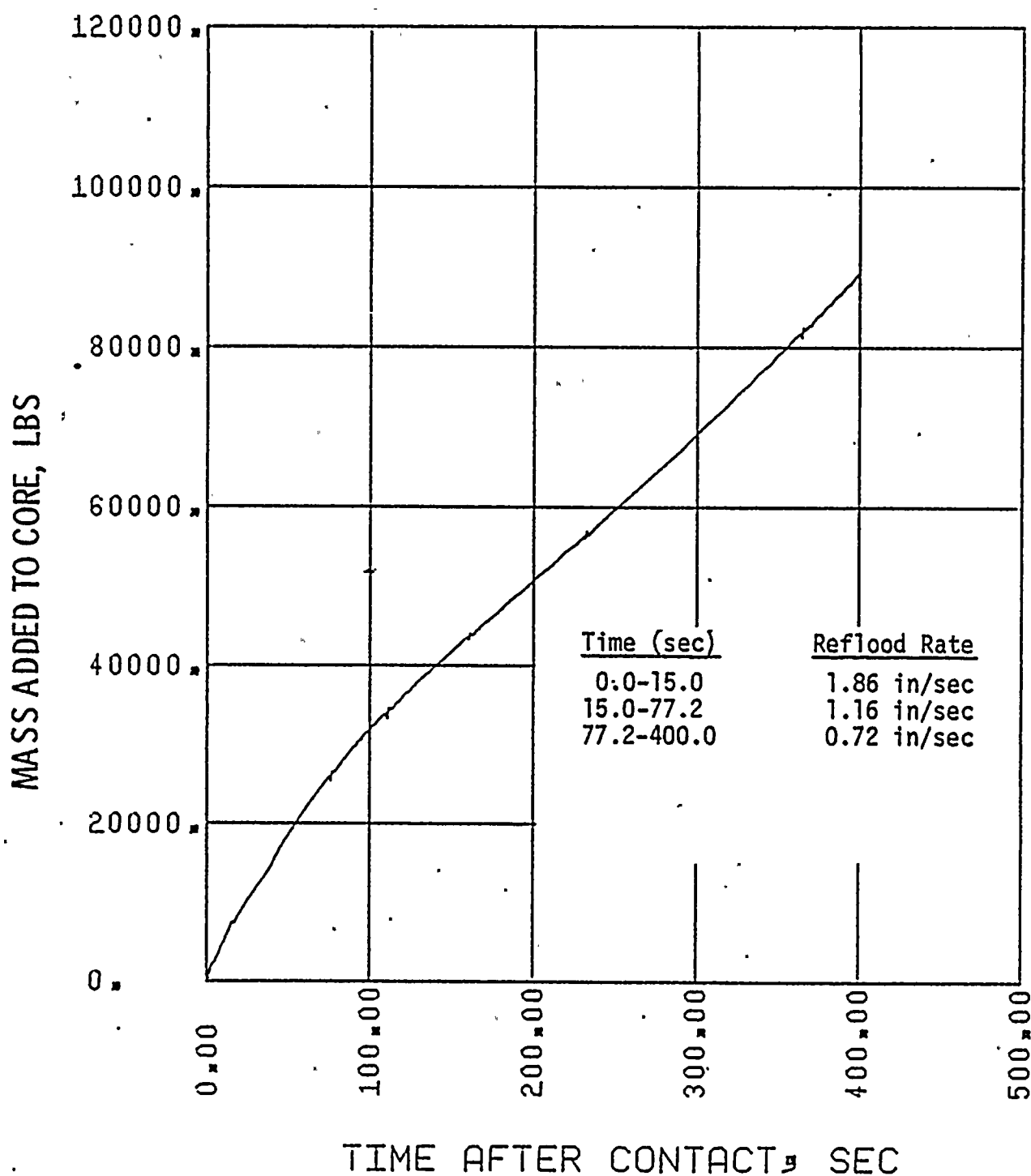




FIGURE III.H

ST. LUCIE UNIT I
ISOLATED SAFETY INJECTION TANK
0.8 x DOUBLE ENDED GUILLOTINE BREAK IN PUMP DISCHARGE LEG
PEAK CLAD TEMPERATURE

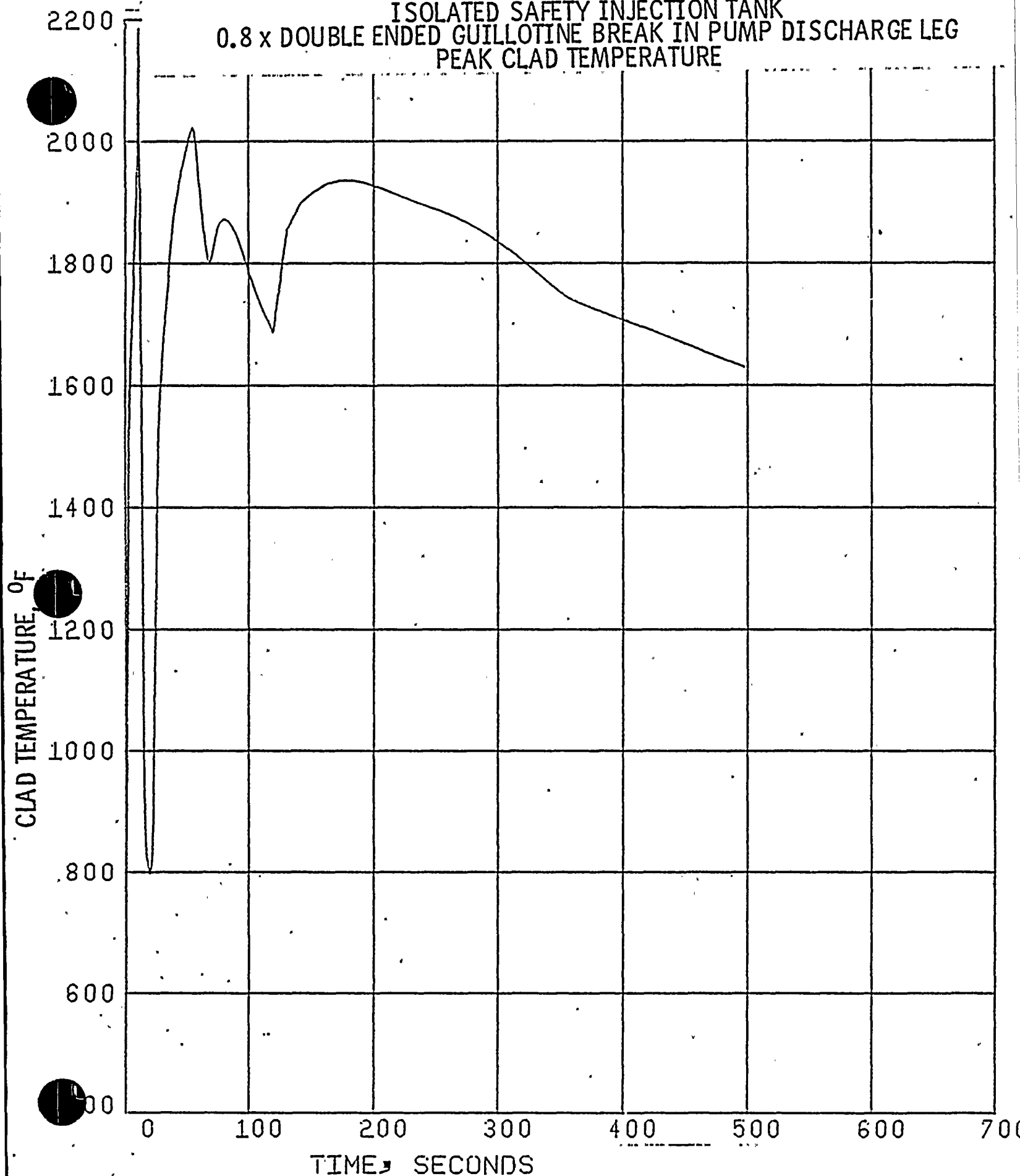


FIGURE III.I
ST. LUCIE UNIT I
ISOLATED SAFETY INJECTION TANK
0.8 x DOUBLE ENDED GUILLOTINE BREAK IN PUMP DISCHARGE LEG
MID-ANNULUS FLOW

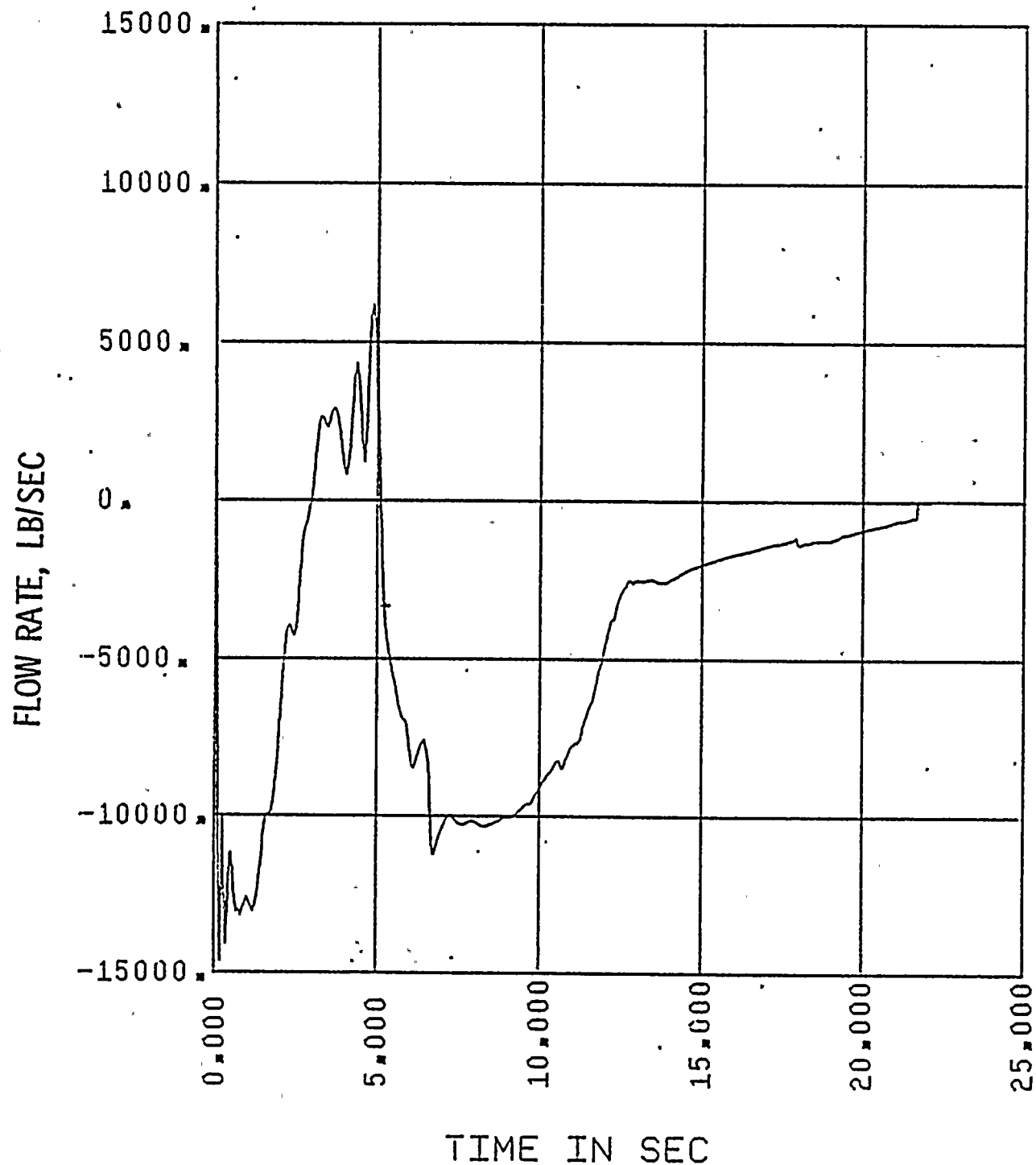


FIGURE III. J
ST. LUCIE UNIT I
ISOLATED SAFETY INJECTION TANK
0.8 x DOUBLE ENDED GUILLOTINE BREAK IN PUMP DISCHARGE LEG
QUALITIES ABOVE AND BELOW THE CORE

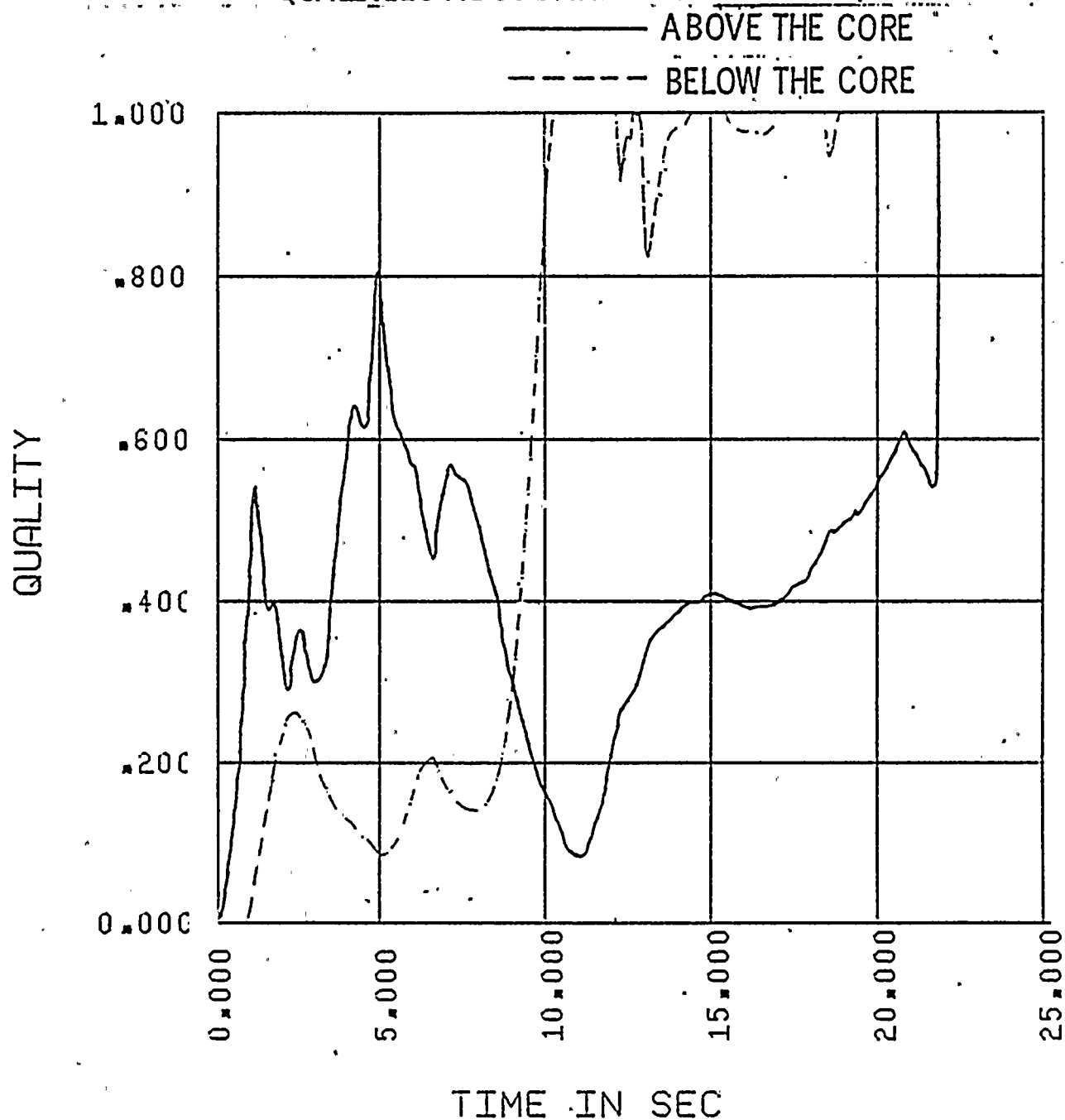


FIGURE III.K
ST. LUCIE UNIT I
ISOLATED SAFETY INJECTION TANK
0.8 x DOUBLE ENDED GUILLOTINE BREAK IN PUMP DISCHARGE LEG
CORE PRESSURE DROP

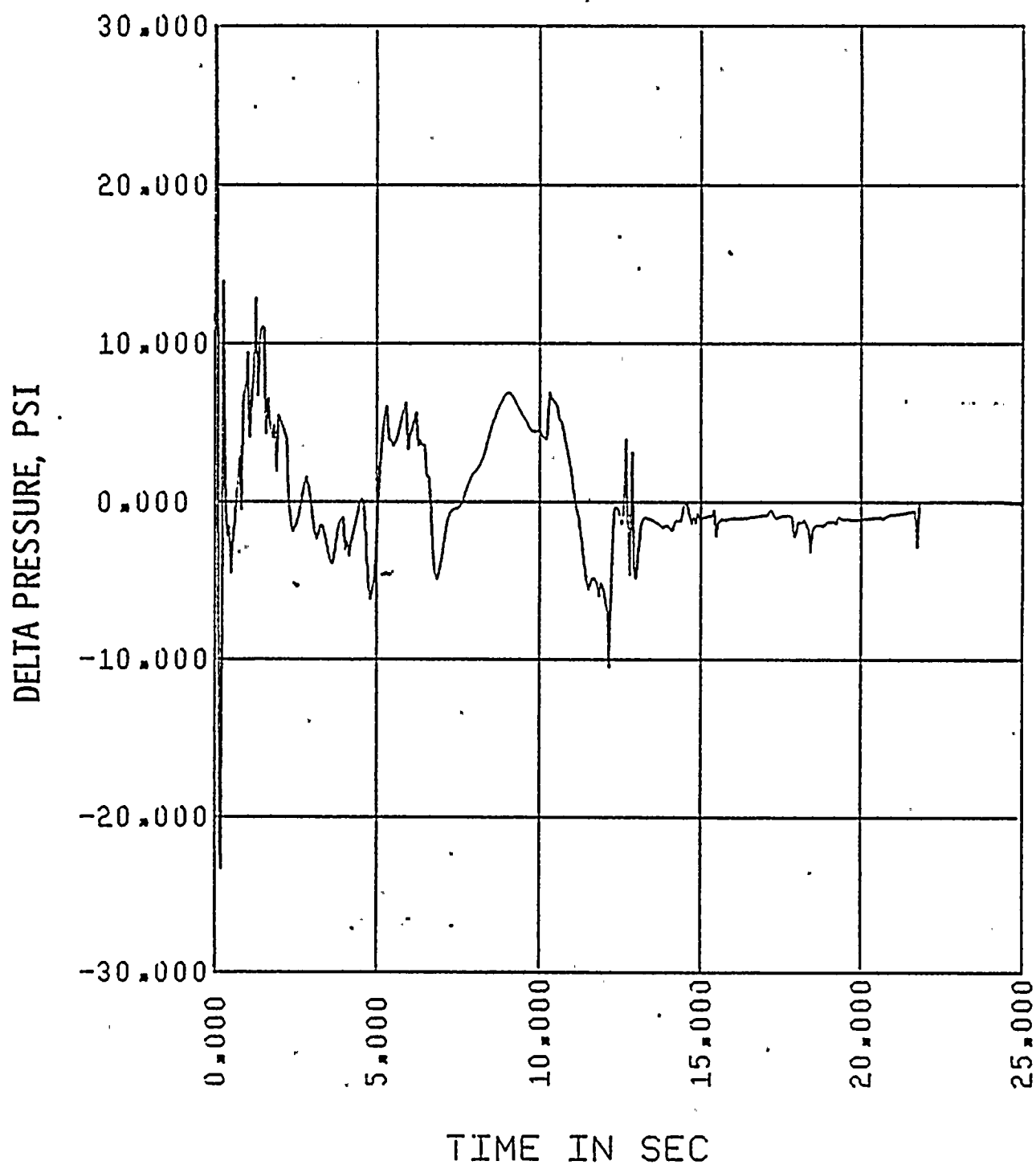


FIGURE III.L
ST. LUCIE UNIT I
ISOLATED SAFETY INJECTION TANK
0.8 x DOUBLE ENDED GUILLOTINE BREAK IN PUMP DISCHARGE LEG
SAFETY INJECTION FLOW INTO INTACT DISCHARGE LEGS

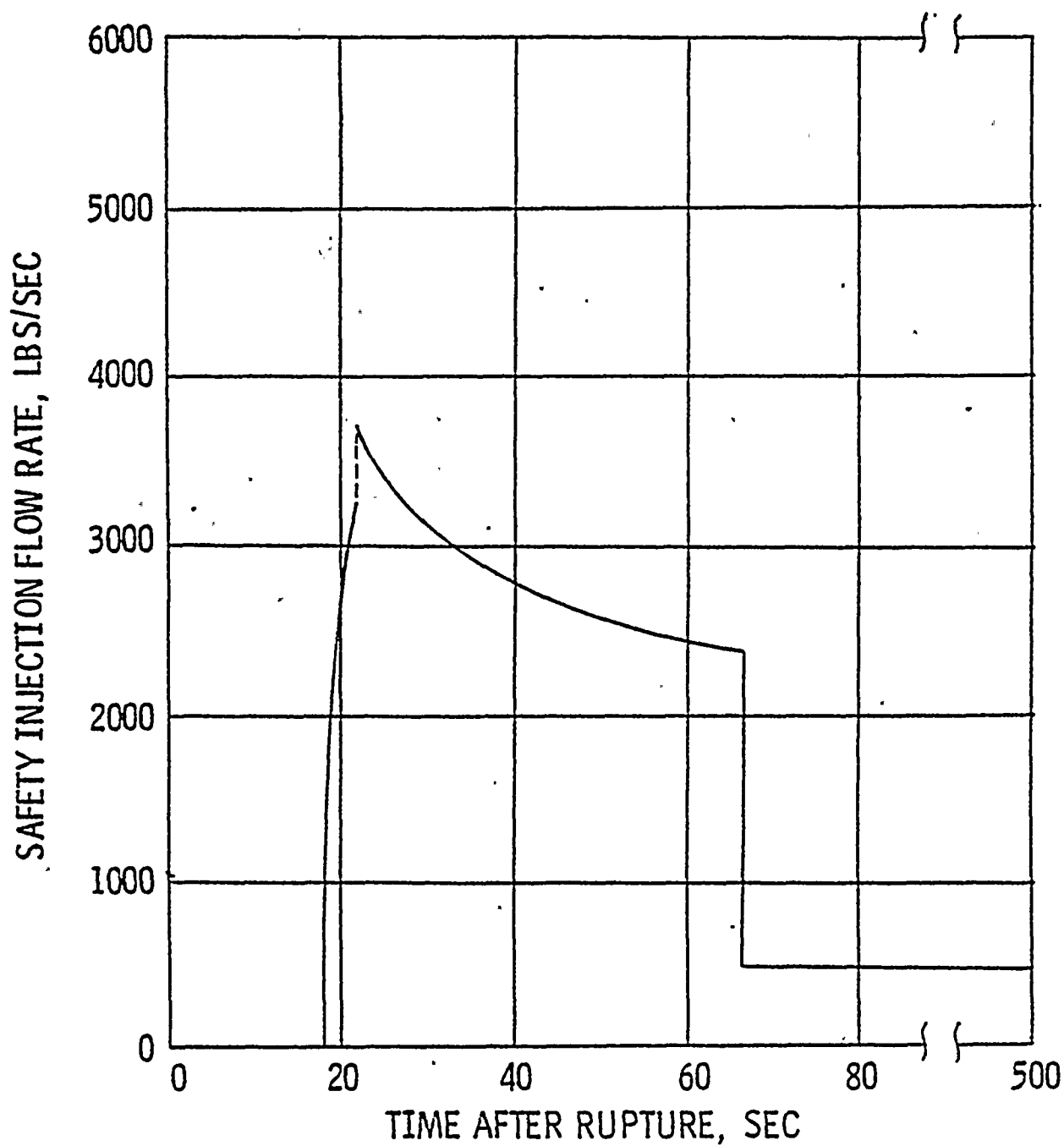


FIGURE III.M
ST. LUCIE UNIT I
ISOLATED SAFETY INJECTION TANK
0.8 x DOUBLE ENDED GUILLOTINE BREAK IN PUMP DISCHARGE LEG
WATER LEVEL IN DOWNCOMER DURING REFLOOD

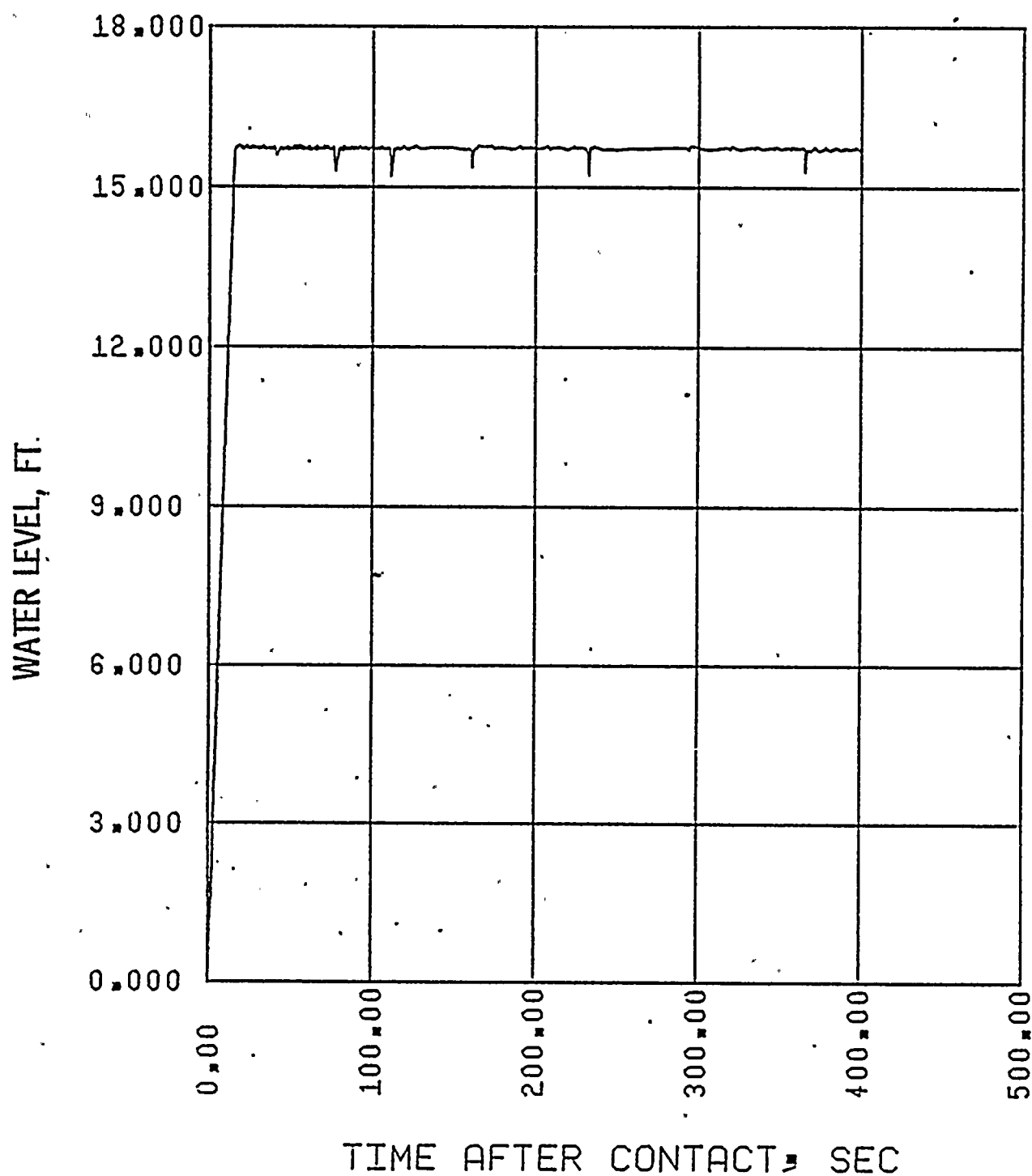


FIGURE III.N

ST. LUCIE UNIT I

ISOLATED SAFETY INJECTION TANK

0.8 x DOUBLE ENDED GUILLOTINE BREAK IN PUMP DISCHARGE LEG

HOT SPOT GAP CONDUCTANCE

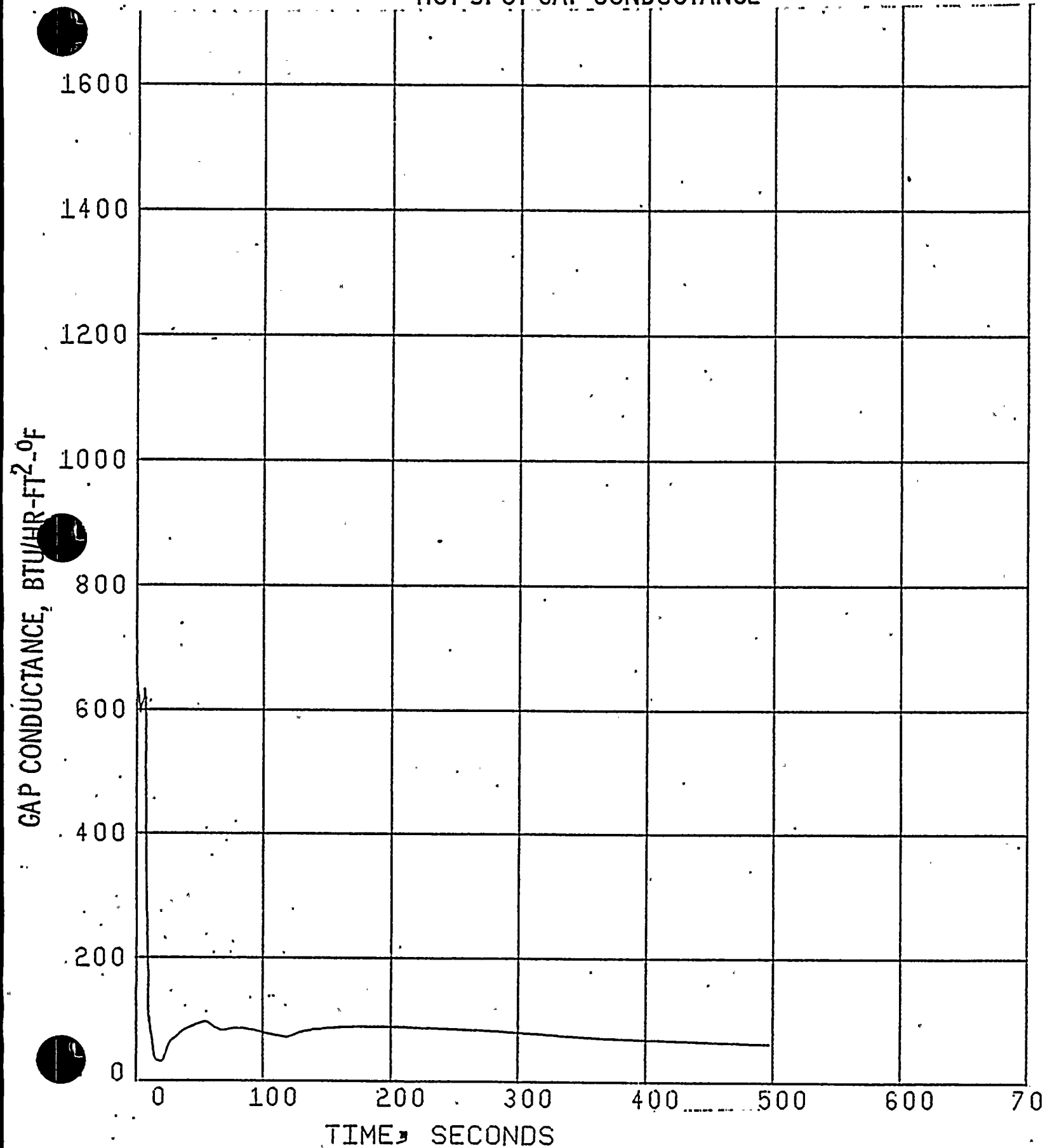


FIGURE III.0

ST. LUCIE UNIT I

ISOLATED SAFETY INJECTION TANK

0.8 x DOUBLE ENDED GUILLOTINE BREAK IN PUMP DISCHARGE LEG

PEAK LOCAL CLAD OXIDATION

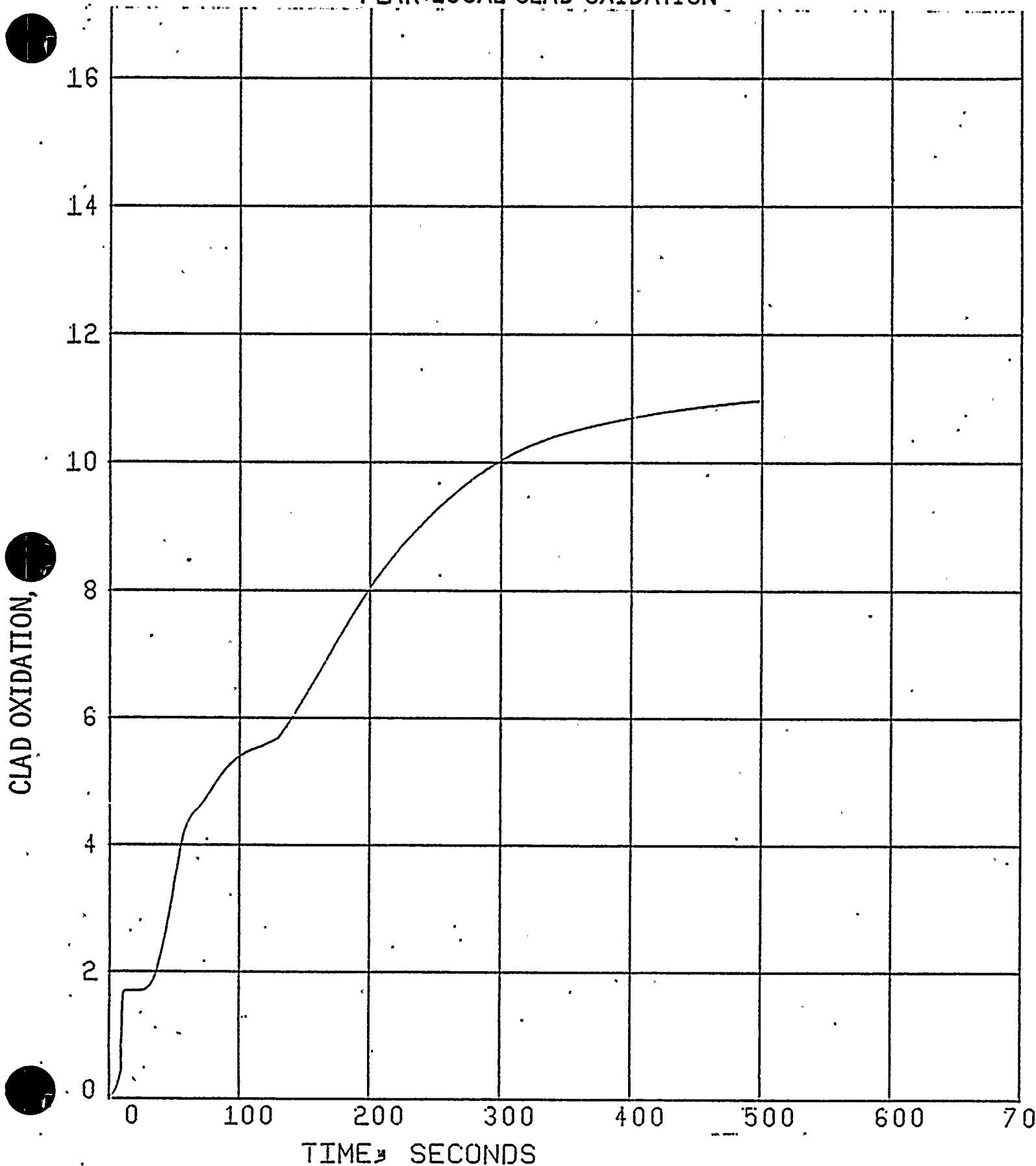


FIGURE III. P

ST. LUCIE UNIT I

ISOLATED SAFETY INJECTION TANK

0.8 x DOUBLE ENDED GUILLOTINE BREAK IN PUMP DISCHARGE LEG
CLAD TEMPERATURE, CENTERLINE FUEL TEMPERATURE, AVERAGE
FUEL TEMPERATURE AND COOLANT TEMPERATURE FOR HOTTEST NODE

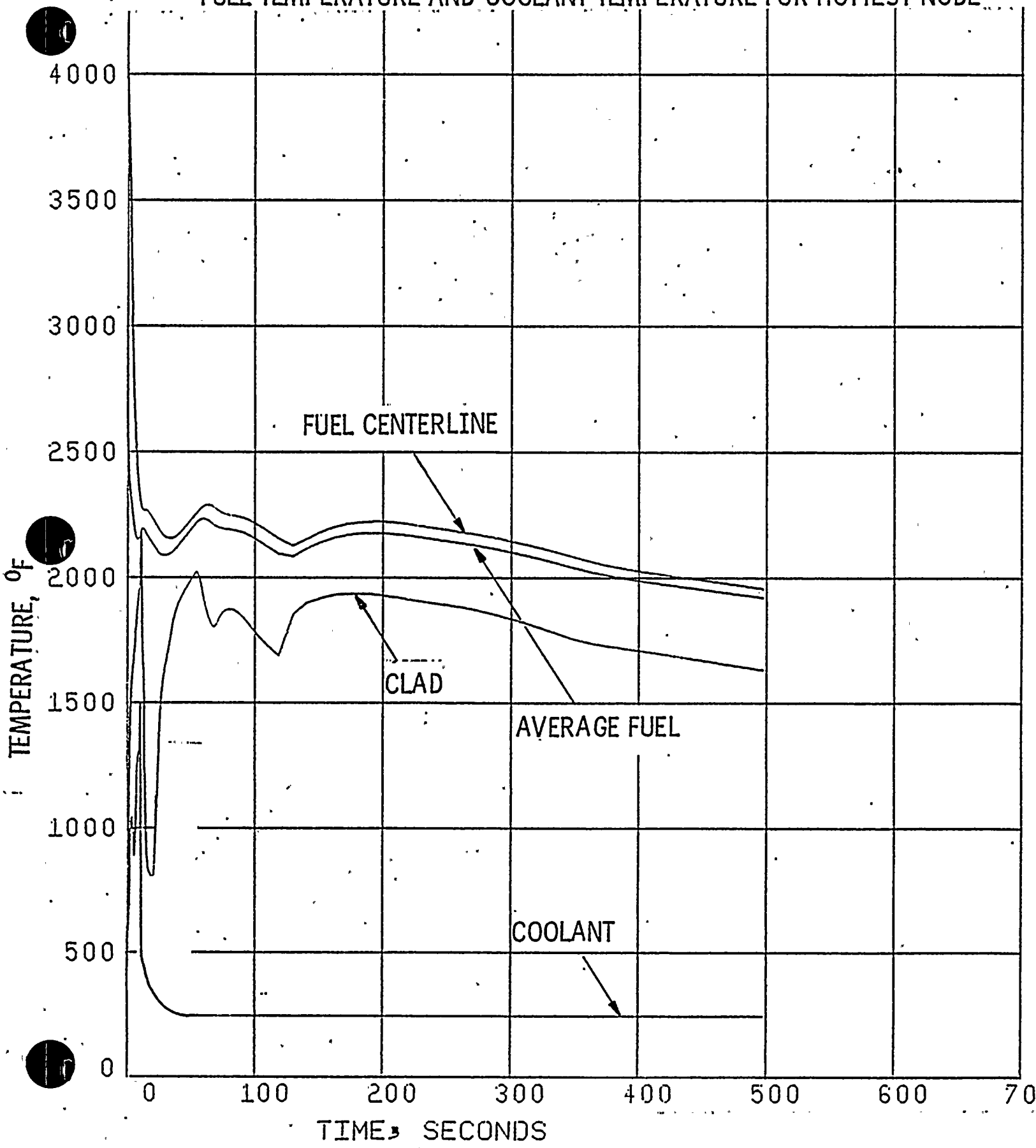


FIGURE III.Q

ST. LUCIE UNIT I

ISOLATED SAFETY INJECTION TANK

0.8 x DOUBLE ENDED GUILLOTINE BREAK IN PUMP DISCHARGE LEG

HOT SPOT HEAT TRANSFER COEFFICIENT

HEAT TRANSFER COEFFICIENT, BTU/HR-FT²-°F

180

160

140

120

100

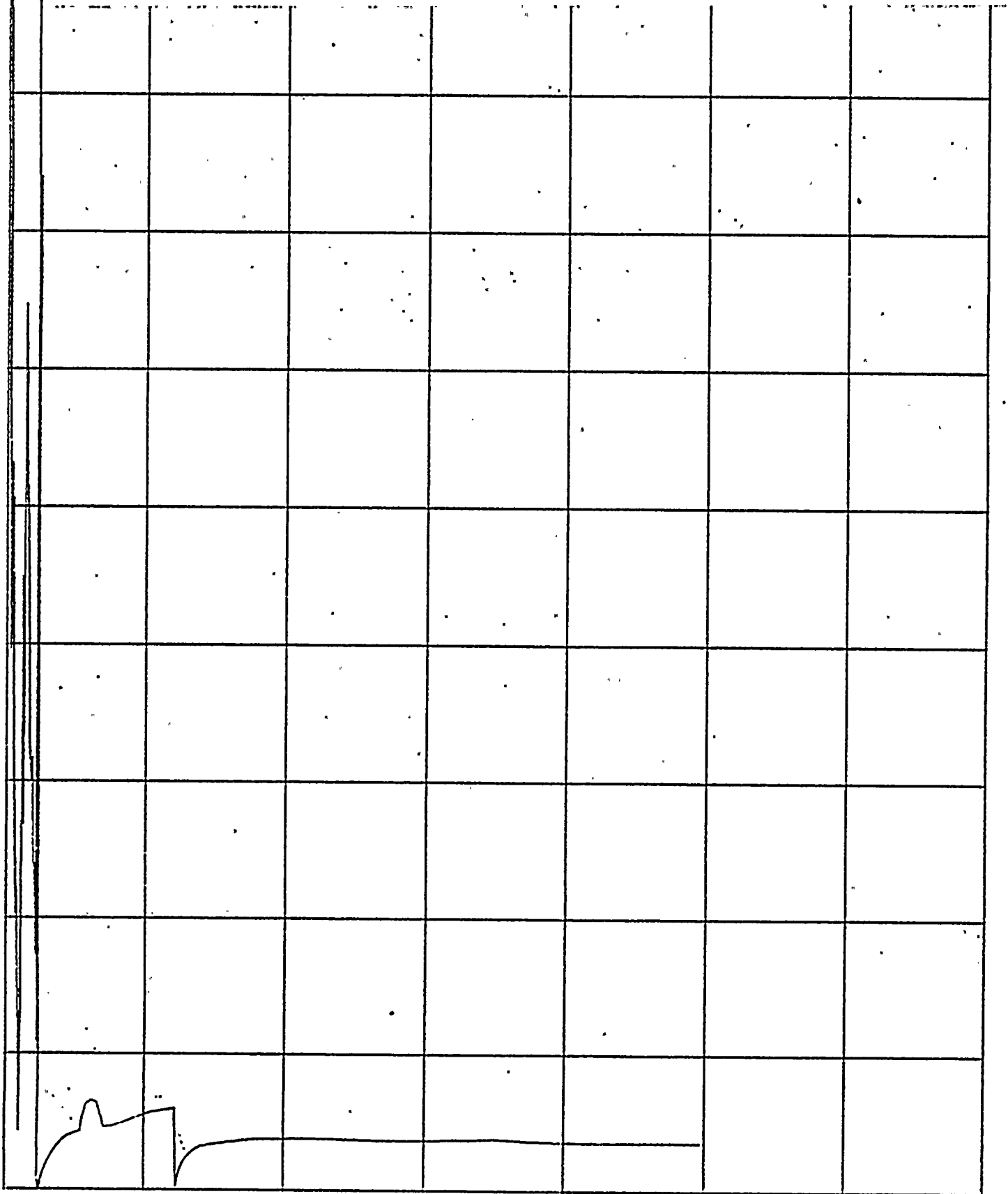
80

60

40

20

0



TIME, SECONDS

FIGURE III. R
ST. LUCIE UNIT I
ISOLATED SAFETY INJECTION TANK
0.8 x DOUBLE ENDED GUILLOTINE BREAK IN PUMP DISCHARGE LEG
HOT SPOT HEAT TRANSFER COEFFICIENT DURING REFLOOD

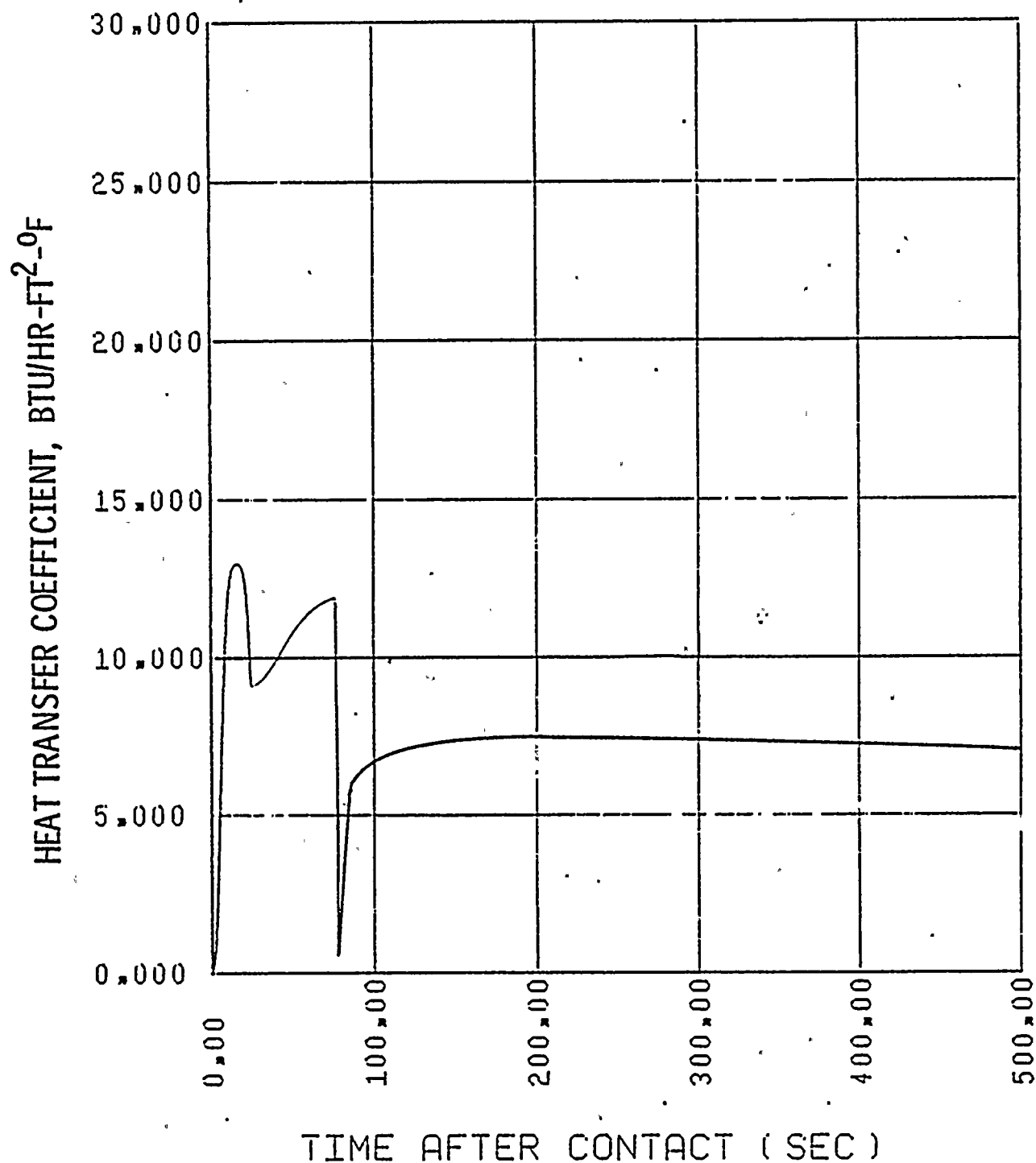


FIGURE III. S
ST. LUCIE UNIT I
ISOLATED SAFETY INJECTION TANK
0.8 x DOUBLE ENDED GUILLOTINE BREAK IN PUMP DISCHARGE LEG
CONTAINMENT TEMPERATURE

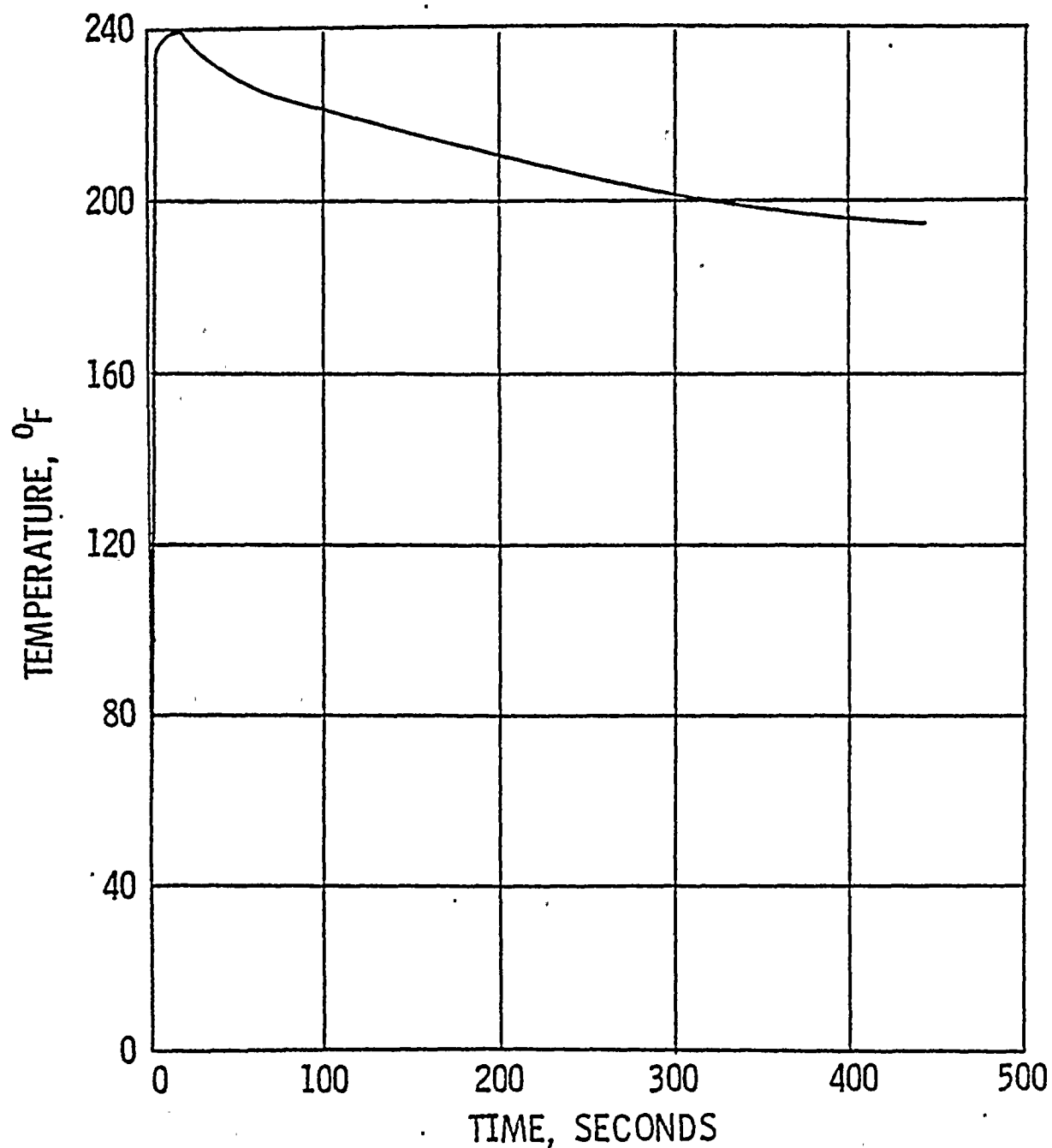


FIGURE III. T
ST. LUCIE UNIT I
ISOLATED SAFETY INJECTION TANK
0.8 x DOUBLE ENDED GUILLOTINE BREAK IN PUMP DISCHARGE LEG
SUMP TEMPERATURE

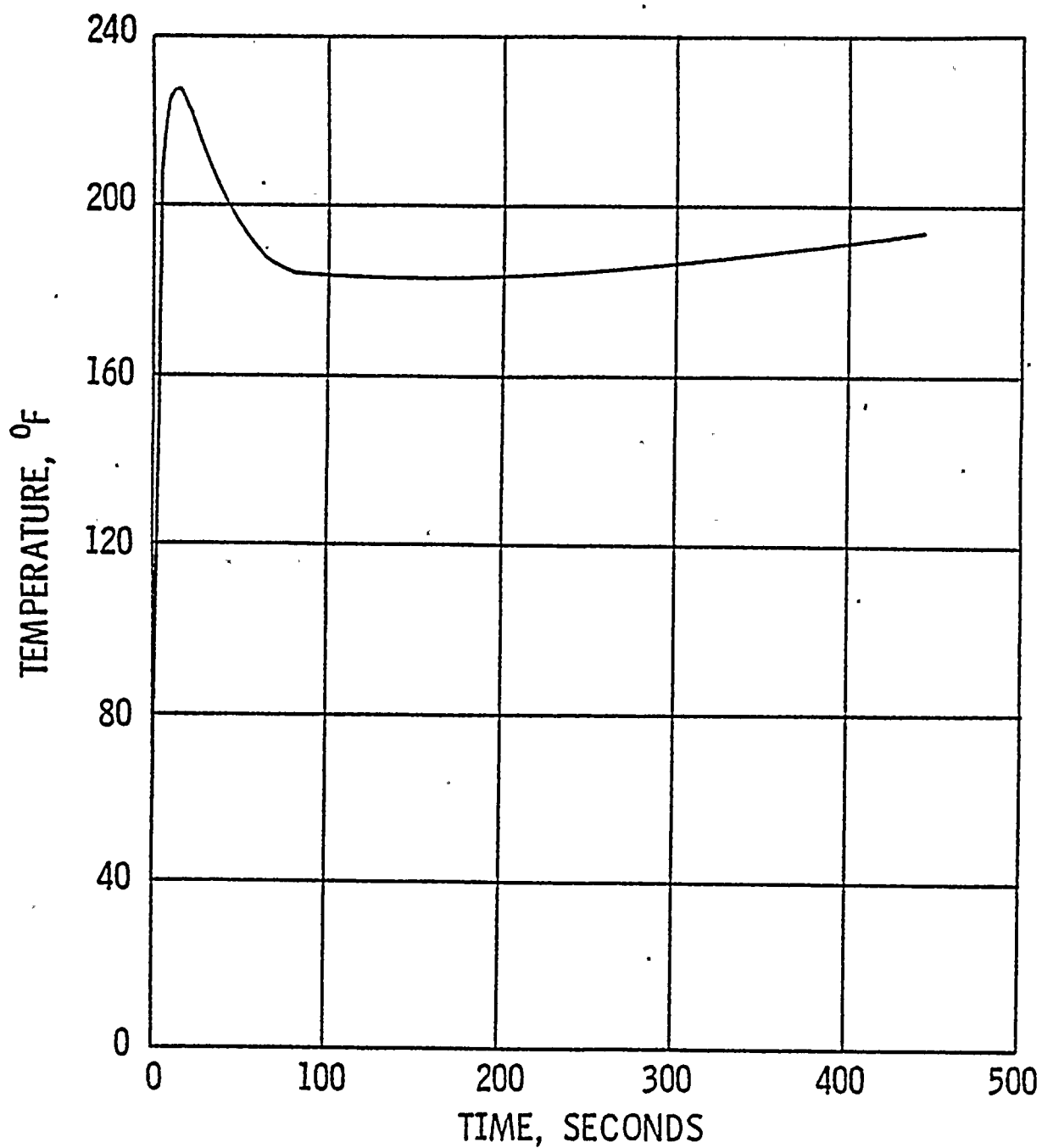


FIGURE III.U
ST. LUCIE UNIT I
ISOLATED SAFETY INJECTION TANK
0.8 x DOUBLE ENDED GUILLOTINE BREAK IN PUMP DISCHARGE LEG
HOT ROD INTERNAL GAS PRESSURE

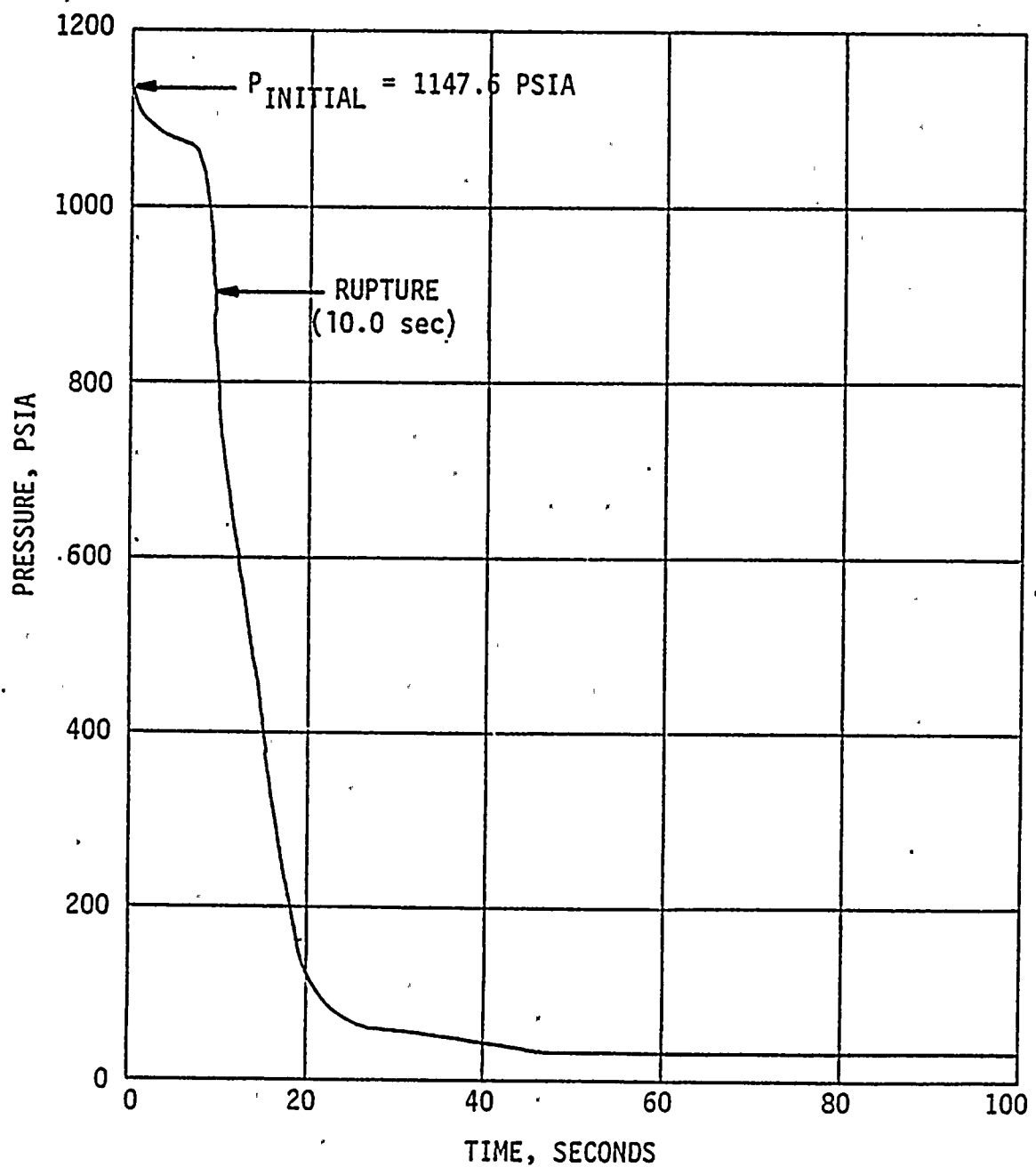


FIGURE III.V
ST. LUCIE UNIT I
ISOLATED SAFETY INJECTION TANK
0.8 x DOUBLE ENDED GUILLOTINE BREAK IN PUMP DISCHARGE LEG
CORE BULK CHANNEL FLOW RATE

